



# The Water Colour Simulator WASI

## User manual for WASI version 5

Peter Gege



The actual version of WASI and of this manual can be downloaded from the web site of the International Ocean-Colour Coordinating Group (IOCCG):

<http://www.ioccg.org/data/software.html>

## Copyright

The software was developed by Dr. Peter Gege, German Aerospace Center (DLR), Institut für Methodik der Fernerkundung, 82234 Oberpfaffenhofen, Germany. He owns all copyrights.

- WASI version 5 is a public domain software and can be used free of charge.
- There is no warranty in case of errors.
- There is no user support.
- Commercial distribution is not allowed.
- Commercial use is not allowed unless an agreement with the author is made.
- Publication of results obtained from using the software requires to
  - quote the use of WASI in the text,
  - cite a recent publication about WASI,
  - inform Peter Gege via email,
  - send a PDF of the paper to Peter Gege.

WASI version: 5  
Date: 25 June 2019  
Author: Peter Gege  
Contact: peter.gege@dlr.de



## Table of contents

1.	Introduction.....	6
2.	Models .....	7
2.1	Absorption.....	7
2.1.1	Pure water .....	7
2.1.2	CDOM .....	7
2.1.3	Phytoplankton.....	8
2.1.4	Non-algal particles.....	10
2.2	Backscattering.....	12
2.2.1	Pure water .....	12
2.2.2	Phytoplankton.....	13
2.2.3	Non-algal particles.....	13
2.3	Attenuation .....	15
2.3.1	Diffuse attenuation for downwelling irradiance.....	15
2.3.2	Diffuse attenuation for upwelling irradiance.....	15
2.3.3	Attenuation for upwelling radiance .....	16
2.4	Surface reflectance .....	17
2.5	Irradiance reflectance .....	18
2.5.1	Deep water .....	18
2.5.2	Shallow water .....	18
2.6	Radiance reflectance .....	19
2.6.1	Deep water .....	19
2.6.2	Shallow water .....	19
2.6.3	Above the surface .....	20
2.7	Bottom reflectance .....	22
2.7.1	For irradiance sensors .....	22
2.7.2	For radiance sensors .....	23
2.8	Downwelling irradiance .....	24
2.8.1	Above the water surface .....	24
2.8.2	Below the water surface.....	26
2.8.3	At depth z.....	26
2.9	Sky radiance .....	28
2.10	Upwelling radiance .....	29
2.10.1	Below the water surface.....	29
2.10.2	Above the water surface .....	29
2.11	Fluorescence.....	31
2.11.1	Phytoplankton .....	31
2.12	Mixed pixel .....	34
2.13	Depth of light penetration .....	35
3.	Forward mode .....	36
3.1	Graphical user interface .....	36
3.2	Calculation of a single spectrum .....	38
3.2.1	Mode selection.....	38
3.2.2	Spectrum type selection.....	38
3.2.3	Parameter selection.....	38
3.2.4	Calculation options .....	38
3.2.5	Start calculation .....	40
3.2.6	Example .....	40
3.3	Calculation of a series of spectra.....	43
3.3.1	General.....	43

3.3.2	Specification of the iteration.....	43
3.3.3	Data storage .....	44
3.3.4	Example .....	45
4.	Inverse modes .....	47
4.1	Graphical user interface .....	47
4.2	Inversion of a single spectrum .....	49
4.2.1	Spectrum selection.....	49
4.2.2	Definition of initial values.....	50
4.2.3	Fit strategy .....	51
4.2.4	Definition of fit region and number of iterations.....	52
4.3	Inversion of a series of spectra.....	53
4.3.1	Selection of spectra.....	53
4.3.2	Definition of initial values.....	53
4.4	Optimization of inversion.....	55
4.4.1	Irradiance reflectance of deep water.....	55
4.4.2	Irradiance reflectance of shallow water.....	59
4.4.3	Radiance reflectance of deep water .....	62
4.4.4	Radiance reflectance of shallow water .....	63
4.4.5	Downwelling irradiance.....	64
5.	Reconstruction mode .....	65
5.1	Definition of parameter values.....	65
5.2	Definition of output information.....	67
6.	2D mode.....	69
6.1	Image data format.....	69
6.2	Preview settings.....	70
6.3	Image import and pixel information.....	71
6.4	Image masking .....	71
6.5	Guidelines for data processing .....	72
6.5.1	Preprocessing.....	72
6.5.2	Define mask .....	73
6.5.3	Load masked image .....	75
6.5.4	Select preview parameter.....	76
6.5.5	Define fit settings.....	77
6.5.6	Run fit .....	78
6.5.7	Visualize results.....	79
7.	Background mode .....	81
8.	Model options .....	82
8.1	Downwelling irradiance .....	82
8.2	Irradiance reflectance .....	84
8.3	Absorption .....	88
8.4	Bottom reflectance .....	90
9.	Implicit spectra .....	92
10.	Program options .....	94
10.1	Data format.....	94
10.2	Directories .....	97
10.3	Display options.....	98
10.4	General options .....	98
11.	References .....	100
	Appendix 1: Installation .....	106
	Appendix 2: WASI5.INI .....	107
	Appendix 3: Parameters .....	113

Appendix 4: Constants .....	114
Appendix 5: Input spectra .....	115
Appendix 6: Calculated spectra.....	116
Appendix 7: Spectrum types .....	118
Appendix 8: Demo data.....	120
Appendix 9: Changes compared to version 4.1.....	121

## 1. Introduction

The Water Color Simulator WASI is a software tool for simulating and analyzing the most common types of spectral measurements of open waters under outdoor conditions. The deep-water version is described in Gege (2004), the shallow-water version in Gege and Albert (2006), and the version for processing image data in Gege (2014).

The spectrum types and major calculation options are listed in Table 1.1. A more comprehensive summary including the fit parameters is given in Appendix 7. WASI can be used to generate the spectra of Table 1.1 ("Forward mode"), or to analyze such spectra ("Inverse mode"). Both modes can be combined to perform sensitivity studies ("Reconstruction mode"). The three modes of operation are described in chapter 3 (forward mode), chapter 4 (inverse mode) and chapter 5 (reconstruction mode). Model options are depicted in chapter 6, program options in chapter 8. The installation of WASI is described in Appendix 1.

All calculations are based on analytical models with experimentally easily accessible parameters, which are well established in the "ocean color" community and experimentally and theoretically validated. These models are described in detail in chapter 2; the corresponding references are cited in chapter 9.

The program consists of an executable file, WASI5.EXE, an initialization file, WASI5.INI, and a database consisting of 34 spectra. WASI5.INI is an ASCII file that comprises all paths and file names of the data files, parameter values, constants and user settings. An example listening is given in Appendix 2. Much effort was spent to make the user interface as clear as possible. Since most settings in the different pop-up windows are self-explanatory, not every detail is described in this manual.

Spectrum type	Model options
Absorption coefficient	Of water constituents Of natural water bodies
Attenuation coefficient	For downwelling irradiance
Specular reflectance	Wavelength dependent Constant
Irradiance reflectance	For deep water For shallow water
Radiance reflectance	Below surface for deep water Below surface for shallow water Above surface for deep water Above surface for shallow water
Bottom reflectance	For irradiance sensors For radiance sensors
Downwelling irradiance	Above surface Below surface
Upwelling radiance	Below surface Above surface

Table 1.1: Spectrum types and major model options.

## 2. Models

### 2.1 Absorption

The bulk absorption coefficient of natural water,  $a(\lambda)$ , is the sum of the absorption coefficients of pure water and of the water constituents:

$$a(\lambda) = a_w(\lambda) + (T - T_0) \frac{da_w(\lambda)}{dT} + a_{wc}(\lambda). \quad (2.1)$$

The absorption coefficient of pure water is split up into a temperature-independent term  $a_w(\lambda)$ , which is valid at a reference temperature  $T_0$ , and a temperature gradient  $da_w(\lambda)/dT$ , with  $T$  being the actual water temperature.

The huge variety of particles and molecules present in all natural waters is usually grouped into three classes with distinct spectral absorption: colored dissolved organic matter (CDOM), phytoplankton (phy), and non-algal particles (NAP). The resulting absorption coefficient of the water constituents is the sum of the components' absorption coefficients:

$$a_{wc}(\lambda) = a_{CDOM}(\lambda) + a_{phy}(\lambda) + a_{NAP}(\lambda). \quad (2.2)$$

#### 2.1.1 Pure water

The spectra  $a_w(\lambda)$  and  $da_w(\lambda)/dT$  provided with WASI5 are shown in Figure 2.1.  $a_w(\lambda)$  is a combination from different sources for a temperature of  $T_0 = 20$  °C. 190-196.6 nm: Warren (1995); 200-227 nm: Quickenden and Irvin (1980); 260-300 nm: Wang (2008); 304-386 nm: Lu (2006); 387.5-710 nm: Pope and Fry (1997); 712.3 – 1838 nm: Kou et al. (1993). The gaps in between have been interpolated using an Akima fit. The spectrum  $da_w(\lambda)/dT$  was measured by Röttgers et al. (2013).

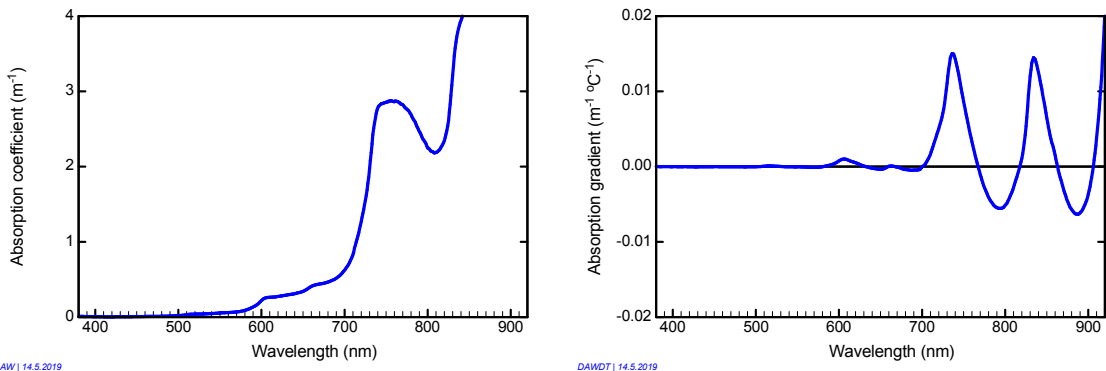


**Figure 2.1: Pure water absorption coefficient,  $a_w(\lambda)$ , and temperature gradient of water absorption,  $da_w(\lambda)/dT$ .**

#### 2.1.2 CDOM

CDOM (colored dissolved organic matter) is the colored fraction of the water constituents passing a filter with a pore size of 0.2 µm. Historical names are, besides others, Gelbstoff (Kalle 1938) and yellow substance.

The concentration of CDOM is usually expressed in the remote sensing community in terms of the absorption coefficient at a reference wavelength  $\lambda_0$ :

$$C_Y = a_{CDOM}(\lambda_0), \quad (2.3)$$

and the wavelength dependency of CDOM absorption by an absorption coefficient  $a_Y^N(\lambda)$  that is normalized at the wavelength  $\lambda_0$ . Hence,

$$a_{CDOM}(\lambda) = C_Y \cdot a_Y^N(\lambda). \quad (2.4)$$

The index “Y” is used to associate the optical quantity “yellow substance” with the model parameters rather than mass-specific parameters. In WASI,  $a_Y^N(\lambda)$  can either be read from file or calculated using the usual exponential approximation (Nyquist 1979; Bricaud et al. 1981):

$$a_Y^N(\lambda) = \exp\{-S \cdot (\lambda - \lambda_0)\}, \quad (2.5)$$

with  $S$  denoting the spectral slope. Default values are  $\lambda_0 = 440$  nm and  $S = 0.014 \text{ nm}^{-1}$ , which can be considered representative of a great variety of water types (Bricaud et al. 1981; Carder et al. 1989). The spectrum  $a_Y^N(\lambda)$  for these default values is shown in Figure 2.3.

It has been shown (Gege 2000) for measurements at Lake Constance that the errors of approximation (2.5) are below 10 % only for a wavelength interval of  $\sim 60$  nm around  $\lambda_0$ , and that a better approximation is a sum of 3 Gaussian distributions (with the x-axis in units of  $\text{cm}^{-1}$ ). The Gaussian model is physically more reasonable than the exponential model and offers a deeper understanding of the chemical interactions affecting CDOM molecular structure (Schwarz et al. 2002). Thus, a spectrum (`Y_Gauss.AN`) is provided with WASI which represents the line shape of  $a_Y^N(\lambda)$  in terms of the Gaussian model for the average parameters determined for Lake Constance (Table 1 in Gege 2000). It is shown in Figure 2.3.

*Note:* If the mass-specific absorption coefficient  $a_{CDOM}^*(\lambda_0)$  is known,  $C_Y$  can be converted to mass concentration  $C_{CDOM}$  (in units of  $\text{g m}^{-3}$ ) using the relationship

$$C_{CDOM} = \frac{C_Y}{a_{CDOM}^*(\lambda_0)}. \quad (2.6)$$

However, this conversion introduces a large uncertainty since  $a_{CDOM}^*(\lambda_0)$  is highly variable within a reported range from  $0.27$  to  $2.16 \text{ m}^2 \text{ g}^{-1}$  at  $\lambda_0 = 380$  nm (Sipelgas et al. 2003). To avoid the uncertainty resulting from this variability, and since  $C_{CDOM}$  is frequently of minor interest, this conversion is rarely performed in remote sensing and not implemented in WASI.

### 2.1.3 Phytoplankton

The high number of phytoplankton species occurring in natural waters and their differences in pigment composition can lead to a high variability of the specific absorption coefficient of phytoplankton. To account for this natural variability, WASI separates the phytoplankton group into 6 optical classes. This is done by assigning 6 specific absorption spectra  $a_i^*(\lambda)$  and 6 concentrations  $C_i$  to phytoplankton. The absorption coefficient of a mixture of different phytoplankton classes is then modelled in WASI as follows:

$$a_{phy}(\lambda) = \sum_{i=0}^5 C_i \cdot a_i^*(\lambda). \quad (2.7)$$

The total phytoplankton concentration is the sum of the concentrations of all 6 classes:

$$C_{phy} = \sum_{i=0}^5 C_i. \quad (2.8)$$

$C_i$  denotes chlorophyll-a concentration. If the phytoplankton can be approximated by a single specific absorption spectrum, five of the  $C_i$  are set equal zero. This is the common approach.

The spectra  $a_i^*(\lambda)$  of the WASI database are shown in Figure 2.2. The five spectra  $a_1^*(\lambda) \dots a_5^*(\lambda)$  represent the optical classes “cryptophyta type L”, “cryptophyta type H”, “dia-

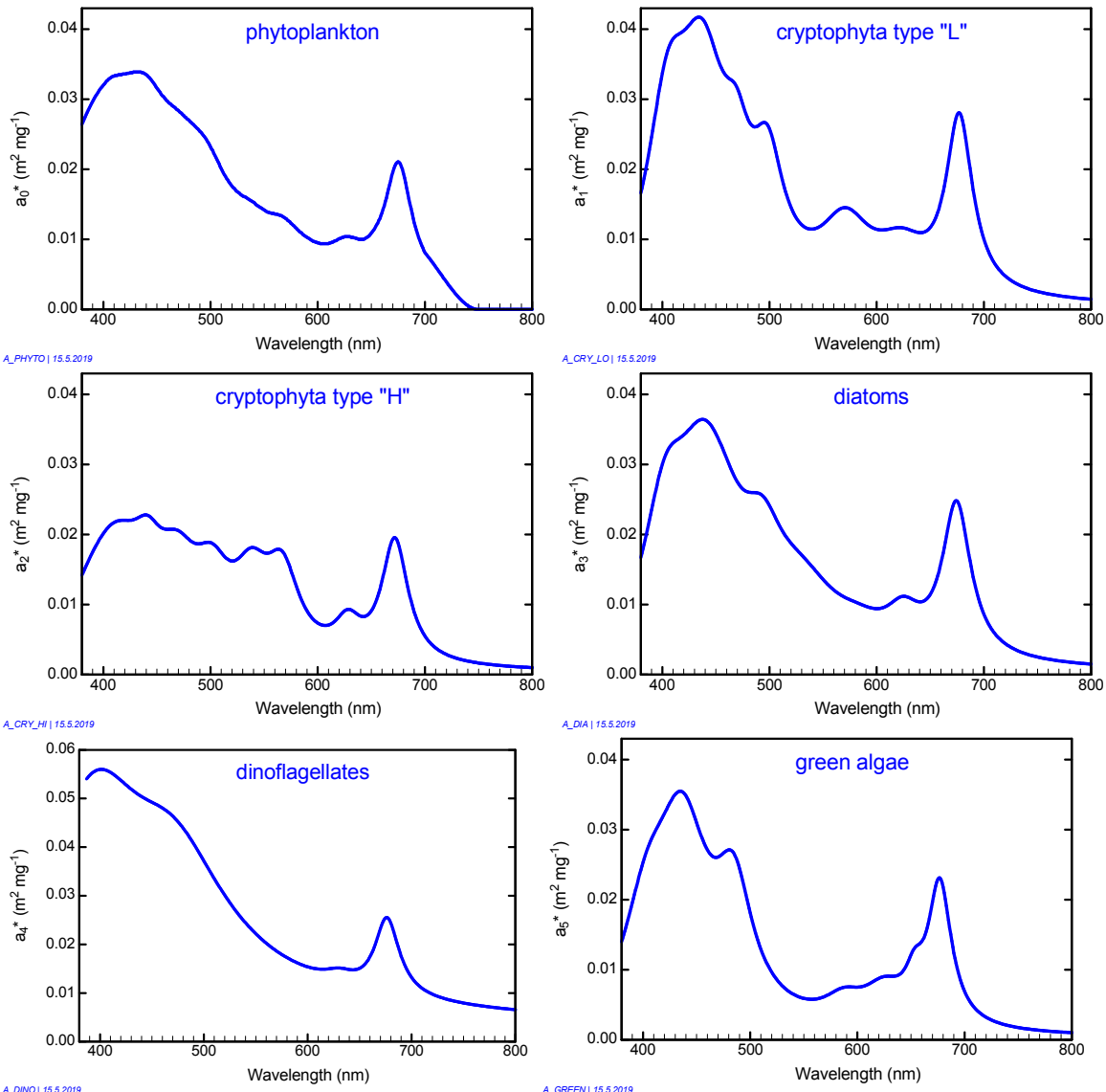


**Figure 2.2: Specific absorption coefficients of 6 phytoplankton classes,  $a_i^*(\lambda)$ .**

toms”, “dinoflagellates”, and “green algae”. These were derived from pure cultures grown in the laboratory (Gege 1994, 1995, 1998b). The scaling of  $a_3^*(\lambda)$ ,  $a_4^*(\lambda)$  and  $a_5^*(\lambda)$  was adjusted to match field measurements (Gege 2012b).

The spectrum  $a_0^*(\lambda)$ , labeled "phytoplankton" in Figure 2.2, is a weighted sum of the five spectra  $a_1^*(\lambda) \dots a_5^*(\lambda)$  and represents a typical mixture for Lake Constance. It was calculated by Heege (2000) using phytoplankton absorption spectra<sup>1</sup> and pigment data<sup>2</sup> from 32 days in 1990 and 1991, and he validated it using 139 irradiance reflectance and 278 attenuation measurements<sup>3</sup> from 1990 to 1996.

## 2.1.4 Non-algal particles

The sum of all absorbing non-algal particles in the water is nowadays called NAP. Historical names are detritus, tripton (Gitelson et al. 2008) or bleached particles (Doerffer and Schiller 2007). As the particles are of various origins, the spectral properties of NAP can change significantly. WASI imports a normalized absorption spectrum,  $a_{NAP}^N(\lambda)$ , from file. NAP absorption is calculated as

$$a_{NAP}(\lambda) = C_{NAP} \cdot a_{NAP}^*(\lambda_0) \cdot a_{NAP}^N(\lambda). \quad (2.9)$$

$a_{NAP}^N(\lambda)$  is normalized at the same wavelength  $\lambda_0$  as CDOM.  $a_{NAP}^*(\lambda_0)$  denotes the specific absorption coefficient of NAP at the wavelength  $\lambda_0$ . The concentration  $C_{NAP}$  is calculated as the sum of the two NAP components considered in the backscattering model described in chapter 2.2.3:

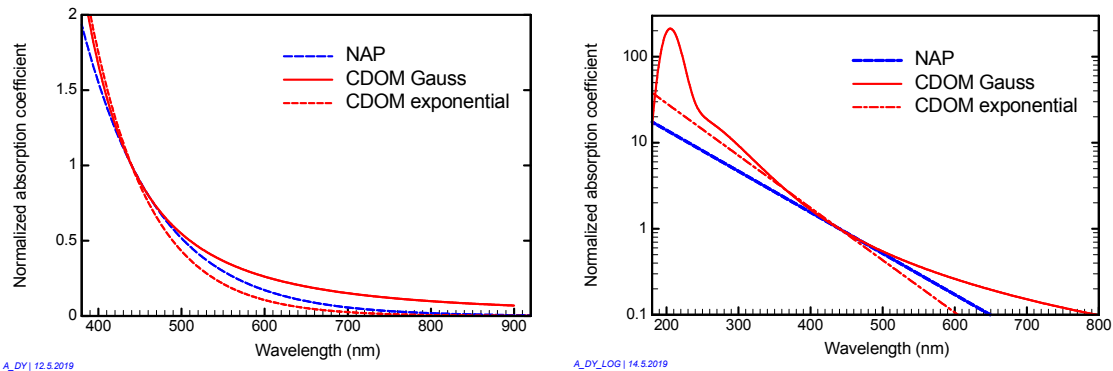


Figure 2.3: Normalized absorption coefficients of CDOM,  $a_Y^*(\lambda)$ , and NAP,  $a_{NAP}^N(\lambda)$ . Left: y-axis linear, right: y-axis logarithmic.

$$C_{NAP} = C_X + C_{Mie}. \quad (2.10)$$

For  $\lambda_0$  in the blue,  $a_{NAP}^*(\lambda_0)$  varies at least by an order of magnitude from  $0.01 \text{ m}^2 \text{ g}^{-1}$  (Lobo et al. 2014) to  $0.12 \text{ m}^2 \text{ g}^{-1}$  (Xue et al. 2017). WASI uses by default  $a_{NAP}^*(440) = 0.041 \text{ m}^2 \text{ g}^{-1}$ , which is the average of 328 measurements in different coastal waters around Europe (Babin et al. 2003a).

<sup>1</sup> Derived from above-water reflectance spectra by inverse modelling (Gege 1994, 1995).

<sup>2</sup> Measured at the University of Constance by Beese, Richter, and Kenter.

<sup>3</sup> Measured by Tilzer, Hartig, and Heege (Tilzer et al. 1995, Heege 2000).

The spectral shape can be approximated reasonably well in many cases with an exponential function (Babin et al. 2003a). The default spectrum provided with WASI was accordingly calculated as  $a_{NAP}^N(\lambda) = \exp\{-S_{NAP} \cdot (\lambda - \lambda_0)\}$  using  $\lambda_0 = 440$  nm and  $S_{NAP} = 0.011$  nm<sup>-1</sup> (D'Sa et al. 2006). It is shown in Figure 2.3.

*Note:* Spectral shape,  $a_{NAP}^N(\lambda)$ , and specific absorption coefficient,  $a_{NAP}^*(\lambda_0)$ , depend on the particle types in the water, which can strongly differ regionally and seasonally. The defaults provided with WASI can be used as an approximation, but it is recommended to replace them with regional information whenever available.

## 2.2 Backscattering

The backscattering coefficient of water,  $b_b$ , is the sum of the backscattering coefficients of pure water (index "w"), phytoplankton (phy) and non-algal particles (NAP):

$$b_b(\lambda) = b_{b,w}(\lambda) + b_{b,phy}(\lambda) + b_{b,NAP}(\lambda). \quad (2.11)$$

CDOM backscattering is negligible, thus it is omitted in Eq. (2.11). Typical spectral shapes and magnitudes of backscattering are illustrated in Figure 2.4.

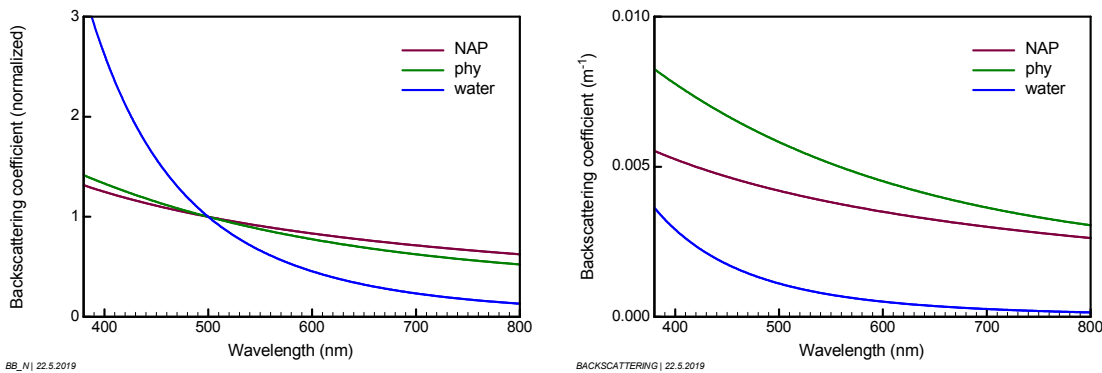


**Figure 2.4:** Typical backscattering coefficients of non-algal particles, phytoplankton and water. Left: Normalized spectra for comparison of spectral shape. Right: Absolute values for comparison of amplitudes for conditions common in clear coastal and inland waters:  $C_{phy} = 5 \text{ mg m}^{-3}$ ,  $b_{b,phy}^*(550) = 0.001 \text{ m}^2 \text{ mg}^{-1}$ ,  $C_{Mie} = 1 \text{ g m}^{-3}$ ,  $b_{b,Mie}^*(500) = 0.0042 \text{ m}^2 \text{ g}^{-1}$ ,  $n = -1$ .

The spectra labeled “NAP” and “phy” are very similar because scattering and backscattering of phytoplankton and non-algal particles depend more on the size distribution than on chemical composition. Since measuring backscattering coefficients during field campaigns does not allow a clear assignment to phytoplankton and non-algal particles, such distinction is frequently not made, and just the bulk backscattering coefficient of both phytoplankton and non-algal particles is considered:

$$b_{b,TSM}(\lambda) = b_{b,phy}(\lambda) + b_{b,NAP}(\lambda). \quad (2.12)$$

The sum of the concentrations of phytoplankton and non-algal particles is called total suspended matter (TSM):

$$C_{TSM} = C_{phy} + C_{NAP}. \quad (2.13)$$

### 2.2.1 Pure water

The backscattering coefficient of pure water is calculated using the empirical relation of Morel (1974):

$$b_{b,w}(\lambda) = b_1 \cdot \left( \frac{\lambda}{\lambda_1} \right)^{-4.32}. \quad (2.14)$$

The specific backscattering coefficient,  $b_1$ , depends on salinity. It is  $b_1 = 0.00111 \text{ m}^{-1}$  for fresh water and  $b_1 = 0.00144 \text{ m}^{-1}$  for oceanic water with a salinity of 35–38 ‰, when  $\lambda_1 = 500 \text{ nm}$  is chosen as reference wavelength.

## 2.2.2 Phytoplankton

The backscattering coefficient of phytoplankton is calculated as the product of phytoplankton concentration  $C_{phy}$ , specific phytoplankton backscattering coefficient  $b_{b,phy}^*$  at a reference wavelength  $\lambda_S$ , and normalized phytoplankton scattering coefficient  $b_{phy}^N(\lambda)$ :

$$b_{b,phy}(\lambda) = C_{phy} \cdot b_{b,phy}^* \cdot b_{phy}^N(\lambda). \quad (2.15)$$

As described in section 2.1.3, WASI can distinguish between 6 optical classes of phytoplankton with different specific absorption coefficients. Since backscattering has usually not such prominent spectral features as absorption (compare Figure 2.4 with Figure 2.2), no such distinction is made for phytoplankton backscattering, and  $C_{phy}$  is calculated using Eq. (2.8) as the sum of all 6 classes.

The spectrum  $b_{phy}^N(\lambda)$  provided with WASI was obtained by fitting a measurement of  $b_{b,phy}(\lambda)$  for green algae from Lake Garda in the range from 400 to 900 nm (C. Giardino, personal communication) and extrapolating the fit curve to the range from 350 to 1000 nm (Figure 2.4). The specific phytoplankton backscattering coefficient of this measurement,  $b_{b,phy}^* = 0.0010 \text{ m}^2 \text{ mg}^{-1}$  at  $\lambda_S = 550 \text{ nm}$ , is set as default in WASI.  $b_{phy}^N(\lambda)$  is imported from file while  $b_{b,phy}^*$  is a tunable parameter.

## 2.2.3 Non-algal particles

For the non-algal particles (NAP) a mixture of two types with spectrally different backscattering coefficients is implemented:

$$b_{b,NAP}(\lambda) = C_X \cdot b_{b,X}^* \cdot b_X^N(\lambda) + C_{Mie} \cdot b_{b,Mie}^* \cdot \left( \frac{\lambda}{\lambda_S} \right)^n. \quad (2.16)$$

The first type is defined by a normalized scattering coefficient with arbitrary wavelength dependency,  $b_X^N(\lambda)$ , the second type by a scattering coefficient following the Angström law  $(\lambda/\lambda_S)^n$ . The concentrations are denoted  $C_X$  and  $C_{Mie}$ , respectively. The specific backscattering coefficients  $b_{b,X}^*$  and  $b_{b,Mie}^*$  assign physical units to the unitless functions  $b_X^N(\lambda)$  and  $(\lambda/\lambda_S)^n$ .

**Particles of Type I.** Particles of Type I are defined by a normalized scattering coefficient with arbitrary wavelength dependency,  $b_X^N(\lambda)$ , which is imported from file.  $C_X$  is the concentration and  $b_{b,X}^*$  the specific backscattering coefficient. The user has several options for calculation:

- $b_{b,X}^*$  can be treated either as constant with a default value of  $0.0086 \text{ m}^2 \text{ g}^{-1}$  (Heege 2000), or as  $b_{b,X}^* = A \cdot C_X^B$ . Such a non-linear dependency of scattering on concentration was observed for phytoplankton (Morel 1980). It may be used for Case 1 water types, while  $b_{b,X}^*$

= constant is appropriate for Case 2 waters with significant sources of NAP. Typical values of the empirical constants are  $A = 0.0006 \text{ m}^2 \text{ g}^{-1}$  and  $B = -0.37$  (Sathyendranath et al. 1989), which are set as defaults in WASI.

- $b_X^N(\lambda)$  can either be read from file, or it can be calculated as  $b_X^N(\lambda) = a_0^*(\lambda_L)/a_0^*(\lambda)$ , where  $a_0^*(\lambda)$  is the specific absorption coefficient of phytoplankton class no. 0 (see Eq. (2.7)), and  $\lambda_L$  denotes a reference wavelength ( $\lambda_L = 550 \text{ nm}$  by default). This method assumes that particle backscattering originates mainly from phytoplankton cells, and couples absorption and scattering according to the Case 1 waters model of Sathyendranath et al. (1989). However, such coupling may be used in exceptional cases only, since living algae have a negligible influence on the backscattering process by oceanic waters (Ahn et al. 1992), and in Case 2 waters particle scattering is weakly related to phytoplankton absorption in general. In WASI,  $b_X^N(\lambda) = 1$  is set as default.

**Particles of Type II.** Particles of Type II are defined by the normalized scattering coefficient  $(\lambda/\lambda_S)^n$ , where the Angström exponent  $n$  is related to the particle size distribution.  $C_{Mie}$  is the concentration and  $b_{b,Mie}^*$  the specific backscattering coefficient. The parameters are set by default to  $b_{b,Mie}^* = 0.0042 \text{ m}^2 \text{ g}^{-1}$ ,  $\lambda_S = 500 \text{ nm}$ ,  $n = -1$ , which are representative for Lake Constance (Heege 2000).

In the open ocean, the exponent  $n$  typically ranges from -1 for low to 0 for high (above  $2 \mu\text{g/l}$ ) chlorophyll-a concentrations (Morel 1988, Morel and Maritorena 2001). In coastal waters, the backscattering coefficients are spectrally rather flat, corresponding to  $n$  values around zero (Babin et al. 2003, Chami et al. 2005). Mass-specific scattering coefficients are typically in the order of 0.5 to  $1.0 \text{ m}^2 \text{ g}^{-1}$  at  $555 \text{ nm}$  (Babin et al. 2003), and the ratio of backscattering to total scattering ranges from about 0.2 % to 3 % (Chami et al. 2005, Antoine et al. 2011), hence  $b_{b,Mie}^*$  is in the range from about 0.001 to  $0.03 \text{ m}^2 \text{ g}^{-1}$  for  $\lambda_S = 555 \text{ nm}$ .

## 2.3 Attenuation

The diffuse attenuation coefficient of irradiance  $E$  is defined as  $K = -(1/E) dE/dz$ , where  $z$  is the depth. Similarly, the attenuation coefficient of radiance  $L$  is defined as  $k = -(1/L) dL/dz$ . Attenuation is an apparent optical property (AOP) and depends not only on the properties of the medium, but additionally on the geometric distribution of the illuminating light field.

### 2.3.1 Diffuse attenuation for downwelling irradiance

The most important attenuation coefficient is  $K_d$ , as it describes the decrease of natural illumination under water.  $K_d$  has been studied extensively; see Bukata et al. (1995) for a literature overview. The following approximation is used frequently and implemented in WASI:

$$K_d(\lambda) = \kappa_0 \frac{a(\lambda) + b_b(\lambda)}{\cos \theta'_{\text{sun}}}, \quad (2.17)$$

with  $\theta'_{\text{sun}}$  the sun zenith angle in water. It originates from Gordon (1989), who has shown by Monte Carlo simulations for oceanic waters that this equation provides an accuracy of  $\sim 3\%$  near the water surface for sun zenith angles below  $60^\circ$ .  $a(\lambda)$  is calculated according to Eq. (2.10),  $b_b(\lambda)$  using Eq. (2.11). The coefficient  $\kappa_0$  depends on the scattering phase function. Gordon (1989) determined a value of  $\kappa_0 = 1.0395$  from Monte Carlo simulations in Case 1 waters, Albert and Mobley (2003) found a value of  $\kappa_0 = 1.0546$  from simulations in Case 2 waters using the radiative transfer program Hydrolight (Mobley et al. 1993). Some authors use Eq. (2.17) with  $\kappa_0 = 1$  (Sathyendranath and Platt 1988, 1997; Gordon et al. 1975). In WASI,  $\kappa_0$  is read from the WASI5.INI file; the default value is 1.0546.

### 2.3.2 Diffuse attenuation for upwelling irradiance

As the angular distribution of the light backscattered in water is usually different from that reflected at the bottom, two attenuation coefficients are used for upwelling irradiance:  $K_{uW}$  for the radiation from the water, and  $K_{uB}$  for the radiation from the bottom. The following parameterization is adopted from Albert and Mobley (2003):

$$K_{uW}(\lambda) = [a(\lambda) + b_b(\lambda)] \cdot [1 + \omega_b(\lambda)]^{1.9991} \cdot \left[ 1 + \frac{0.2995}{\cos \theta'_{\text{sun}}} \right]. \quad (2.18)$$

$$K_{uB}(\lambda) = [a(\lambda) + b_b(\lambda)] \cdot [1 + \omega_b(\lambda)]^{1.2441} \cdot \left[ 1 + \frac{0.5182}{\cos \theta'_{\text{sun}}} \right]. \quad (2.19)$$

The function  $\omega_b(\lambda)$  depends on absorption  $a(\lambda)$  and backscattering  $b_b(\lambda)$  of the water body:

$$\omega_b(\lambda) = \frac{b_b(\lambda)}{a(\lambda) + b_b(\lambda)}. \quad (2.20)$$

Eqs. (2.18) and (2.19) are used implicitly in the model of irradiance reflectance in shallow waters, see Eq. (2.29).

### 2.3.3 Attenuation for upwelling radiance

For upwelling radiance two attenuation coefficients are used:  $k_{uW}$  for the radiation backscattered in the water, and  $k_{uB}$  for the radiation reflected from the bottom. The following parameterization is adopted from Albert and Mobley (2003):

$$k_{uW}(\lambda) = \frac{a(\lambda) + b_b(\lambda)}{\cos \theta'_v} \cdot [1 + \omega_b(\lambda)]^{3.5421} \cdot \left[ 1 - \frac{0.2786}{\cos \theta'_{\text{sun}}} \right]. \quad (2.21)$$

$$k_{uB}(\lambda) = \frac{a(\lambda) + b_b(\lambda)}{\cos \theta'_v} \cdot [1 + \omega_b(\lambda)]^{2.2658} \cdot \left[ 1 + \frac{0.0577}{\cos \theta'_{\text{sun}}} \right]. \quad (2.22)$$

These equations are used implicitly in the model of radiance reflectance in shallow waters, see Eq. (2.33).

## 2.4 Surface reflectance

An above-water radiance sensor looking down to the water surface measures the sum of two radiance components: one from the water body, one from the surface. The first comprises the desired information about the water constituents; the second is an unwanted add-on which has to be corrected. However, correction is difficult. For example, the method from the SeaWiFS protocols (Mueller and Austin 1995), which is widely used in optical oceanography, leads to rms errors of the corrected water leaving radiance as large as 90 % under typical field conditions (Toole et al. 2000). Thus, WASI offers different methods.

The radiance reflected from the surface,  $L_r(\lambda)$ , is a fraction  $\rho_L$  of sky radiance  $L_s(\lambda)$ :

$$L_r(\lambda) = \rho_L \cdot L_s(\lambda) \quad (2.23)$$

$L_s(\lambda)$  is the average radiance of that area of the sky that is specularly reflected into the sensor. It can be imported from file or calculated using Eq. (2.59).  $\rho_L$  is the Fresnel reflectance and depends on the angle of reflection. The value can either be specified by the user or it can be calculated from the viewing angle  $\theta_v$  using the Fresnel equation for unpolarized light (Jerlov 1976):

$$\rho_L = \frac{1}{2} \left| \frac{\sin^2(\theta_v - \theta'_v)}{\sin^2(\theta_v + \theta'_v)} + \frac{\tan^2(\theta_v - \theta'_v)}{\tan^2(\theta_v + \theta'_v)} \right|. \quad (2.24)$$

$\theta'_v$  is the angle of refraction, which is related to  $\theta_v$  by Snell's law  $n_w \sin\theta'_v = \sin\theta_v$ , where  $n_w \approx 1.33$  is the refractive index of water. For viewing angles near nadir,  $\rho_L \approx 0.02$ .

The ratio of the radiance reflected from the water surface to the downwelling irradiance,

$$R_{rs}^{surf}(\lambda) = \frac{L_r(\lambda)}{E_d(\lambda)} = \rho_L \cdot \frac{L_s(\lambda)}{E_d(\lambda)}, \quad (2.25)$$

is called surface reflectance.  $E_d(\lambda)$  and  $L_s(\lambda)$  can either be imported from file, or one or both can be calculated using Eq. (2.40) or (2.59). If the wavelength-independent model of surface reflection is chosen, it is

$$R_{rs}^{surf} = \frac{\rho_L}{\pi}. \quad (2.26)$$

Toole et al. (2000) showed that  $R_{rs}^{surf}(\lambda)$  is nearly spectrally flat at overcast sky, but clearly not for clear-sky conditions. Thus, Eq. (2.25) should be used in general, and Eq. (2.26) at most for days with overcast sky.

## 2.5 Irradiance reflectance

The ratio of upwelling irradiance to downwelling irradiance in water,  $R(\lambda) = E_u^-(\lambda) / E_d^-(\lambda)$ , is called irradiance reflectance (Mobley 1994). It is an apparent optical property (AOP) and depends not only on the properties of the medium, but also on the geometric distribution of the incoming light.

### 2.5.1 Deep water

A suitable parameterization which separates to a large extent the parameters of water and of the illumination was found by Gordon et al. (1975):

$$R(\lambda) = f \cdot \omega_b(\lambda) + Q \cdot r_{rs,F}^-(\lambda). \quad (2.27)$$

$r_{rs,F}^-(\lambda)$  denotes the contribution caused by fluorescence; it is calculated using Eq. (2.66). The function  $\omega_b(\lambda)$ , which is given by Eq. (2.20), depends only on inherent optical properties of the water body, absorption and backscattering. The factor  $f$  comprises the illumination dependencies. It can be treated either as an independent parameter with a default value of 0.33 according to Gordon et al. (1975), or the relationship of Albert and Mobley (2003) can be used:

$$f = 0.1034 \cdot (1 + 3.3586 \cdot \omega_b - 6.5358 \cdot \omega_b^2 + 4.6638 \cdot \omega_b^3) \cdot \left(1 + \frac{2.4121}{\cos \theta'_{\text{sun}}}\right). \quad (2.28)$$

$\theta'_{\text{sun}}$  is the sun zenith angle in water. Eq. (2.28) takes into consideration the fact that  $f$  depends not only on the geometric structure of the light field, expressed by the parameter  $\theta'_{\text{sun}}$ , but also on the absorption and scattering properties of the water. Some alternate models of  $f$  are also included in WASI and can be used if desired, namely those of Kirk (1984), Morel and Gentili (1991), and Sathyendranath and Platt (1997). The equations are given in chapter 6.2.

Independently from Gordon, Prieur (1976) found the relation  $R(\lambda) = f \cdot b_b(\lambda) / a(\lambda)$ . It is also included in WASI. However, the Gordon algorithm (2.27) is favored and set as default, because it restricts the  $\omega_b$  values to the physically reasonable range from 0 to 1, which is not the case for the Prieur equation.

### 2.5.2 Shallow water

For shallow water, the parameterization of Albert and Mobley (2003) is used:

$$\begin{aligned} R^{sh}(\lambda) &= R(\lambda) \cdot [1 - A_1 \cdot \exp\{- (K_d(\lambda) + K_{uw}(\lambda)) \cdot z_B\}] \\ &\quad + A_2 \cdot R^b(\lambda) \cdot \exp\{- (K_d(\lambda) + K_{ub}(\lambda)) \cdot z_B\} \end{aligned} \quad (2.29)$$

The first term on the right-hand side is the reflectance of a water layer of thickness  $z_B$ , the second term the contribution of the bottom. Bottom reflectance  $R^b(\lambda)$  is calculated using Eq. (2.38). The  $K$ 's account for attenuation within the water layer and are calculated using Eqs. (2.17), (2.18) and (2.19). The empirical constants are  $A_1 = 1.0546$  and  $A_2 = 0.9755$  according to Albert and Mobley (2003) and cannot be changed by the user.

## 2.6 Radiance reflectance

The ratio of upwelling radiance to downwelling irradiance,  $r_{rs}(\lambda) = L_u(\lambda)/E_d(\lambda)$ , is called *radiance reflectance*. It is an apparent optical property (AOP), i.e. it depends on the geometric distribution of the incoming light and on the viewing angle.

### 2.6.1 Deep water

The radiance reflectance below the water surface is, for optically deep water, proportional to  $R(\lambda)$ :

$$r_{rs}^-(\lambda) = \frac{R(\lambda)}{Q}. \quad (2.30)$$

This follows from the definitions  $r_{rs}^- = L_u^-/E_d^-$ ,  $Q = E_u^-/L_u^-$  and  $R = E_u^-/E_d^-$ .  $R(\lambda)$  is either calculated using Eq. (2.27), or imported from file. The factor  $Q$ , which is a measure of the anisotropy of the light field in water, is treated here as a wavelength-independent parameter with a default value of 5 sr. It depends on the geometric distribution of the upwelling and downwelling light, and thus on the scattering and absorption properties of the water body. Consequently,  $Q$  depends on wavelength. This is here not accounted for since no convenient parameterization of  $Q$  is known. Yet, an alternative to Eq. (2.30) with a convenient parameterization of the factor  $f_{rs}$  was found by Albert and Mobley (2003):

$$r_{rs}^-(\lambda) = f_{rs} \cdot \omega_b(\lambda) + r_{rs,F}(\lambda). \quad (2.31)$$

$r_{rs,F}(\lambda)$  is the contribution caused by fluorescence and calculated using Eq. (2.66). Note that fluorescence is also included in Eq. (2.31) through  $R(\lambda)$  according to Eq. (2.27). The following parameterization of the factor  $f_{rs}$  is valid for both deep and shallow waters (Albert and Mobley 2003):

$$f_{rs}(\lambda) = 0.0512 \cdot (1 + 4.6659 \cdot \omega_b(\lambda) - 7.8387 \cdot \omega_b(\lambda)^2 + 5.4571 \cdot \omega_b(\lambda)^3) \cdot \left(1 + \frac{0.1098}{\cos \theta'_{sun}}\right) \cdot \left(1 + \frac{0.4021}{\cos \theta'_{v}}\right). \quad (2.32)$$

Parameters of  $f_{rs}$  are  $\omega_b$  of Eq. (2.20), the sun zenith angle in water,  $\theta'_{sun}$ , and the viewing angle in water,  $\theta'_{v}$ . The original equation has an additional term for wind speed. However, as its contribution is very low, it is neglected in WASI.  $f_{rs}$  can be calculated alternately as  $f_{rs} = f/Q$  using the ill-favored parameter  $Q$ .

### 2.6.2 Shallow water

For optically shallow water the following parameterization is chosen (Albert and Mobley 2003):

$$r_{rs}^{sh-}(\lambda) = r_{rs}^-(\lambda) \cdot [1 - A_{rs,1} \cdot \exp\{-(K_d(\lambda) + k_{uW}(\lambda)) \cdot z_B\}] + A_{rs,2} \cdot R_{rs}^b(\lambda) \cdot \exp\{-(K_d(\lambda) + k_{uB}(\lambda)) \cdot z_B\} \quad (2.33)$$

The first term on the right-hand side is the reflectance of a water layer of thickness  $z_B$ , the second term the contribution of the bottom. Bottom reflectance  $R_{rs}^b(\lambda)$  is calculated using Eq. (2.39).  $K_d$ ,  $k_{uW}$  and  $k_{uB}$  account for attenuation within the water layer and are calculated using Eqs. (2.17), (2.21) and (2.22), respectively. The empirical constants are set to  $A_{rs,1} = 1.1576$  and  $A_{rs,2} = 1.0389$  according to Albert and Mobley (2003) and cannot be changed by the user.

### 2.6.3 Above the surface

The radiance reflectance above the water surface is the sum of a contribution from the water,  $R_{rs}(\lambda)$ , and from the surface,  $R_{rs}^{surf}(\lambda)$ :

$$r_{rs}(\lambda) = R_{rs}(\lambda) + R_{rs}^{surf}(\lambda). \quad (2.34)$$

$R_{rs}(\lambda)$ , which is the ratio of the water leaving radiance  $L_w(\lambda)$  to the downwelling irradiance above the water surface  $E_d(\lambda)$ , is called *remote sensing reflectance*. The surface reflectance  $R_{rs}^{surf}(\lambda)$  can be calculated using Eq. (2.25) or Eq. (2.26).

Remote sensing reflectance is related to radiance and irradiance in water as follows:

$$R_{rs}(\lambda) = \frac{L_w(\lambda)}{E_d(\lambda)} = \frac{\frac{1 - \sigma_L^-}{n_w^2} \cdot L_u^-(\lambda)}{E_d(\lambda)} = \frac{(1 - \sigma_L^-)(1 - \sigma)}{n_w^2} \cdot \frac{L_u^-(\lambda)}{E_d^-(\lambda) - \rho_u \cdot E_u^-(\lambda)}$$

Eq. (2.62) was used to replace  $L_w(\lambda)$ , and Eq. (2.50) with  $f_{dd} = f_{ds} = 1$  and the approximation  $\sigma = (\rho_{ds} \approx \rho_{dd})$  to express  $E_d(\lambda)$  in terms of  $E_d^-(\lambda)$  and  $E_u^-(\lambda)$ . By using  $L_u^-(\lambda) = E_u^-(\lambda)/Q$ , multiplying numerator and denominator term with  $R(\lambda)/E_u^-(\lambda)$  (where  $R(\lambda) = E_u^-(\lambda)/E_d^-(\lambda)$ ), the following equation is obtained:

$$R_{rs}(\lambda) = \frac{(1 - \sigma)(1 - \sigma_L^-)}{n_w^2 \cdot Q} \cdot \frac{R(\lambda)}{1 - \rho_u \cdot R(\lambda)}. \quad (2.35)$$

Replacing  $R(\lambda)$  with  $r_{rs}^-(\lambda)$  according to Eq. (2.30) yields the following relationship:

$$R_{rs}(\lambda) = \frac{(1 - \sigma)(1 - \sigma_L^-)}{n_w^2} \cdot \frac{r_{rs}^-(\lambda)}{1 - \rho_u \cdot Q \cdot r_{rs}^-(\lambda)}. \quad (2.36)$$

This equation was used, for example, by Lee et al. (1998) for comparing simulated reflectance spectra above and below the surface and calculating the conversion factors, for which they found as typical values  $(1 - \sigma)(1 - \sigma_L^-)/n_w^2 = 0.518$  and  $\rho_u \cdot Q = 1.562$ . The factor  $Q$ , which is difficult to assess in practice, can be avoided by replacing in the denominator  $Q \cdot r_{rs}^-$  with  $R$ :

$$R_{rs}(\lambda) = \frac{(1 - \sigma)(1 - \sigma_L^-)}{n_w^2} \cdot \frac{r_{rs}^-(\lambda)}{1 - \rho_u \cdot R(\lambda)}. \quad (2.37)$$

The three equations (2.35), (2.36) and (2.37) are formally identical. The factors  $\sigma$ ,  $\sigma_L^-$  and  $\rho_u$  are the reflection factors for  $E_d$ ,  $L_u^-$  and  $E_u^-$ , respectively.  $\sigma$  depends on the radiance distribu-

tion and on surface waves. Typical values are 0.02 to 0.03 for clear sky conditions and solar zenith angles below 45°, and 0.05 to 0.07 for overcast skies (Jerlov 1976; Preisendorfer and Mobley 1985, 1986). It is set to  $\sigma = 0.03$  by default.  $\sigma_L^-$  can either be calculated as a function of  $\theta_v$  using Eq. (2.24), or a constant value can be taken.  $\rho_u$  is in the range of 0.50 to 0.57 with a value of 0.54 being typical (Jerome et al. 1990; Mobley 1999). The defaults of the other constants are set to  $Q = 5$  sr and  $n_w = 1.33$ .

Which of the equations is used depends on the application:

- Eq. (2.35) is useful when  $R_{rs}(\lambda)$  shall be connected to  $R(\lambda)$ , for example if in-situ measurements of  $R(\lambda)$  were performed as "ground truth" for a remote sensing instrument.
- Eq. (2.36) links remote sensing reflectance in water to that in air. Since the same spectrum type is used above and below the water surface, it is the most convenient parameterization. This equation is used by default.
- Eq. (2.37) avoids the use of the factor  $Q$ , which is difficult to assess. The equation is useful, for example, for optical closure experiments which investigate the consistency of measurements above and below the water surface by measuring simultaneously the spectra  $R_{rs}(\lambda)$ ,  $R(\lambda)$ , and  $r_{rs}^-(\lambda)$ .

Eq. (2.35), (2.36) or (2.37) is also used to calculate the corresponding spectrum  $R_{rs}^{sh}(\lambda)$  for shallow water.  $R(\lambda)$  is replaced by  $R^{sh}(\lambda)$ , and  $r_{rs}^-(\lambda)$  by  $r_{rs}^{sh-}(\lambda)$  in the case of optically shallow water.

## 2.7 Bottom reflectance

The models of bottom reflectance are used to calculate reflectance and radiance spectra in shallow waters. Furthermore, they can be applied as well to land surfaces, if the input spectra are replaced by suitable albedo spectra from terrestrial bottom types.

### 2.7.1 For irradiance sensors

The irradiance reflectance of a surface is called albedo. When  $N$  different surfaces of albedo  $a_n(\lambda)$  are viewed simultaneously, the measured albedo is the following sum:

$$R^b(\lambda) = \sum_{n=0}^{N-1} f_n \cdot a_n(\lambda). \quad (2.38)$$

$f_n$  is the areal fraction of surface number  $n$  within the sensor's field of view; it is  $\Sigma f_n = 1$ . This equation is implemented in WASI for  $N = 6$  bottom substrate types. The six spectra  $a_n(\lambda)$  provided with WASI are shown in Figure 2.5:

0. **Constant:** an artificial spectrum with constant albedo of 10 %.
1. **Sand:** coarse-grain sand from the sea floor of the Baltic Sea in the Wismar bay (Germany); measured in air (Schnalzger 2017).
2. **Silt:** fine-grained sediment from the sea floor of the Baltic Sea in the Wismar bay (Germany); measured in air (Schnalzger 2017).
3. **Sea grass:** sea grass *Zostera marina* from the Wismar bay in the Baltic Sea (Germany); measured in air (Schnalzger 2017).
4. **Mussel:** blue mussel *Mytilus edulis* (bright type) from Wismar bay in the Baltic Sea (Germany); measured in air (Schnalzger 2017).
5. **Macrophyte:** green macrophyte *Chara aspera* from Lake Constance (Germany); measured in water (Pinnel 2005).

*Note:* the spectral range of the measurements doesn't cover the maximum range of the simulations (350 to 1000 nm by default). To have valid numerical data from 350 to 1000 nm, the missing data at the lower and upper end of the spectral range were filled with the first and last measured value, respectively. These extrapolated data cannot be assumed to be correct.

Type and optical properties of the bottom substrate can differ significantly from one location to the next. The user can exchange the default spectra provided with WASI in the menu “Options – Models – Bottom”.

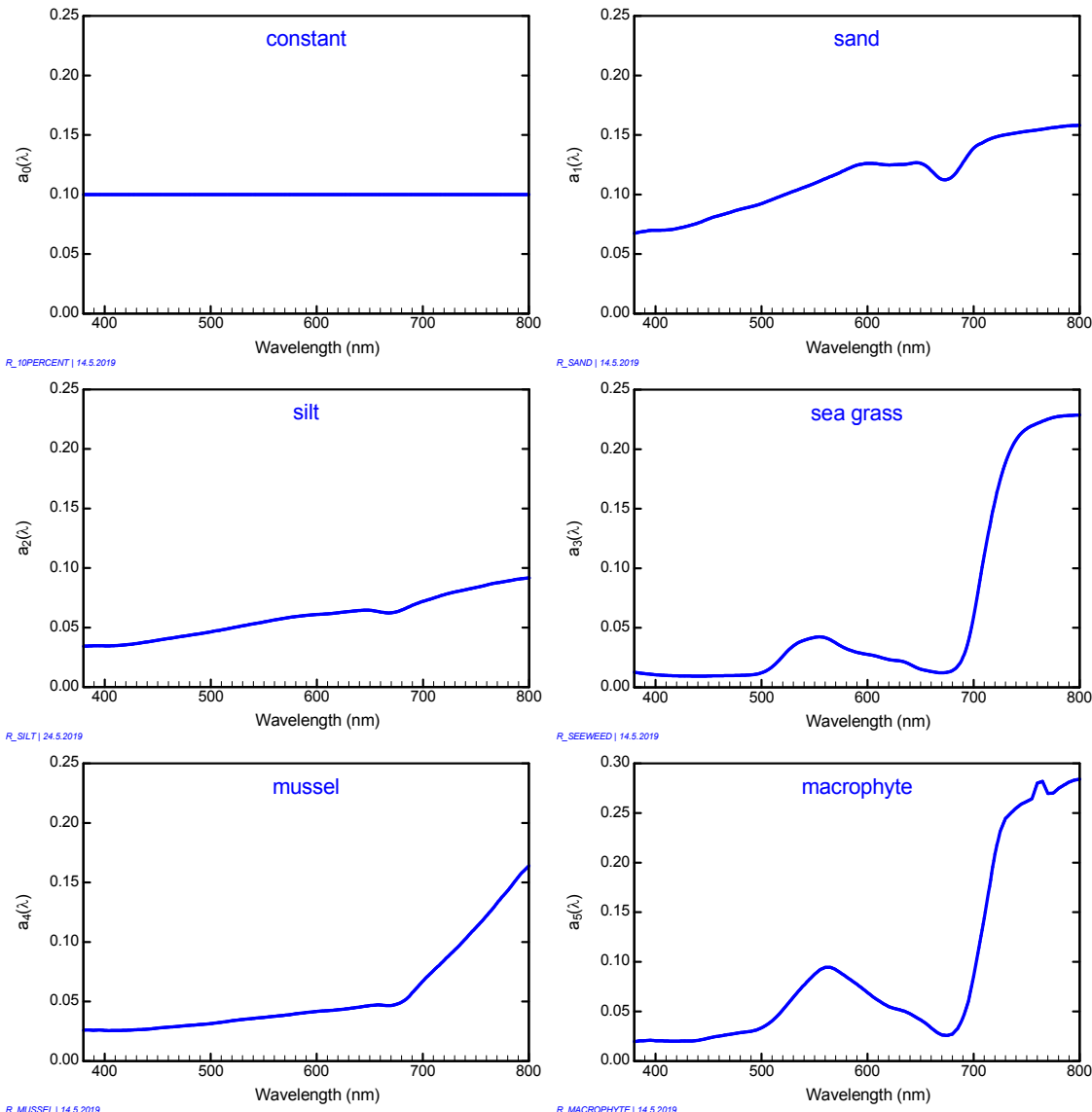


**Figure 2.5: Spectral albedo  $a_n(\lambda)$  (irradiance reflectance) of 6 bottom substrate types.**

### 2.7.2 For radiance sensors

When the upwelling radiation is measured by a radiance sensor, the corresponding radiance reflectance can be expressed as follows:

$$R_{rs}^b(\lambda) = \sum_{n=0}^{N-1} f_n \cdot B_n \cdot a_n(\lambda). \quad (2.39)$$

$B_n$  is the proportion of radiation which is reflected towards the sensor. In WASI, the  $B_n$ 's of all surfaces are assumed to be angle-independent. The default values are set to  $B_n = 1/\pi = 0.318 \text{ sr}^{-1}$ , which represents isotropic reflection (Lambertian surfaces).

## 2.8 Downwelling irradiance

### 2.8.1 Above the water surface

The downwelling irradiance spectrum,  $E_d(\lambda)$ , is split into a direct and a diffuse component:

$$E_d(\lambda) = f_{dd} \cdot E_{dd}(\lambda) + f_{ds} \cdot E_{ds}(\lambda). \quad (2.40)$$

$E_{dd}(\lambda)$  is the direct component of the downwelling irradiance, representing the sun disk in the sky as light source. The radiation from the sky, i.e. the diffuse downwelling irradiance, is split into two components:  $E_{ds}(\lambda) = E_{dsr}(\lambda) + E_{dsa}(\lambda)$ , with  $E_{dsr}(\lambda)$  representing Rayleigh scattering, and  $E_{dsa}(\lambda)$  aerosol scattering. The parameters  $f_i$  are the intensities of the "light sources"  $E_i$  relative to conditions with undisturbed illumination geometry. These reference conditions (with  $f_i = 1$ ) are defined by a cloudless atmosphere, unobscured view of the upper hemisphere, and an horizontally oriented sensor with an angular response equal to the cosine of the incidence angle.  $0 \leq f_i < 1$  corresponds to measurements when intensity is decreased (due to shadows, sensor tilt or deviations from the cosine response),  $f_i > 1$  when intensity is increased.

The calculation of  $E_i(\lambda)$  is based on equations and data of Gregg and Carder (1990), which these authors derived from Bird and Riordan (1986). The adopted equations are recalled briefly. Eq. (2.40) extends these models by adding weights  $f_i$  which allow simulation and analysis of measurements at non-standard conditions.

The three components of downwelling irradiance are calculated as follows:

$$E_{dd}(\lambda) = E_0(\lambda) \cos\theta_{\text{sun}} T_r(\lambda) T_{aa}(\lambda) T_{as}(\lambda) T_{oz}(\lambda) T_o(\lambda) T_{wv}(\lambda), \quad (2.41)$$

$$E_{dsr}(\lambda) = \frac{1}{2} E_0(\lambda) \cos \theta_{\text{sun}} (1 - T_r(\lambda)^{0.95}) T_{aa}(\lambda) T_{oz}(\lambda) T_o(\lambda) T_{wv}(\lambda), \quad (2.42)$$

$$E_{dsa}(\lambda) = E_0(\lambda) \cos \theta_{\text{sun}} T_r(\lambda)^{1.5} T_{aa}(\lambda) T_{oz}(\lambda) T_o(\lambda) T_{wv}(\lambda) (1 - T_{as}(\lambda)) F_a. \quad (2.43)$$

$E_0(\lambda)$  is the extraterrestrial solar irradiance corrected for earth-sun distance and orbital eccentricity,  $\theta_{\text{sun}}$  the solar zenith angle,  $F_a$  aerosol forward scattering probability, and the  $T_i$  denote transmittance of the atmosphere after scattering or absorption of component  $i$  ( $T_r$ : Rayleigh scattering,  $T_{aa}$ : aerosol absorption,  $T_{as}$ : aerosol scattering,  $T_{oz}$ : ozone absorption,  $T_o$ : oxygen absorption,  $T_{wv}$  water vapour absorption). The  $T_i$  are given by:

$$T_r(\lambda) = \exp[-M'/(115.6406\lambda^4 - 1.335\lambda^2)], \quad (2.44)$$

$$T_{aa}(\lambda) = \exp[-(1 - \omega_a)\tau_a(\lambda)M], \quad (2.45)$$

$$T_{as}(\lambda) = \exp[-\omega_a\tau_a(\lambda)M], \quad (2.46)$$

$$T_{oz}(\lambda) = \exp[-a_{oz}(\lambda)H_{oz}M_{oz}], \quad (2.47)$$

$$T_o(\lambda) = \exp \frac{-1.41a_o(\lambda) \cdot M'}{\left[1 + 118.3a_o(\lambda) \cdot M'\right]^{0.45}}, \quad (2.48)$$

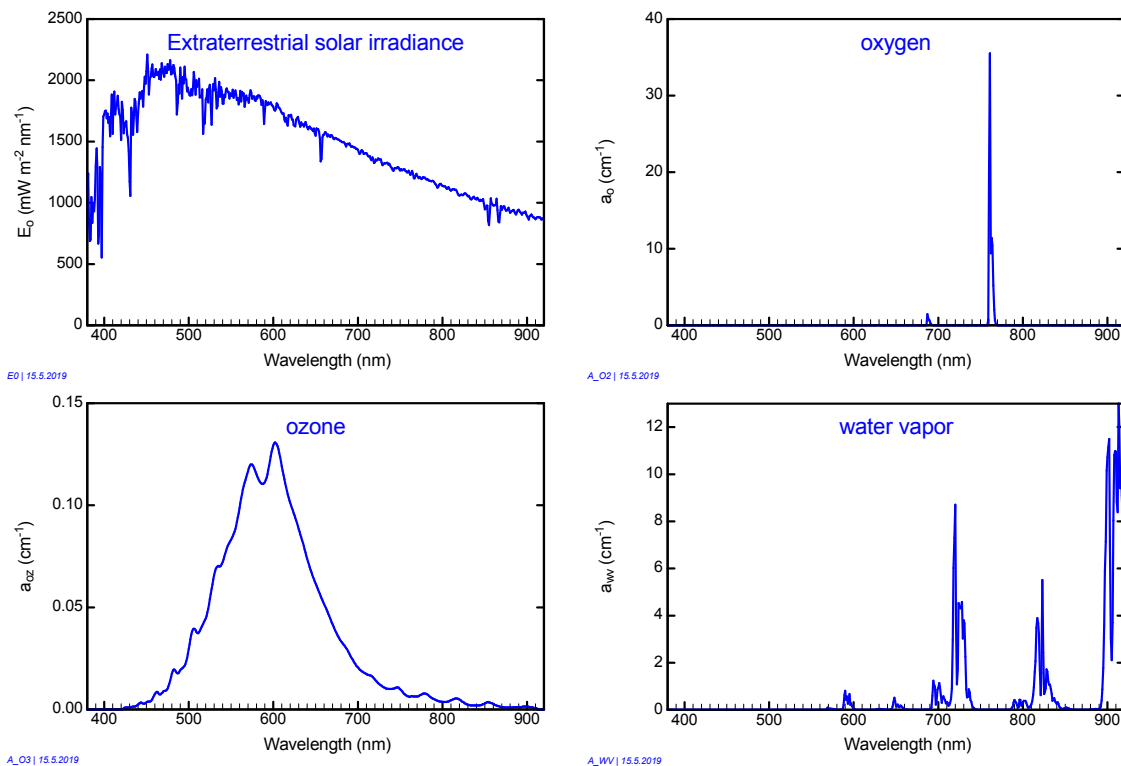


**Figure 2.6: The four input spectra of the irradiance model.**

$$T_{wv}(\lambda) = \exp \frac{-0.2385 a_{wv}(\lambda) \cdot WV \cdot M}{[1 + 20.07 a_{wv}(\lambda) \cdot WV \cdot M]^{0.45}}. \quad (2.49)$$

The atmospheric path length is  $M = 1/[\cos\theta_{\text{sun}} + a(90^\circ + b - \theta_{\text{sun}})^{-c}]$ . The numerical values used by Gregg and Carder ( $a = 0.15$ ,  $b = 3.885^\circ$ ,  $c = 1.253$ ) were replaced by updated values  $a = 0.50572$ ,  $b = 6.07995^\circ$ ,  $c = 1.6364$  from Kasten and Young (1989).  $M' = MP/(1013.25 \text{ mbar})$  is the path length corrected for nonstandard atmospheric pressure  $P$ , and  $M_{\text{o}_3} = 1.0035/(\cos^2\theta_{\text{sun}} + 0.007)^{1/2}$  is the path length for ozone.

Aerosol is parameterized in terms of aerosol optical thickness,  $\tau_a = \beta \cdot (\lambda/\lambda_a)^{-\alpha}$ , and aerosol single scattering albedo,  $\omega_a = (-0.0032AM + 0.972) \cdot \exp(3.06 \cdot 10^{-4}RH)$ . The Angström exponent  $\alpha$  determines the wavelength dependency, the turbidity coefficient  $\beta$  is a measure of concentration. The reference wavelength  $\lambda_a$  is set in WASI by default to 550 nm.<sup>4</sup>  $\alpha$  typically ranges from 0.2 to 2,  $\beta$  from 0.16 to 0.50.  $\beta$  is related to horizontal visibility  $V$  and aerosol scale height  $H_a$ :  $\beta = \tau_a(550) = 3.91 \cdot H_a/V$ . Typical values are 8 to 24 km for  $V$ , and 1 km for  $H_a$ . The parameters of  $\omega_a$  are air mass type,  $AM$ , which ranges from 1 (typical of open-ocean aerosols) to 10 (typical of continental aerosols), and relative humidity,  $RH$ , with typical values from 46 to 91 %. Aerosol forward scattering probability is calculated using the equation  $F_a = 1 - 0.5 \exp[(B_1 + B_2 \cos\theta_{\text{sun}}) \cdot \cos\theta_{\text{sun}}]$  with  $B_1 = B_3[1.459 + B_3(0.1595 + 0.4129B_3)]$ ,  $B_2 = B_3[0.0783 + B_3(-0.3824 - 0.5874B_3)]$ ,  $B_3 = \ln(1 - \langle \cos\theta_{\text{sun}} \rangle)$ , and  $\langle \cos\theta_{\text{sun}} \rangle = -0.1417\alpha + 0.82$ . Water vapor concentration,  $WV$ , is expressed in units of precipitable water, which typically ranges from 0 to 5 cm.

<sup>4</sup> Frequently  $\lambda_a = 1 \mu\text{m}$  is set, e.g. Gregg and Carder (1990).

The calculations make use of four spectra which are imported from file:  $E_0(\lambda)$ ,  $a_o(\lambda)$ ,  $a_{oz}(\lambda)$ , and  $a_{wy}(\lambda)$ . The spectra provided with WASI are shown in Figure 2.6. They were calculated using the radiative transfer model MODTRAN-3 (Gege 2012a).

## 2.8.2 Below the water surface

The downwelling irradiance just below the water surface (indicated by the symbol 0–) is calculated as follows:

$$E_d(\lambda, 0-) = f_{dd} \cdot (1 - \rho_{dd}) \cdot E_{dd}(\lambda) + f_{ds} \cdot (1 - \rho_{ds}) \cdot E_{ds}(\lambda) + \rho_u \cdot E_u(\lambda, 0-). \quad (2.50)$$

The factors  $f_{dd}$  and  $f_{ds}$  are much more variable in water than in air, because the wavy water surface induces strong focusing effects (Dera and Stramski 1993, Zanefeld et al. 2001).  $\rho_{dd}$  and  $\rho_{ds}$  describe the losses of downwelling irradiance at the air–water interface,  $E_u(\lambda, 0-)$  is the upwelling spectral irradiance in water, and  $\rho_u$  is the reflection factor of the water surface for  $E_u(\lambda, 0-)$ . The reflection factor for the direct downwelling component is calculated using the Fresnel equation (Jerlov 1976)

$$\rho_{dd} = \frac{1}{2} \left| \frac{\sin^2(\theta_{sun} - \theta'_{sun})}{\sin^2(\theta_{sun} + \theta'_{sun})} + \frac{\tan^2(\theta_{sun} - \theta'_{sun})}{\tan^2(\theta_{sun} + \theta'_{sun})} \right|; \quad (2.51)$$

that of the diffuse downwelling component using the empirical equation (Gege 2012a)

$$\rho_{ds} = 0.06087 + 0.03751 \cdot (1 - \cos\theta_{sun}) + 0.1143 \cdot (1 - \cos\theta_{sun})^2; \quad (2.52)$$

and that of the upwelling component is set to  $\rho_u = 0.54$  by default (Jerome et al. 1990, Mobley 1999). Using the irradiance reflectance  $R(\lambda) = E_u(\lambda, 0-) / E_d(\lambda, 0-)$  to remove  $E_u(\lambda, 0-)$  from Eq. (2.50) leads to the following expression:

$$E_d(\lambda, 0-) = f_{dd} \cdot (1 - \rho_{dd}) \cdot E_{dd}(\lambda) + f_{ds} \cdot (1 - \rho_{ds}) \cdot [1 + \rho_u \cdot R(\lambda) \cdot (1 + r_d(\lambda, 0-))] \cdot E_{ds}(\lambda). \quad (2.53)$$

$r_d(\lambda, 0-) = f_{dd}/f_{ds} \cdot E_{dd}(\lambda, 0-) / E_{ds}(\lambda, 0-)$  is the ratio of direct to diffuse irradiance just beneath the water surface. It is calculated using the equation (Gege 2012a)

$$r_d(\lambda, 0-) = \frac{f_{dd}}{f_{ds}} \cdot \frac{1 - \rho_{dd}}{1 - \rho_{ds}} \cdot \frac{2 \cdot T_r(\lambda) \cdot T_{as}(\lambda)}{1 - T_r(\lambda)^{0.95} + 2 \cdot T_r(\lambda)^{1.5} \cdot [1 - T_{as}(\lambda)] \cdot F_a}. \quad (2.54)$$

Equation (2.53) is used in WASI for calculating  $E_d(\lambda, 0-)$ .  $R(\lambda)$  is calculated using Eq. (2.27) without fluorescence, i.e.  $R_{rs,F}^-(\lambda) = 0$  is set. Downwelling irradiance below the surface in shallow water,  $E_d^{sh}(\lambda, 0-)$ , is also calculated using Eq. (2.53), but with  $R^{sh}(\lambda)$  instead of  $R(\lambda)$ .

## 2.8.3 At depth z

Since the path lengths are different for the direct and the diffuse component, their depth dependencies are calculated separately. The direct component is attenuated along a path with length  $z / \cos\theta'_{sun}$ :

$$E_{dd}(\lambda, z) = E_{dd}(\lambda, 0-) \exp \left\{ - \frac{[a(\lambda) + b_b(\lambda)] \cdot z \cdot l_{dd}}{\cos \theta'_{sun}} \right\}. \quad (2.55)$$

$l_{dd}$  is the path length of direct radiation relative to sensor depth; it is set equal to one by default. The diffuse component of downwelling irradiance at depth  $z$  is related to that below the surface as follows:

$$E_{ds}(\lambda, z) = E_{ds}(\lambda, 0-) \exp \{ -[a(\lambda) + b_b(\lambda)] \cdot z \cdot l_{ds} \}. \quad (2.56)$$

The average path length of diffuse radiation relative to sensor depth,  $l_{ds}$ , is calculated using the following approximation:

$$l_{ds} = 1.1156 + 0.5504 \cdot (1 - \cos \theta'_{sun}). \quad (2.57)$$

The downwelling irradiance at depth  $z$  is the following sum:

$$E_d(\lambda, z) = f_{dd} \cdot E_{dd}(\lambda, z) + f_{ds} \cdot [1 + \rho_u \cdot R(\lambda) \cdot (1 + r_d(\lambda, 0-))] \cdot E_{ds}(\lambda, z). \quad (2.58)$$

Equations (2.53) to (2.56) were validated using Hydrolight simulations (Gege 2012a); however, the upwelling radiation reflected at the water surface in downward direction was neglected in that paper (corresponding to  $\rho_u = 0$ ).

## 2.9 Sky radiance

A parameterization similar to  $E_d(\lambda)$  is implemented for the sky radiance,  $L_s(\lambda)$ :

$$L_s(\lambda) = g_{dd} \cdot E_{dd}(\lambda) + g_{dsr} \cdot E_{dsr}(\lambda) + g_{dsa} \cdot E_{dsa}(\lambda). \quad (2.59)$$

The radiance downwelling from a part of the sky is treated as a weighted sum of three wavelength dependent functions,  $E_{dd}(\lambda)$ ,  $E_{dsr}(\lambda)$  and  $E_{dsa}(\lambda)$ , which are given by Eqs. (2.41) to (2.43). In contrast to Eq. (2.40), the two diffuse components are treated separately since Rayleigh scattering has a much stronger angle dependency than aerosol scattering. The parameters  $g_{dd}$ ,  $g_{dsr}$  and  $g_{dsa}$  are the intensities (in units of  $\text{sr}^{-1}$ ) of  $E_{dd}(\lambda)$ ,  $E_{dsr}(\lambda)$  and  $E_{dsa}(\lambda)$ , respectively. The radiance  $\rho_L \cdot g_{dd} \cdot E_{dd}(\lambda)$  that is reflected at the water surface into a radiance sensor is known as sun glint, and the radiance  $\rho_L \cdot [g_{dsr} \cdot E_{dsr}(\lambda) + g_{dsa} \cdot E_{dsa}(\lambda)]$  as sky glint.

Note that  $L_s(\lambda)$  doesn't represent the radiance of a "piece of sky" at the coordinates  $(\theta_v, \phi_v)$ , as the term "sky radiance" may indicate. The functions  $E_{dd}(\lambda)$ ,  $E_{dsr}(\lambda)$  and  $E_{dsa}(\lambda)$  have been developed to parameterize the downwelling *irradiance*, but not *radiance*. Hence they are only functions of the sun zenith angle, but not of the sun azimuth angle or the viewing angles  $\theta_v, \phi_v$ . The purpose of  $L_s(\lambda)$  in WASI is modeling of upwelling radiance that originates from the upper hemisphere and is reflected at the water surface [ $\rho_L \cdot L_s(\lambda)$  in Eq. (2.61)]. Since the water surface is almost never perfectly flat, this radiance originates from different locations of the sky, thus a parameterization of  $L_s(\lambda)$  in terms of  $(\theta_v, \phi_v)$  is not considered useful.

$g_{dd}$ ,  $g_{dsr}$  and  $g_{dsa}$  can be used as fit parameters to correct reflections at the water surface. For forward modeling, the user has to specify a value for each parameter. The defaults are  $g_{dd} = 0.02$ ,  $g_{dsr} = g_{dsa} = 1/\pi = 0.32$ .

## 2.10 Upwelling radiance

The upwelling radiance is that part of the downwelling irradiance which is reflected back from the water into a down-looking radiance sensor. Calculation is based on a model of  $R_s$  and a model or a measurement of  $E_d$ .

### 2.10.1 Below the water surface

In water, Eq. (2.50) is used for calculating  $E_d^-(\lambda)$  and Eq. (2.30) or Eq. (2.31) for  $r_{rs}^-(\lambda)$ . The upwelling radiance is then calculated as follows:

$$L_u^-(\lambda) = r_{rs}^-(\lambda) \cdot E_d^-(\lambda) + L_F(\lambda). \quad (2.60)$$

$L_F(\lambda)$  denotes fluorescence radiance; it is calculated using Eq. (2.73). In shallow waters  $r_{rs}^{sh-}(\lambda)$  is used instead of  $r_{rs}^-(\lambda)$ , and  $E_d^{sh-}(\lambda)$  instead of  $E_d^-(\lambda)$ .

### 2.10.2 Above the water surface

The radiance upwelling from water is the sum of the water leaving radiance,  $L_w(\lambda)$ , and of radiance from the surface,  $L_{surf}(\lambda)$ :

$$L_u(\lambda) = L_w(\lambda) + L_{surf}(\lambda). \quad (2.61)$$

The water leaving radiance is related to the upwelling radiance in water,  $L_u^-$ , as follows:

$$L_w(\lambda) = \frac{1 - \sigma_L^-(\theta'_v)}{n_w^2} \cdot L_u^-(\lambda). \quad (2.62)$$

$\theta'_v$  is the zenith angle of the observer in water. The radiance upwelling in the water is weakened at the water-air boundary by two effects: specular reflection (factor  $1 - \sigma_L^-$ ) and refraction (flux dilution by widening of the solid angle, factor  $1/n_w^2$ ).

$L_u^-(\lambda)$  is calculated using Eq. (2.60). The reflection factor for upwelling radiance is set to  $\sigma_L^- = 0.02$  by default. This value, which is valid for a nadir-looking sensor, can be changed in the WASI5.INI file.

The radiance from the surface originates from specular reflection of downwelling radiance ( $L_d$ ) in viewing direction ( $\theta_v$ ). For a perfectly plane water surface the reflected light comes from the direction  $-\theta_v$ :

$$L_{surf}(\lambda, \theta_v) = \sigma(\theta_v) \cdot L_d(\lambda, -\theta_v). \quad (2.63)$$

The reflection factor  $\sigma(\theta_v)$  is given by the Fresnel equation (2.24). The viewing zenith angles in air,  $\theta_v$ , and water,  $\theta'_v$ , are related through Snell's law  $n_w \cdot \sin \theta'_v = \sin \theta_v$  with  $n_w$  the refractive index of water. If the water surface is wavy, the more general model of Eq. (2.23) is used:

$$L_{surf}(\lambda) = \rho_L \cdot L_s(\lambda). \quad (2.64)$$

The symbol  $\theta_v$  is omitted for simplicity. WASI uses this equation by default for calculating  $L_{surf}(\lambda)$  in Eq. (2.61). The sky radiance  $L_s(\lambda)$  can either be calculated using Eq. (2.59), or a measured spectrum can be imported from file. The reflection factor for downwelling radiance,  $\rho_L$ , can either be calculated using the Fresnel equation (2.24), or it can be set constant. The default  $\rho_L = 0.02$  is valid for a nadir-looking sensor. By setting  $\rho_L = 0$  the water leaving radiance can be calculated. Further,  $n_w = 1.33$  is set as default.

## 2.11 Fluorescence

Fluorescence is an inelastic process where a fraction  $\eta_F$  of photons incident at wavelength  $\lambda'$  is emitted at longer wavelengths  $\lambda$ . The ratio  $\eta_F(\lambda, \lambda') = N/N'$  is called fluorescence quantum yield, where  $N$  and  $N'$  denote the number of photons at wavelength intervals  $[\lambda, \lambda+d\lambda]$  and  $[\lambda', \lambda'+d\lambda']$ , respectively (Gordon 1979). The subscript "F" is used to indicate fluorescence, and the prime superscript to denote quantities which are functions of excitation wavelengths.

When fluorescence is expressed in terms of radiation quantities, care must be taken whether radiation is expressed in units of photon numbers or energy. Conversion makes use of the equation  $E = hc/\lambda$  for the energy of a single photon:  $N$  photons with a wavelength of  $\lambda$  have the energy  $E = N hc/\lambda$  and  $N'$  photons with  $\lambda'$  have  $E' = N' hc/\lambda'$ , hence  $E/E' = N/N' \cdot \lambda'/\lambda$ . Consequently, the ratio of radiation parameters in energy units is equal to that ratio in photon number units times the factor  $\lambda'/\lambda$ . In particular, if incident and emitted photon fluxes  $F$  and  $F'$  are expressed in units of  $\text{W m}^{-3}$ , the fluorescence quantum yield is given by

$$\eta_F(\lambda, \lambda') = \frac{N}{N'} = \frac{F}{F'} \cdot \frac{\lambda}{\lambda'}. \quad (2.65)$$

Fluorescence is calculated in WASI in terms of upwelling spectral radiance  $L_F(\lambda)$  (in units of  $\text{W m}^{-2} \text{ nm}^{-1} \text{ sr}^{-1}$ ) as described below. It is the additive term in Eq. (2.60) to the radiance caused by reflection. The fluorescence component of radiance reflectance is obtained by dividing  $L_F(\lambda)$  by  $E_d(\lambda)$ :

$$r_{rs,F}(\lambda) = \frac{L_F(\lambda)}{E_d(\lambda)}. \quad (2.66)$$

$E_d(\lambda)$  is calculated using Eq. (2.58). Eq. (2.66) is used in Eq. (2.31).

### 2.11.1 Phytoplankton

Phytoplankton shows a characteristic fluorescence peak at 685 nm with a full width at half maximum (FWHM) of 25 nm. It originates almost completely (~95%, Owens 1991) from photosystem II (PS-II). Phytoplankton can use approximately the spectral range from 400 to 700 nm for photosynthesis. This photosynthetic active radiation (PAR) is absorbed within the phytoplankton cells by light harvesting antenna. The excited electrons of the antenna pigments are transferred to PS-II, where water molecules are splitted and oxygen is formed (Abbott and Letelier 1999). The energy wasted here causes the 685 nm fluorescence peak. Consequently, since it is irrelevant which pigment had absorbed the incident photon, chlorophyll-a fluorescence quantum yield  $\eta_{chl}(\lambda)$  is largely independent of  $\lambda'$ . A comprehensive overview of the photosynthesis processes is given by Babin et al. (1996).

The flux absorbed by the phytoplankton in depth  $z$  is given by:

$$F'(z) = \int_{PAR} \sum_{i=0}^5 C_i \cdot a_i *(\lambda') \cdot E_0(\lambda', z) d\lambda', \quad (2.67)$$

where  $C_i$  denotes concentration of phytoplankton class number  $i$ ,  $a_i^*(\lambda')$  the specific absorption coefficient of that class, and  $E_0(\lambda', z)$  the scalar irradiance. Since irradiance at depth  $z$  is related to irradiance at the water surface by the Lambert-Beer law,

$$E_0(\lambda', z) = E_0(\lambda', 0) \cdot \exp[-K(\lambda') \cdot z], \quad (2.68)$$

with  $K(\lambda')$  the attenuation coefficient of scalar irradiance,  $F'(z)$  can be expressed as follows:

$$F'(z) = \int_{PAR} \sum_{i=0}^5 C_i \cdot a_i^*(\lambda') \cdot E_0(\lambda', 0) \cdot \exp[-K(\lambda') \cdot z] d\lambda'. \quad (2.69)$$

The flux (in units of  $\text{W m}^{-3}$ ) emitted by a layer at depth  $z$  at wavelength  $\lambda$  is:

$$F(\lambda, z) = \eta_{chl}(\lambda) \cdot F'(z) \cdot \frac{\lambda'}{\lambda}, \quad (2.70)$$

see Eq. (2.65).  $\eta_{chl}(\lambda)$  can be described quite accurately by a Gaussian function:

$$\eta_{chl}(\lambda) = \frac{\eta_{chl}(\lambda_F)}{(2\pi\sigma_F^2)^{1/2}} \exp\left[-\frac{(\lambda - \lambda_F)^2}{2\sigma_F^2}\right]. \quad (2.71)$$

Since fluorescence is in good approximation isotropic, the radiance (in units of  $\text{W m}^{-2} \text{ sr}^{-1}$ ) emitted by a layer of thickness  $dz$  is given by:

$$dL_F(\lambda, z) = \frac{1}{4\pi} F(\lambda, z) dz. \quad (2.72)$$

For a downward looking sensor in depth  $z$ , the fluorescence radiance is the sum of contributions from layers at depths  $z' > z$  down to the bottom (depth  $z_B$ ), weighted by the transmission of the water column between sensor and each layer. The transmission is obtained from the Lambert-Beer law using the attenuation coefficient for upwelling radiance,  $k_u$ . Hence,

$$\begin{aligned} L_F(\lambda, z) &= \int_z^{z_B} dL_F(\lambda, z') \cdot \exp[-k_u(\lambda) \cdot (z' - z)] dz' = \\ &= \frac{1}{4\pi} \int_z^{z_B} \eta_{chl}(\lambda) \cdot \frac{\lambda'}{\lambda} \cdot F'(z') \cdot \exp[-k_u(\lambda) \cdot (z' - z)] dz' = \\ &= \frac{1}{4\pi} \int_z^{z_B} \int_{PAR} \sum_{i=0}^5 C_i \cdot a_i^*(\lambda') \cdot \eta_{chl}(\lambda) \cdot \frac{\lambda'}{\lambda} \cdot E_0(\lambda', 0) \cdot \exp[-(K(\lambda') + k_u(\lambda)) \cdot z'] \cdot \exp[k_u(\lambda) \cdot z] dz' d\lambda'. \end{aligned}$$

Solving the integral over depth leads to:

$$L_F(\lambda, z) = \frac{\eta_{chl}(\lambda)}{4\pi\lambda} \int_{PAR} \sum_{i=0}^5 C_i \cdot a_i^*(\lambda') \left[ e^{-K(\lambda') \cdot z} - e^{-K(\lambda') \cdot z_B - k_u(\lambda) \cdot (z_B - z)} \right] \frac{E_0(\lambda', 0)}{K(\lambda') + k_u(\lambda)} \lambda' d\lambda'. \quad (2.73)$$

Similar equations are used by Maritorena et al. (2000) and Huot et al. (2005) for optically deep water ( $z_B = \infty$ ). Note that the factor  $\lambda'/\lambda$  is missing in their equations since they use photon number units ( $\text{mol m}^{-3} \text{ s}^{-1}$  for fluxes,  $\text{mol m}^{-2} \text{ s}^{-1} \text{ sr}^{-1} \text{ nm}^{-1}$  for spectral radiances).

$E_0(\lambda', 0)$  is calculated from the downwelling vector irradiance using the approximation

$$E_0(\lambda', 0) = f_{E0} \cdot E_d(\lambda', 0-) \quad (2.74)$$

with  $f_{E0} = 1.30$  (Maritorena et al. 2000) and  $E_d(\lambda', 0-)$  from Eq. (2.50).  $K(\lambda')$  is approximated by  $K_d(\lambda')$  using Eq. (2.17), and  $k_u(\lambda)$  is calculated using Eq. (2.21).

The chlorophyll-a fluorescence quantum yield,  $\eta_{chl}(\lambda_F)$ , can be treated as fit parameter in WASI with a default value of 0.01 (Gilerson et al. 2007). The parameters of the Gaussian shaped fluorescence peak are set by default to  $\lambda_F = 685$  nm and  $\sigma_F = 10.6$  nm, which corresponds to a FWHM of 25 nm. The wavelength range of PAR is set to 400–700 nm.

## 2.12 Mixed pixel

If a downward looking above-water sensor has not only water in its field of view, but a reflecting object is covering a part of the observed area, the measured reflectance is the sum of both reflectances, weighted with the areal fractions:

$$r_{rs}^m(\lambda) = (1 - f_{nw}) \cdot r_{rs}(\lambda) + f_{nw} \cdot \frac{a^{nw}(\lambda)}{\pi}. \quad (2.75)$$

The superscript 'm' of  $r_{rs}^m$  indicates a mixed pixel measurement.  $a^{nw}(\lambda)$  is the object's albedo (irradiance reflectance) and  $f_{nw}$  its areal fraction; the index 'nw' stands for 'non-water'. The object's angular reflection is assumed isotropic, thus a factor  $\pi$  is used to convert albedo to remote sensing reflectance.  $r_{rs}(\lambda)$  is calculated using Eq. (2.34). Examples of such objects are whitecaps or objects floating on the water surface; macrophytes or other natural or artificial underwater structures penetrating the surface; and measurements at the shoreline covering partly the land and partly the water.

The upwelling radiance of a mixed pixel,  $L_u^m(\lambda)$ , is calculated as follows:

$$L_u^m(\lambda) = (1 - f_{nw}) \cdot L_u(\lambda) + f_{nw} \cdot E_d(\lambda) \cdot \frac{a^{nw}(\lambda)}{\pi}. \quad (2.76)$$

$L_u(\lambda)$  is calculated using Eq.(2.61), and  $E_d(\lambda)$  using Eq. (2.40) with  $f_{dd} = f_{ds} = 1$ .

The default setting of WASI is  $f_{nw} = 0$ , i.e. contamination of the measurement by non-water targets is excluded. The user can however specify a spectrum  $a^{nw}(\lambda)$  and then simulate or analyze mixed pixel measurements. Using  $f_{nw}$  as fit parameter allows spectral unmixing of water and the non-water object.

## 2.13 Depth of light penetration

The light penetration depth  $z_{Ed}$  is defined as the depth where the incident irradiance has decreased to a specified percentage  $p_{Ed}$ . It is a measure of water clarity. Calculation makes use of the approximation  $E_d(z) = E_d(0) \exp\{-K_d z\}$ . Solving it for a given fraction  $p_{Ed} = E_d(z) / E_d(0)$  leads to:

$$z_{Ed}(\lambda) = -\frac{\ln p_{Ed}}{K_d(\lambda)}. \quad (2.77)$$

$K_d(\lambda)$  is calculated using Eq. (2.17).  $p_{Ed}$  is set by default to 1 % since the average of  $z_{Ed}(\lambda)$  over the photosynthetic active radiation (PAR) range 400 to 700 nm then yields the euphotic zone depth,  $z_{1\%}$ , which is not only a quality index of an ecosystem but also an important property for primary production and heat transfer in the upper water column (Lee et al. 2007).  $z_{Ed}(\lambda)$  and its average over the PAR range can be visualized after  $K_d(\lambda)$  has been calculated.<sup>5</sup>

---

<sup>5</sup> Select in the menu bar “Display –  $p_{Ed}$  depth”.  $p_{Ed}$  can be changed in “Options – Models – Irradiance”.

### 3. Forward mode

The forward mode allows calculating a single spectrum or a series of spectra according to user-specified parameter settings. The supported spectrum types are listed in Table 1.1.

#### 3.1 Graphical user interface

Figure 3.1 shows the graphical user interface (GUI) of WASI 5 at the example of the spectrum type "Radiance reflectance".

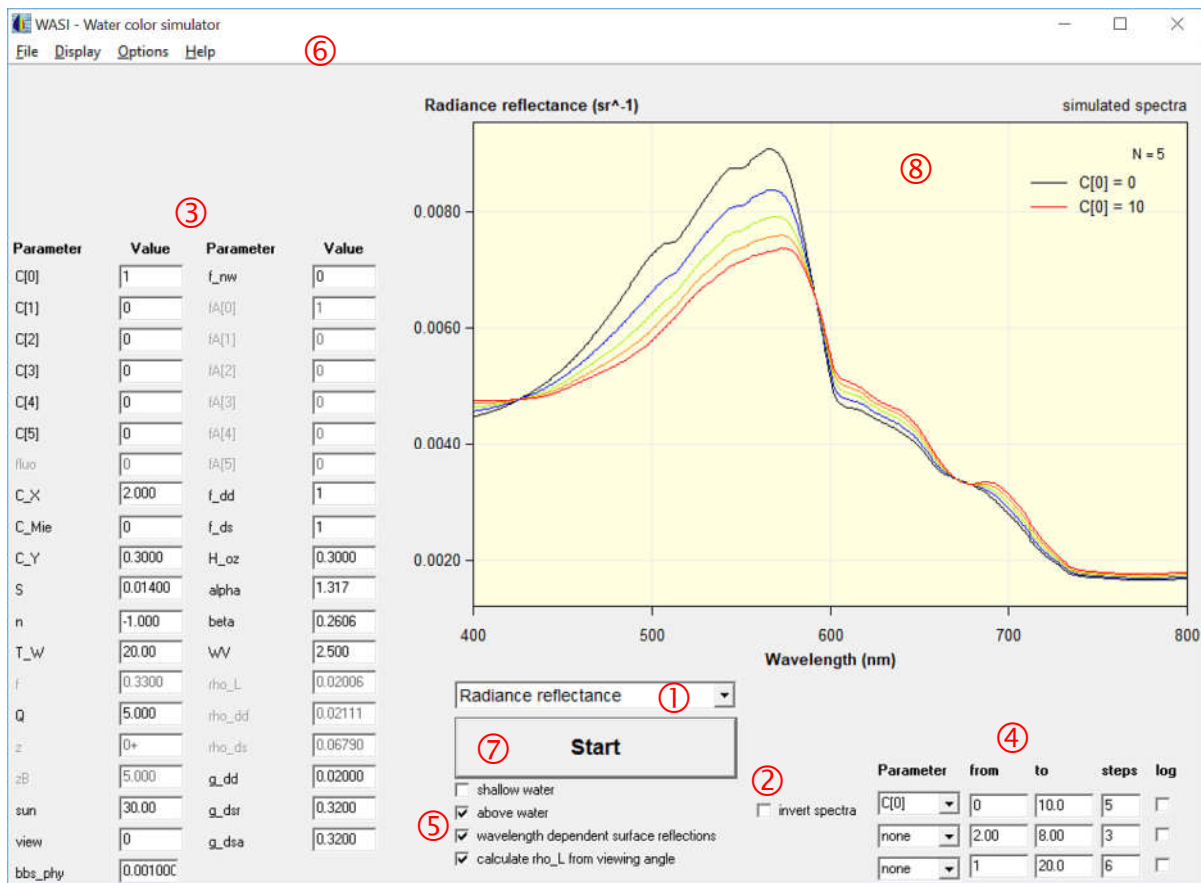
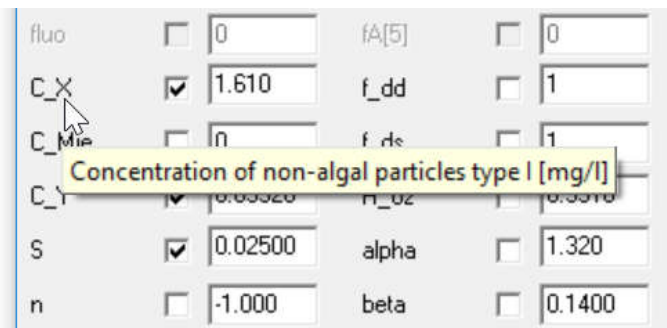


Figure 3.1: Graphical user interface of the forward mode. 1 = Drop-down list for selecting the spectrum type, 2 = Check box for switching between forward and inverse mode, 3 = Parameter list, 4 = Selection panel for specifying the parameter iterations, 5 = Check boxes for selecting model options (model specific), 6 = Menu bar, 7 = Start button, 8 = Plot window.

The GUI consists of 8 elements:

- (1) Drop-down list for selecting the spectrum type. The user selects one of the spectrum types from Table 1.1. If the spectrum type is changed, the parameter list (3) is updated such that only the relevant parameters are activated. Also the model options (5) are updated.
- (2) Check box for switching between forward and inverse mode. In the forward mode, this box is not checked.



**Figure 3.2: Explanation of the parameter under the mouse pointer.**

- (3) Parameter list. This list tabulates the parameters which are relevant for the selected spectrum type. It displays the parameters' symbols (in WASI notation, see Appendix 3) and their actual values. Default values are read from the `WASI5.INT` file, actual values are set by the user by editing the corresponding "Value" fields. Depending on the model options, not all parameters may be relevant. Irrelevant parameters are disabled, i.e. the corresponding symbol and value is displayed in gray color, and the value cannot be edited. A brief explanation of a parameter is shown for a few seconds after moving the mouse over the parameter name (Figure 3.2).
- (4) Selection panel for specifying the iterations. Up to 3 parameters can be iterated simultaneously during one run, thus the panel has 3 rows, one for each parameter. The iterated parameters are selected in the "Parameter" drop-down lists, their minimum and maximum values in the "from" and "to" fields, and their numbers of values in the "steps" fields. The "log" check boxes specify whether the intervals are equidistant on a linear scale (no hook) or on a logarithmic scale (hook).
- (5) Check boxes for selecting model options. Several spectrum types support options which further specify the model, cf. Table 1.1. Each option is either switched on or off.
- (6) Menu bar. Further details concerning the model, data storage and visualization can be specified in various pop-up windows, which are accessed via the menu bar.
- (7) Start button. Calculation is started by pressing this button.
- (8) Plot window. Each spectrum is plotted in this window after calculation. All curves are plotted together in order to visualize the spectral changes for the chosen iterations. A counter in the upper right corner is updated after each plot.

## 3.2 Calculation of a single spectrum

### 3.2.1 Mode selection

For calculating a single spectrum in the forward mode, the following settings must be made:

- Set forward mode: uncheck the "invert spectra" box (② in Figure 3.1);
- No parameter iteration: select "none" in each "parameter" drop-down list (④ in Figure 3.1).

### 3.2.2 Spectrum type selection

WASI allows calculating 8 different types of spectra, see Table 1.1. The desired type is selected in the main window from the drop-down list ① of Figure 3.1.

Several types of spectra support further options, see Table 1.1. If that is the case for the selected type, the options are displayed at the bottom of the main window (⑤ in Figure 3.1). Each option is either switched on or off. The selection is done by checking the corresponding check box. In the example of Figure 3.1 four options are available:

- (1) Shallow water. Since the check box is not marked, radiance reflectance will be calculated for optically deep water; when the hook is set, the calculation will be made for optically shallow water.
- (2) Above water. Since the check box is marked, the radiance reflectance will be calculated for a sensor above the water surface; when the hook is removed, calculation is performed for below the surface.
- (3) Wavelength dependent surface reflections. Since the check box is marked, the wavelength dependent model of Eq. (2.25) will be used to calculate surface reflections. Otherwise the reflections are treated as constant by applying Eq. (2.26).
- (4) Calculate rho\_L from viewing angle. Since the check box is marked, the reflectance factor for sky radiance,  $\rho_L$ , will be calculated using Eq. (2.24). Otherwise,  $\rho_L$  is treated as a parameter that can be defined by the user.

### 3.2.3 Parameter selection

All model parameters are read during program start from the WASI5.INI file. The most relevant parameters are listed at the left side of the main window (③ in Figure 3.1). This list can be edited for the parameters of the actual spectrum type.

### 3.2.4 Calculation options

Several calculation settings are made in the pop-up window "Forward calculation settings" which is shown in Figure 3.3. This pop-up window is accessed from the menu bar via "Options - Forward calculation" (see Figure 10.1)

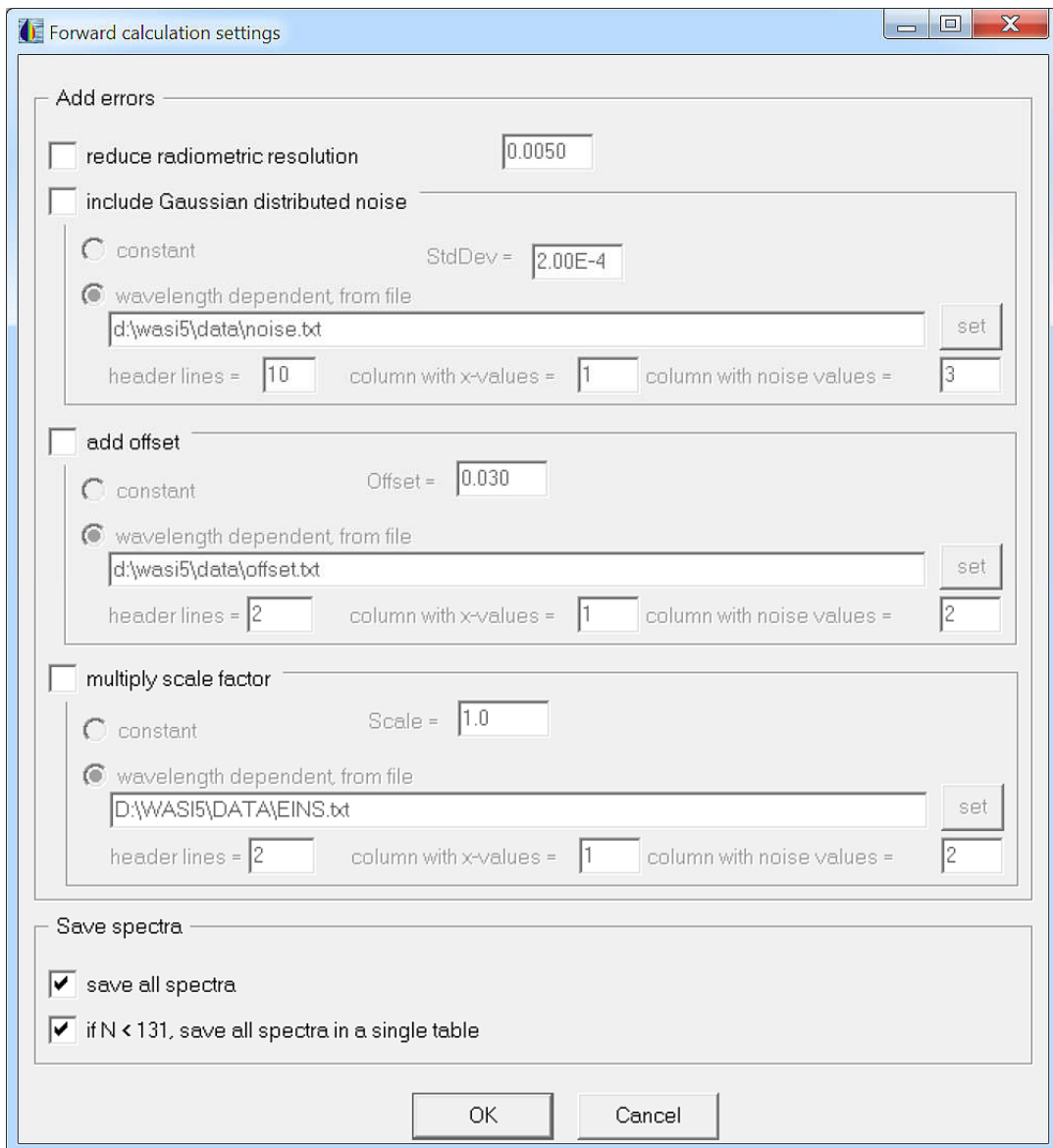


Figure 3.3: The pop-up window "Forward calculation settings".

**Add errors.** Four types of measurement errors can be simulated:

- *Low radiometric resolution.* If the check box "reduce radiometric resolution" is marked with a hook, the numerical accuracy is limited to the value shown in the corresponding input field. For example, 0.005 rounds original real numbers such that values of 0.000, 0.005, 0.010, 0.015, etc. result. If "reduce radiometric resolution" is not selected, the corresponding input field is not enabled.
- *Noise.* If the check box "include Gaussian distributed noise" is marked with a hook, Gaussian distributed noise is added to each calculated value. Its standard deviation can be chosen constant or wavelength dependent. A constant value is specified in the input field "StdDev", a spectrally dependent noise pattern is imported from the specified file.
- *Offset.* If the check box "add offset" is marked, an offset is added to each calculated value. It can be either chosen constant or wavelength dependent. A constant value is specified in the input field "Offset", a spectrally dependent offset is imported from the specified file.
- *Scale.* If the check box "multiply scale factor" is marked, each calculated value is multiplied with a scaling factor. It can be either chosen constant or wavelength dependent. A constant value is specified in the input field "Scale", a spectrally dependent scale is imported from the specified file.

**Save spectra.** Automatic saving of calculated spectra is activated by checking the box "save all spectra". The directory is selected in the "Directories" window, see section 8.2 (Figure 10.4). The calculated spectrum is stored in ASCII format as file `B1.FWD`. Note: If a file with the name `B1.FWD` already exists, it will be overwritten without warning. Two additional files are created automatically in the same directory as the spectrum. First, a copy of the initialization file `WASI5.INI` containing the actual parameter settings. It documents the data and parameters used for calculation. Second, a file `CHANGES.TXT`, which can be ignored; it is relevant only if a series of spectra is calculated. The check box "if N < 131, save all spectra in a single table" is not relevant for calculating a single spectrum.

### 3.2.5 Start calculation

Calculation is started by pressing the "Start" button (⑦ in Figure 3.1).

After calculation, the resulting curve is plotted in the main window (⑧ in Figure 3.1) and stored automatically, if spectra saving is activated in the pop-up window "Forward calculation settings" (Figure 3.3).

### 3.2.6 Example

An example of a spectrum calculated in the forward mode is shown in Figure 3.4. The spectrum type is irradiance reflectance in shallow water. The values of the model parameters are listed in the parameter list at the left-hand side: phytoplankton concentration  $C[0] = 2 \mu\text{g/l}$ ;

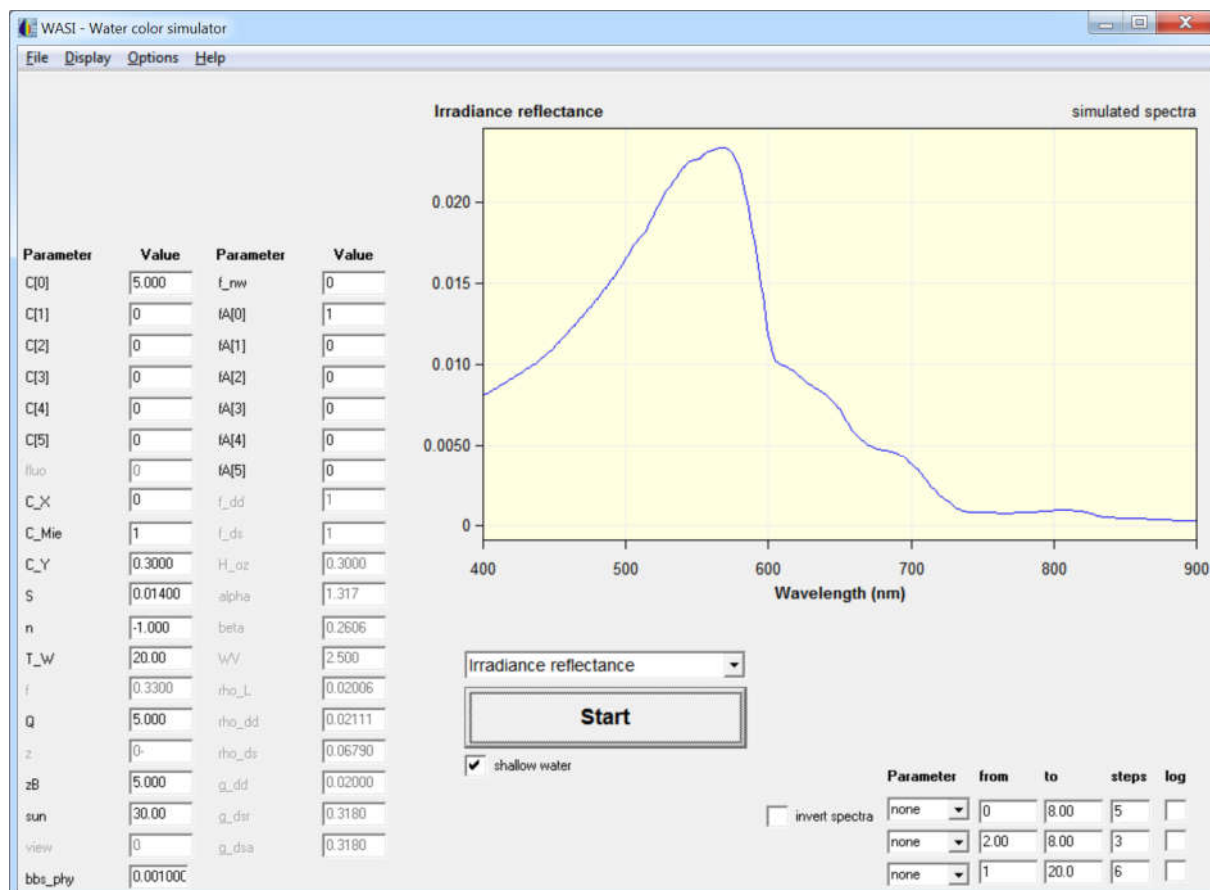


Figure 3.4: A single irradiance reflectance spectrum calculated in the forward mode.

phytoplankton fluorescence quantum yield  $fluo = 0.01$ ; concentration of non-algal particles type I,  $C_X = 0.6 \text{ mg/l}$ ; CDOM absorption at 440 nm,  $C_Y = 0.3 \text{ m}^{-1}$ ; CDOM exponent  $S = 0.014 \text{ nm}^{-1}$ ;  $n$  is irrelevant since  $C_{Mie} = 0$ ; water temperature  $T_W = 20 \text{ }^\circ\text{C}$ ; anisotropy factor  $Q = 5.0$ ; sun zenith angle  $sun = 30.0^\circ$ ; bottom depth  $zB = 5 \text{ m}$ ; areal fraction of bottom surface type no. 1  $fa[1] = 1$ . The concentrations of other water constituents and the areal fractions of other bottom types are set to zero. Irrelevant parameters for the chosen spectrum type are indicated by gray text color. In particular sensor depth  $z$  is irrelevant since irradiance reflectance is defined just below the water surface. The fact that the displayed spectrum is a model curve (and not a measurement) is indicated by "simulated spectra" at top right.

A listening of the first lines of the file with the calculated spectrum is shown in Figure 3.6. The header specifies the spectrum type (irradiance reflectance), informs that the spectrum has been created by the program WASI, gives the software version, specifies the directory used for documentation, lists the files containing additional information (WASI5.INI, CHANGES.TXT), refers to a file with a screenshot of the current plot (WASI\_plot.bmp), and lists the wavelength range (400 to 700 nm) that was used to calculate the average intensity (Avg). The calculated spectrum is listed subsequently to the header.

```
Irradiance reflectance

This file was generated by the program WASI
Version 5.0 (64bit) - Latest update: 20 May 2019
Documentation in directory: D:\WASI5\DATA\demo\tmp
Parameter values in files: WASI5.INI, CHANGES.TXT
Screenshot of plot in file: WASI_plot.bmp
Average from 400 to 700 nm

No. 1
Avg 0.02049

380.00 0.005893
381.00 0.005942
382.00 0.005992
383.00 0.006041
384.00 0.006091
385.00 0.006142
386.00 0.006194
387.00 0.006248
388.00 0.006302
389.00 0.006357
390.00 0.006410
```

Figure 3.5: Listening of the first lines of the spectrum from Figure 3.4.

Whenever a new plot is created in WASI's plot window (⑧ in Figure 3.1), a screenshot is automatically saved to a file named `WASI_plot.bmp`. Figure 3.6 shows this file for the example of Figure 3.4.

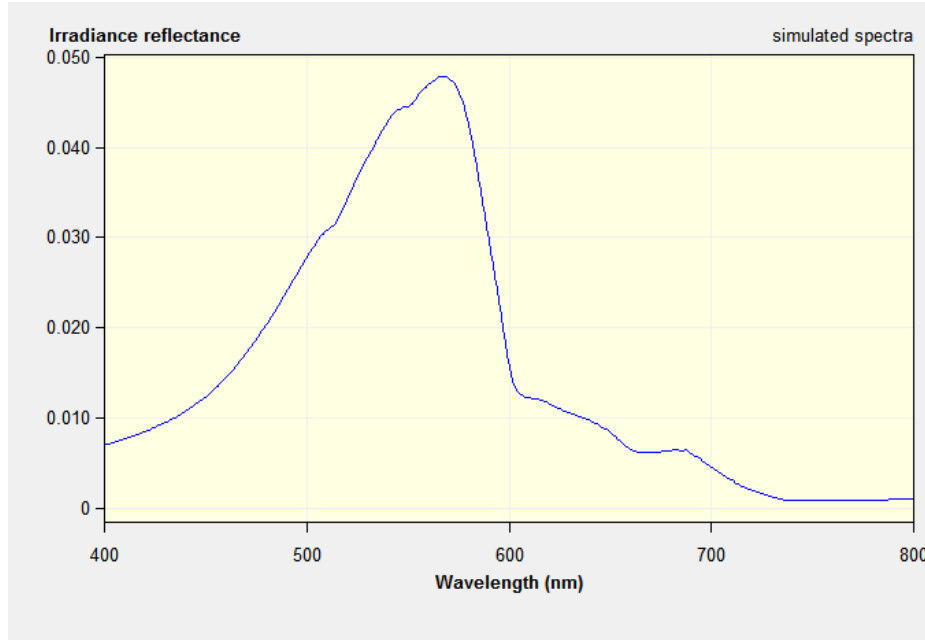


**Figure 3.6:** Screenshot that has been automatically created and stored to file after the calculation of Figure 3.4.

### 3.3 Calculation of a series of spectra

#### 3.3.1 General

Calculating a series of spectra in the forward mode is very similar to calculating a single spectrum. The only difference is that the parameter iterations have to be specified. Hence the steps are as follows:

- Define the spectrum type: select the type from the drop-down list (① in Figure 3.1);
- Set forward mode: uncheck the "invert spectra" box (② in Figure 3.1);
- Specify the parameter values: set the values of all model parameters in the parameter list (③ in Figure 3.1).

Up to three model parameters can be iterated simultaneously as described below. For the iterated parameters the entries in the parameter list are irrelevant since the values are set during iteration.

#### 3.3.2 Specification of the iteration

##### 3.3.2.1 Iteration over 1 parameter

For studying the dependence of a spectrum on a certain parameter, the values of that parameter can be iterated over a user-defined range. WASI allows to iterate the parameters of Appendix 3. As shown in Figure 3.7, the parameter to be iterated has to be selected from one of the three "Parameter" drop-down lists of the selection panel ④ of Figure 3.1 (it is irrelevant, which of the 3 lists); the selection in the two other drop-down lists must be "none". The range of variation of the iterated parameter is specified by a minimum and a maximum value ("from", "to"), and the number of calculated spectra by the number of steps ("steps"). If the check box "log" is marked with a hook, the parameter intervals are equidistant on a logarithmic scale, otherwise they are equidistant on a linear scale.

Parameter	from	to	steps	log
C[0]	0.100	10.0	7	<input checked="" type="checkbox"/>
none	0.100	1	4	<input type="checkbox"/>
none	1	5.00	5	<input type="checkbox"/>

Figure 3.7: Iteration over 1 parameter.

In the example of Figure 3.7 the phytoplankton concentration C[0] is iterated from 0.100 to 10 µg/l in 7 steps which are equidistant on a logarithmic scale, i.e. 7 spectra with concentrations of 0.100, 0.215, 0.464, 1.0, 2.15, 4.64 and 10 µg/l are calculated.

##### 3.3.2.2 Iteration over 2 parameters

When 2 parameters should be iterated, these parameters, their range of variation and the number of steps must be specified analogously to iterating 1 parameter. This is illustrated in Figure 3.8.

Parameter	from	to	steps	log
C[0]	0.100	10.0	7	<input checked="" type="checkbox"/>
C_Y	0.100	1	4	<input type="checkbox"/>
none	1	5.00	5	<input type="checkbox"/>

Figure 3.8: Iteration over 2 parameters.

In the example of Figure 3.8 the phytoplankton concentration C[0] is iterated like in Figure 3.7 from 0.100 to 10 µg/l in 7 steps which are equidistant on a logarithmic scale, and additionally CDOM absorption at 440 nm, C\_Y, is iterated from 0.100 to 1 m<sup>-1</sup> in 4 steps which are equidistant on a linear scale, i.e. absorption values of 0.1, 0.4, 0.7 and 1.0 m<sup>-1</sup> are taken. Spectra are calculated for each combination, hence the number of generated spectra is  $7 \cdot 4 = 28$ .

### 3.3.2.3 Iteration over 3 parameters

When 3 parameters should be iterated, these parameters, their range of variation and the number of steps must be specified analogously to iterating 1 or 2 parameters. This is illustrated in Figure 3.9.

Parameter	from	to	steps	log
C[0]	0.100	10.0	7	<input checked="" type="checkbox"/>
C_Y	0.100	1	4	<input type="checkbox"/>
C_X	1	5.00	5	<input type="checkbox"/>

Figure 3.9: Iteration over 3 parameters.

In the example of Figure 3.9 phytoplankton concentration C[0] and CDOM absorption C\_Y are iterated as in Figure 3.8, and additionally the concentration of non-algal particles type I, C\_X, is iterated from 1 to 5 mg/l in 5 steps which are equidistant on a linear scale, i.e. concentrations of 1, 2, 3, 4 and 5 mg/l are taken. Spectra are calculated for each combination, hence the number of generated spectra is  $7 \cdot 4 \cdot 5 = 140$ .

### 3.3.3 Data storage

Calculated spectra are stored automatically if saving is activated in the "Forward calculation settings" pop-up window shown in Figure 3.3. Each spectrum is stored in a separate file; the file names are `Bnr.fwd` with `nr` = file number. The extension `fwd` indicates that the spectra are the result of forward calculations. The parameters which change from one spectrum to the next are listed in the file `changes.txt`. A copy of the `WASI5.INI` file is created for documenting all parameters and input files. Selection of the directory where all the files are stored is described in section 10.2.

If the number of calculated spectra is below 131, the spectra can alternately be stored in a single file, `spec.fwd`. This option is selected by marking the check box "if N < 131 save all spectra in a single table" in the "Forward calculation settings" pop-up window (see Figure 3.3).

### 3.3.4 Example

An example of a series of spectra calculated in the forward mode is given in Figure 3.10.

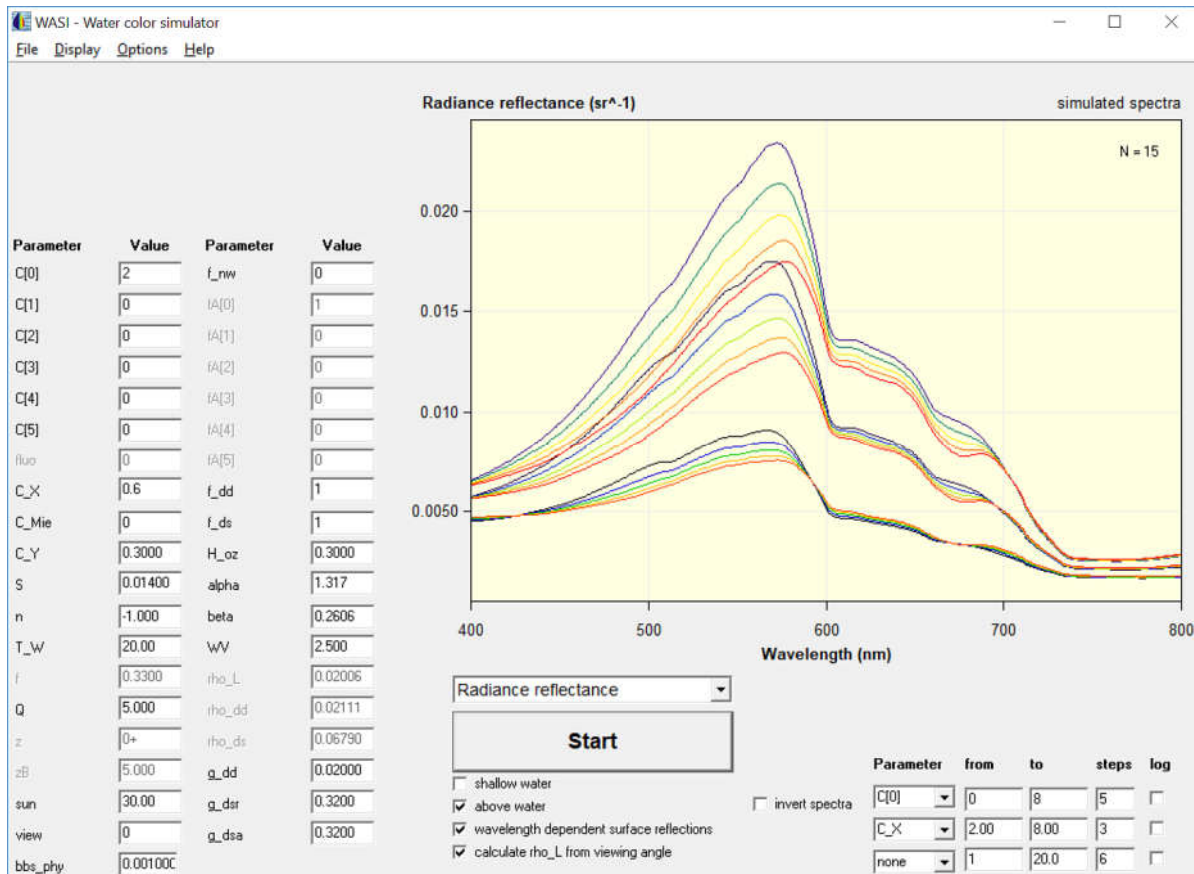


Figure 3.10: A series of radiance reflectance spectra calculated in the forward mode.

The spectrum type of Figure 3.10 is radiance reflectance.  $N = 15$  spectra have been calculated by iterating two parameters: phytoplankton concentration,  $C[0]$ , was changed from 0 to 8  $\mu\text{g/l}$  in 5 steps, i.e. concentrations of 0, 2, 4, 6, 8  $\mu\text{g/l}$  were taken, and the concentration of non-algal particles type I,  $C_X$ , was changed from 2 to 8 mg/l in 3 steps, i.e. concentrations of 2, 5 and 8 mg/l were taken. The values of the other parameters are shown in the parameter list at the left side. The list values of the iterated parameters,  $C[0]$  and  $C_X$ , are invalid.

When "save all spectra" is activated in the "Forward calculation settings" pop-up-window (see Figure 3.3), all 15 spectra are saved in ASCII format as separate files in the specified directory; an example listing of such a file was given above in Figure 3.5. The file names are `B01.fwd`, `B02.fwd`, ... `B15.fwd`.

If the number of calculated spectra is less than 131, and if the check box "if  $N < 131$  save all spectra in a single table" of the "Batch mode options" menu is marked with a hook, a single table with the file name `SPEC.FWD` is created instead of separate files. An example of that table is shown in Figure 3.11.

Radiance reflectance (sr <sup>-1</sup> )					
This file was generated by the program WASI					
Version 5.0 (64bit) - Latest update: 20 June 2019					
Documentation in directory: d:\wasi5\data\demo\tmp					
Parameter values in files: WASI5.INI, CHANGES.TXT					
Screenshot of plot in file: WASI_plot.bmp					
Average from 400 to 700 nm					
No.	1	2	3	4	5
Avg	0.005801	0.01023	0.01364	0.005628	0.009593
380.00	0.004426	0.005344	0.005971	0.004530	0.005389
381.00	0.004426	0.005357	0.005993	0.004529	0.005400
382.00	0.004426	0.005370	0.006016	0.004528	0.005411
383.00	0.004426	0.005384	0.006039	0.004527	0.005422
384.00	0.004426	0.005399	0.006062	0.004526	0.005433
385.00	0.004427	0.005414	0.006087	0.004525	0.005445
386.00	0.004428	0.005429	0.006112	0.004525	0.005458
387.00	0.004429	0.005446	0.006138	0.004526	0.005471
388.00	0.004431	0.005463	0.006165	0.004527	0.005485
389.00	0.004434	0.005480	0.006192	0.004528	0.005499
390.00	0.004436	0.005498	0.006220	0.004529	0.005514

Figure 3.11: The first lines and the first 5 columns of the file SPEC.FWD with the spectra of Figure 3.10.

The parameter values and input files used for calculating the spectra are documented by a copy of the WASI5.INI file, which is stored automatically in the directory of the spectra. The values of the iterated parameters are tabulated in the file CHANGES.TXT. An example of that file is given in Figure 3.12.

This file was generated by the program WASI					
version 5.0 (64bit) - Latest update: 20 June 2019					
List of parameter values which differ from one spectrum to the next					
Common parameter set of all spectra in file: WASI5.INI					
All spectra are the results of forward calculations					
Spectra = Radiance reflectance (sr <sup>-1</sup> )					
Spectrum	C[0]	C_X			
B01.fwd	0	2.000			
B02.fwd	0	5.000			
B03.fwd	0	8.000			
B04.fwd	2.000	2.000			
B05.fwd	2.000	5.000			
B06.fwd	2.000	8.000			
B07.fwd	4.000	2.000			
B08.fwd	4.000	5.000			
B09.fwd	4.000	8.000			
B10.fwd	6.000	2.000			
B11.fwd	6.000	5.000			
B12.fwd	6.000	8.000			
B13.fwd	8.000	2.000			
B14.fwd	8.000	5.000			
B15.fwd	8.000	8.000			

Figure 3.12: The file CHANGES.TXT of the spectra series of Figure 3.10.

## 4. Inverse modes

Inverse modeling is the determination of model parameters for a given spectrum. More precisely, those values of the model parameters must be determined for which the correspondence between model curve and given spectrum is maximal.

Four modes are implemented for inverse modeling of spectra:

- **Single spectrum mode.** Inversion is performed for a single spectrum which the user loads from file. After calculation, an overlay of imported spectrum and model curve is automatically shown on screen and resulting fit parameters, number of iterations, and residuum are displayed. This mode allows to inspect the results for individual measurements. It is useful for optimizing the choice of initial values and the fit strategy before starting a batch job or processing a multi- or hyperspectral image.
- **Batch mode.** A series of spectra from file is inverted. After each single run, an overlay of imported spectrum and model curve is automatically shown on screen. This mode is useful for processing data sets.
- **Reconstruction mode.** Combines forward and inverse modes. Inversion is performed for a series of forward calculated spectra which are not necessarily read from file. The model parameters can be chosen differently for forward and inverse calculations. This mode is useful for performing sensitivity studies. It is described in chapter 5.
- **2D mode.** All non-masked pixels of a multi- or hyperspectral image are inverted. This mode is similar to the batch mode, yet the spectra are imported from an image file. It is described in chapter 6.

### 4.1 Graphical user interface

The graphical user interface (GUI) of WASI in the inverse mode is shown in Figure 4.1. It consists of 8 elements:

- (1) Drop-down list for selecting the spectrum type. Same as in the forward mode.
- (2) Check boxes for specifying the operation mode. In the inverse mode, the box "invert spectra" is checked. Checking "batch mode" enables analysis of a series of spectra. Unchecking "batch mode" inverts a single spectrum (single spectrum mode). The check box "read from file" selects whether the spectra are read from files (hook) or if previously forward calculated spectra are used (reconstruction mode, no hook).
- (3) Parameter list. The list shows the start values of the fit parameters. Defaults are read from the WASI5.INI file, the user can change them by editing the "Value" fields. Checking a "Fit?" box makes the corresponding parameter to a fit parameter, otherwise the parameter is kept constant during inversion. The resulting fit values are displayed after inversion is finished.
- (4) The appearance of this area depends on the mode of operation. In the single spectrum mode and 2D mode, the residuum and the number of iterations are shown here after calcu-

lation is finished. In the batch mode, this area is empty. In the reconstruction mode, the panel of the forward mode for specifying the parameter iterations is displayed.

- (5) Check boxes for selecting model options. Same as in the forward mode.
- (6) Menu bar. Same as in the forward mode.
- (7) Start button. Inverse modeling is started by pressing this button.
- (8) Plot window. The input spectrum is displayed in blue, the fit curve in red. The window is refreshed before a new pair of spectra is plotted, thus only the last pair remains on screen when a series of spectra is analyzed. The file name of the imported spectrum is shown on top right.

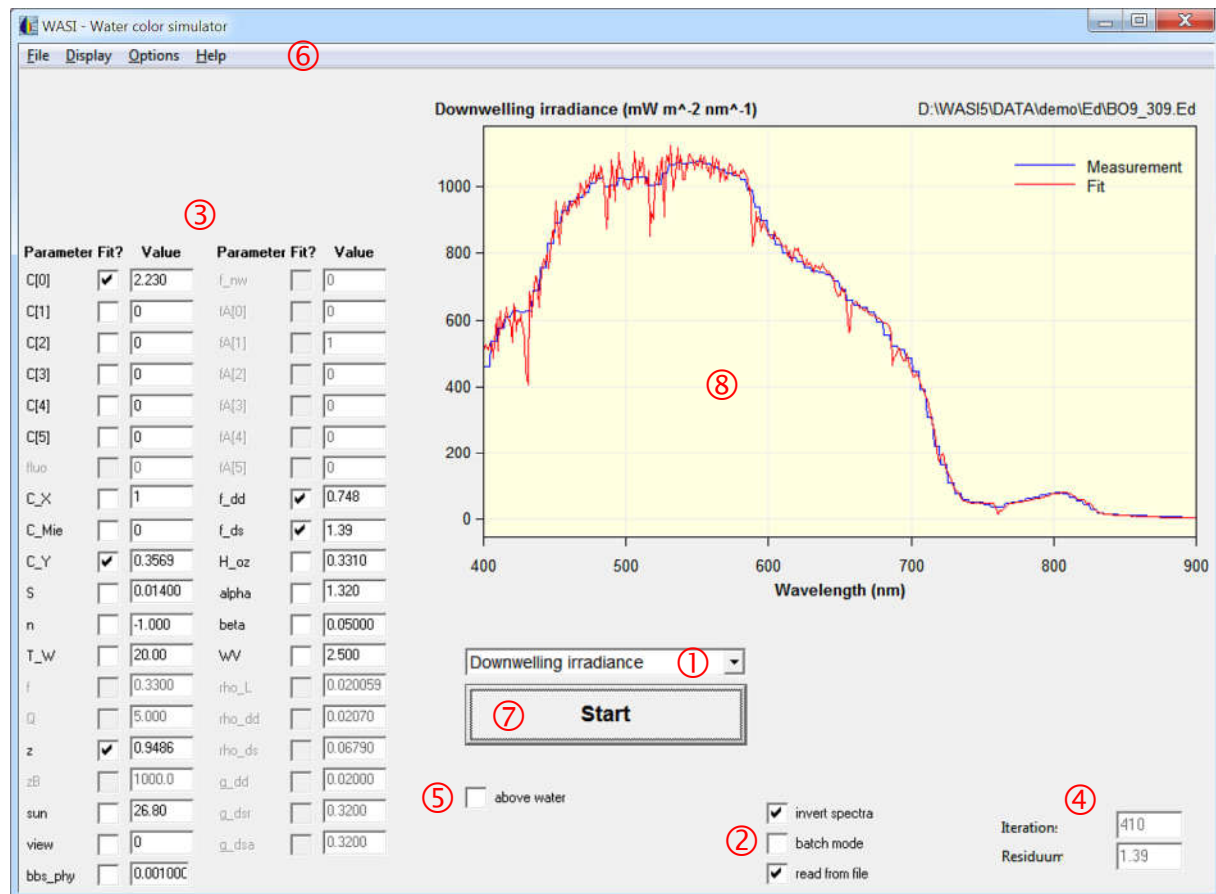


**Figure 4.1:** Graphical user interface of the inverse mode. 1 = Drop-down list for selecting the spectrum type, 2 = Check boxes for specifying the operation mode, 3 = Parameter list, 4 = Display elements depending on mode of operation, 5 = Check boxes for selecting model options (model specific), 6 = Menu bar, 7 = Start button, 8 = Plot window.

In the example of Figure 4.1 a downwelling irradiance spectrum with the filename BO9\_309.Ed, which had been measured by a submersed irradiance sensor, was inverted in the single spectrum mode. During inversion five parameters were fitted ( $C[0]$ ,  $C_Y$ ,  $z$ ,  $f_{dd}$ ,  $f_{ds}$ ), the other parameters were kept constant. Parameters irrelevant for the spectrum type "downwelling irradiance" are inactive, indicated by gray text and gray check boxes. Fit results are  $C[0] = 2.230 \mu\text{g l}^{-1}$ ,  $C_Y = 0.3569 \text{ m}^{-1}$ ,  $z = 0.9486 \text{ m}$ ,  $f_{dd} = 0.748$  and  $f_{ds} = 1.39$ . The fit converged after 410 iterations at a residuum of  $1.39 \text{ mW m}^{-2} \text{ nm}^{-1}$ .

## 4.2 Inversion of a single spectrum

### 4.2.1 Spectrum selection

A single spectrum from file is selected as follows:

- Define the spectrum type: select the type from the drop-down list (① in Figure 4.1);
- Load the spectrum.

Loading the spectrum is illustrated in Figure 4.2. The pull-down menu "File" is opened from the menu bar, and "Load" is selected (top). Then a pop-up window for file selection opens, where the desired file is selected (bottom). *Note:* The window layout depends on the operating system and the language; here the German version of Microsoft Windows 7 is shown.

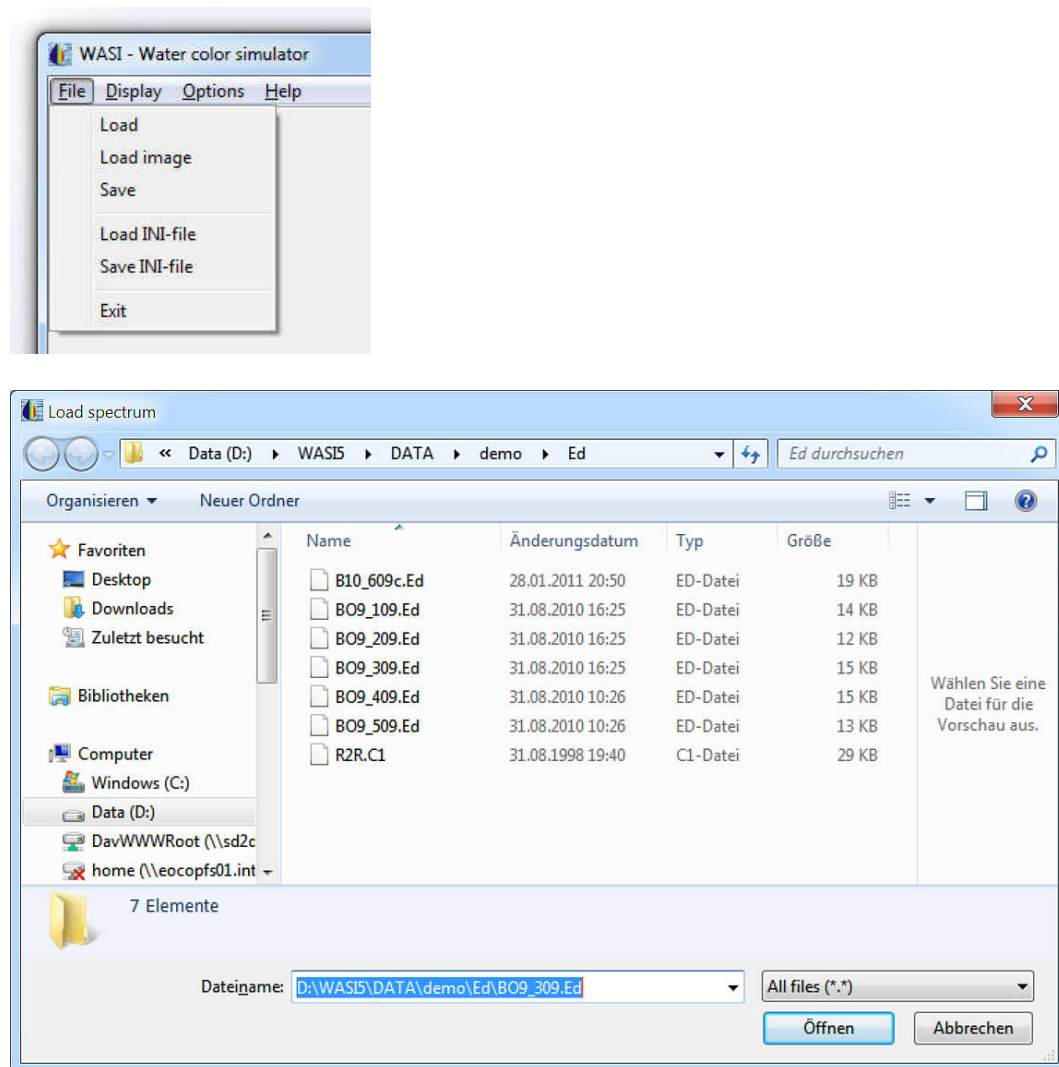


**Figure 4.2: Loading a single spectrum for inversion. Top: Menu bar and pull-down menu "File". Bottom: Pop-up window for selecting the file.**

After the spectrum is loaded, it is automatically displayed in the plot window ⑧ of Figure 4.1, and the program mode is automatically set to "single spectrum mode", i.e. the check boxes ② of Figure 4.1 are set as shown in Figure 4.3. No user action is required.

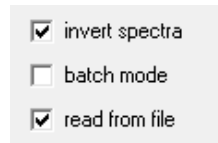


**Figure 4.3: Check box settings of the single spectrum mode.**

#### 4.2.2 Definition of initial values

Initial values of each fit parameter are read from the WASI5.INI file. The user can change them either in the parameter list ③ of Figure 4.1, or in the "Fit parameters" pop-up window, which is more detailed, see Figure 4.4.

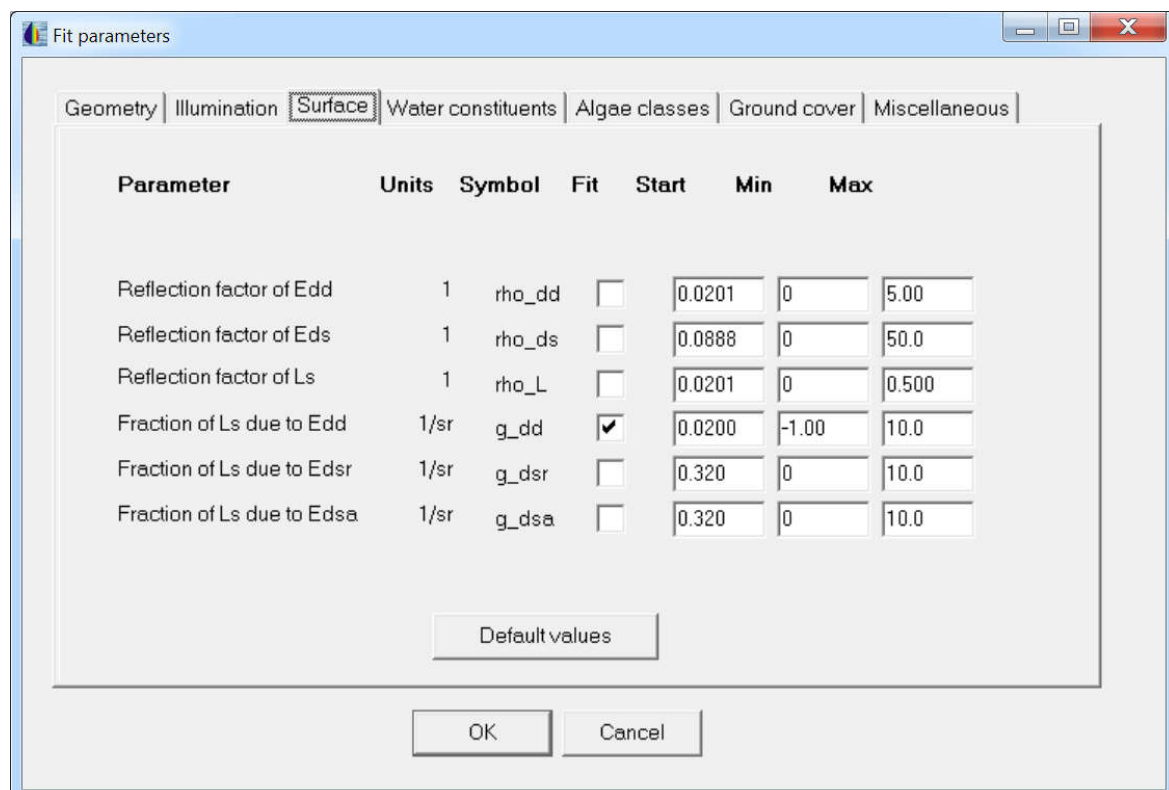


**Figure 4.4: The pop-up window "Fit parameters" with the register card "Surface".**

The pop-up window "Fit parameters" is accessed from the menu bar via "Options - Inverse calculation - Fit parameters" (see Figure 10.1). It has seven register cards which sort the parameters according to the categories Geometry, Illumination, Surface, Water constituents, Algae classes, Ground cover, and Miscellaneous. Figure 4.4 shows as example the register card "Surface". For each parameter, a short description, the physical units, and the symbol are listed. A check box "Fit" determines whether the parameter is fit parameter or kept constant during inverse modeling. The start value, as well as minimum and maximum values that are allowed for the fit routine, can be specified. Pressing the button "Default values" changes the complete set of start values of the displayed register card to the default values from the WASI5.INI file. These default values are stored separately from the start values and can be changed only by editing the WASI5.INI file.

### 4.2.3 Fit strategy

Inverse modeling aims to determine the values of unknown model parameters, called fit parameters. These are determined iteratively as follows. In the first iteration, a model spectrum is calculated for user-defined initial values of the fit parameters. This spectrum is compared with the measured one by calculating the residuum as a measure of correspondence. Then, in the further iterations, the fit parameter values are altered using the Downhill Simplex algorithm (Nelder and Mead 1965, Caceci and Cacheris 1984), resulting in altered model curves and altered residuals. The procedure is stopped when the calculated and the measured spectrum agree as good as possible, which corresponds to the minimum residuum, or if the number of iterations is above a threshold. The values of the fit parameter of the step with the smallest residuum are the fit results. WASI supports two options for residuum calculation:

- wavelength dependent weighting,
- 6 different minimization methods.

The 6 implemented equations to calculate the residuum are summarized in Table 4.1.

no.	method	y-values	residuum
1	least squares	linear	$1/N \cdot \sum g_i \cdot  m_i - f_i ^2$
2	absolute differences	linear	$1/N \cdot \sum g_i \cdot  m_i - f_i $
3	relative differences	linear	$1/N \cdot \sum g_i \cdot  1 - f_i / m_i $
4	least squares	logarithmic	$1/N \cdot \sum g_i \cdot  \ln(m_i) - \ln(f_i) ^2$
5	absolute differences	logarithmic	$1/N \cdot \sum g_i \cdot  \ln(m_i) - \ln(f_i) $
6	relative differences	logarithmic	$1/N \cdot \sum g_i \cdot  1 - \ln(f_i) / \ln(m_i) $

**Table 4.1: Implemented algorithms to calculate the residuum.  $g_i$  = weight of channel i,  $m_i$  = measured value of channel i,  $f_i$  = modelled value of channel i,  $N$  = number of channels with  $g_i \neq 0$ .**

The residuum is calculated by averaging the weighted differences between measured and fit curve over a user-defined wavelength interval. The weights  $g_i$  are specified in the "Weights" register card of the pop-up window "Fit tuning", which is shown in Figure 4.5 and accessed from the menu bar via "Options - Invers calculation - Fit tuning" (see Figure 10.1). Path and file name of that function are displayed in the "File" field; the file can be exchanged by opening a file selection window by pressing the "set" button. The number of header lines and the columns of the x- and y-values have to be specified. If all wavelengths shall be weighted equally, the file contains a constant function. Such a file with 1 as  $g_i$  values, EINS.PRN, is set as default in WASI.

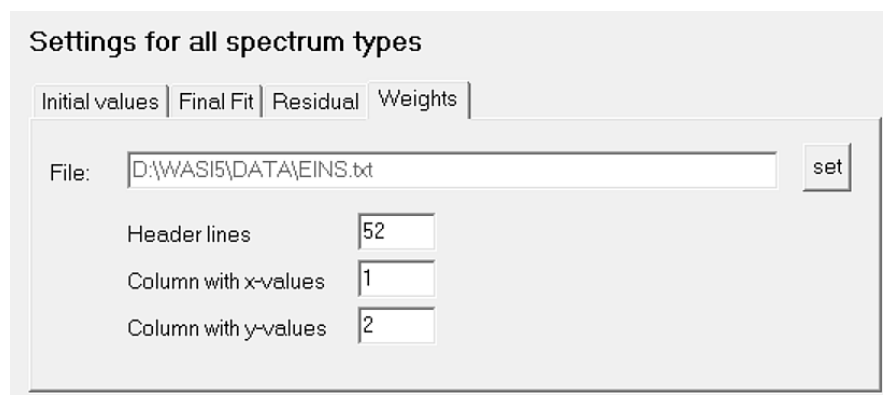


**Figure 4.5: The register card "Weights" of the popup window "Fit tuning".**

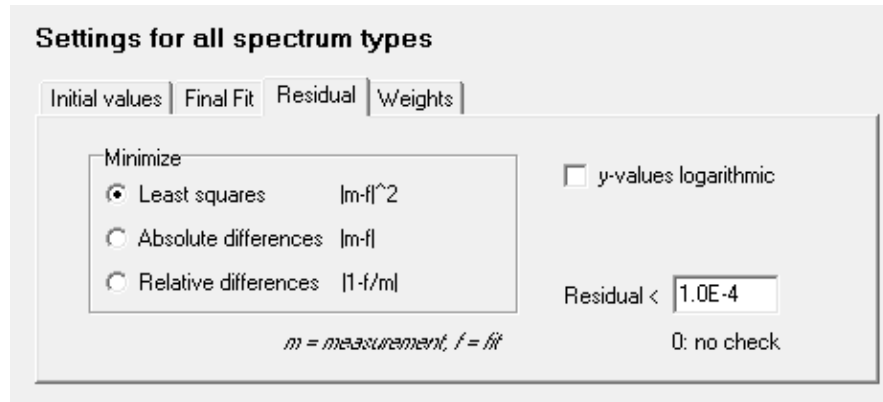


Figure 4.6: The register card "Residual" of the popup window "Fit tuning".

The equation used to calculate the residuum is selected in the "Residual" register card of the pop-up window "Fit tuning", which is shown in Figure 4.6. The allowed maximum of the residuum is set in the input field "Residual <". Inversion stops when the residuum is below the specified value or when the maximum number of iterations is exceeded, which is defined in the "Final fit" register card (Figure 4.7).

#### 4.2.4 Definition of fit region and number of iterations

Which part of the spectrum to fit and which data interval to take for calculating the residuum is specified in the "Final fit" register card of the "Fit tuning" menu, as shown in Figure 4.7. The pop-up window is accessed from the menu bar via "Options - Invers calculation - Fit tuning" (see Figure 10.1). The maximum number of iterations forces the fit routine to stop; the number should be set high enough that a forced stop is exceptional.

*Note:* If data processing requires frequently the maximum number of iterations, the 'Residual <' value should be checked in the 'Residual' register card (Figure 4.6).

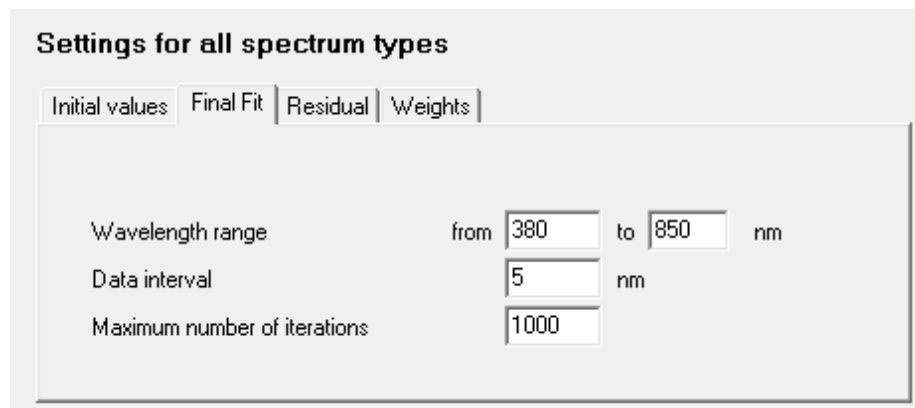


Figure 4.7: The register card "Final fit" of the pop-up window "Fit tuning".

## 4.3 Inversion of a series of spectra

### 4.3.1 Selection of spectra

A series of spectra is selected for inversion as follows:

- Set the path of the input spectra in the menu "Options - directories", field "Read spectra" (Figure 10.4).
- Set the path for storing the results in the menu "Options - directories", field "Save results", input line "Inversion" (Figure 10.4).
- Specify the data format of the input files in the menu "Options - Invers calculation - Data format" (Figure 10.2), field "File format of measurements": define number of header lines, column of x-values, column of y-values. If the sun zenith angle is provided in the input file, check the box "sun zenith angle available" and specify line, column and format of the angle parameter. Specify similarly the file info's if the day of year is given in the input file.
- Activate reading a series of spectra in the menu "Options - Invers calculation - Data in/out" (Figure 10.2), field "Batch processing": check the box "import series of spectra" and choose path and files after clicking the "set" button. Alternately, specify file extension in the input box "Extension".
- The batch mode supports multi-column files in the format  $(x, y_1, y_2, \dots, y_N)$ . To read such files, check in the "Batch processing" field the box "multiple columns per file" and specify the maximum number N of spectra per file by editing the "max. columns" box (Figure 10.2). The column of the first spectrum  $y_1$  is set in the "column with y-values" edit box of the "Field format of measurements" field.
- Activate or deactivate saving of each calculated spectrum in the "Batch processing" field (Figure 10.2) and choose the directory after clicking the "set" button.

As a result of inversion, the fit results are stored in the table `FITPARS.TXT`. This table is generated at the specified path, irrespective whether saving of spectra is activated or deactivated. If saving of spectra is activated, for each input spectrum a file is generated which lists the spectral values of input and fit curve. The file names are identical to the input file names, but the file extensions are set to `INV`.

### 4.3.2 Definition of initial values

When a series of spectra shall be inverted, the initial values can either be chosen identically for every spectrum, or they are determined individually. The selection of the method is done in the "Initial values" register card of the pop-up window "Fit tuning" menu, as shown in Figure 4.8. The pop-up window is accessed from the menu bar via "Options - Invers calculation - Fit tuning".

If the box "identical for all spectra" is checked, the initial values for every spectrum are taken from the parameter list, as described in section 4.1. Otherwise, there are two options: either the results from the previous fit are taken as start values for the subsequent fit, or some start values are determined from the spectrum itself. Which of these options is taken is specified individually for each spectrum type in the register card "Settings for individual spectra types". However, determination of start values from the spectrum itself is not possible for every spectrum type. If there is no register card for a specific spectrum type, or if the register card does

not include a box labeled "Analytic estimate of ...", the results from the previous fit are taken as start values.

Figure 4.8 shows as an example the register card for the spectrum type `Irradiance reflectance`. "Analytic estimate of C\_X and C\_Mie" and "Analytic estimate of C[0] and C\_Y" are activated, i.e. the initial values of the four parameters C\_X, C\_Mie, C[0] and C\_Y are determined from the spectra themselves. The implemented algorithms for automatic determination and the relevant user interfaces are described in section 4.4 "Optimization of inversion".

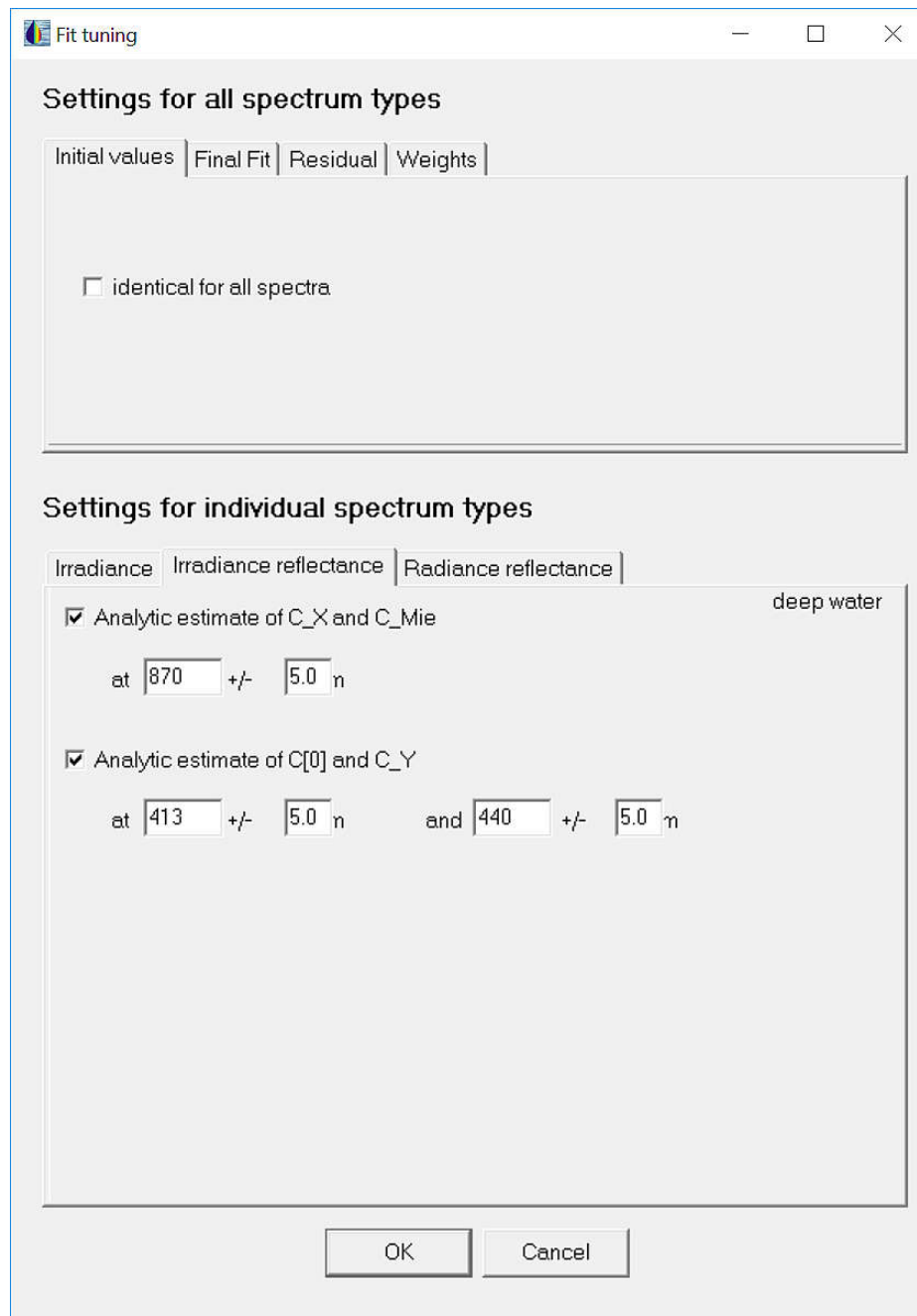


Figure 4.8: The pop-up window "Fit tuning" with the opened register cards "Initial values" and "Irradiance reflectance" of deep water.

## 4.4 Optimization of inversion

### 4.4.1 Irradiance reflectance of deep water

The most important parameters that can be determined from irradiance reflectance spectra of deep water are the concentrations of phytoplankton, CDOM and NAP. A study has been performed which investigated their retrieval sensitivity to errors (Gege 2002). It resulted a very small sensitivity for suspended matter, some sensitivity for CDOM, but very high sensitivity for phytoplankton. The study suggested a procedure for initial values determination, which has been optimized by further simulations. Finally the 5-steps-procedure summarized in Table 4.2 was implemented in WASI. The user can fine-tune the procedure in the "Fit tuning" pop-up window, which is shown in Figure 4.8. It is accessed from the menu bar via "Options - Invers calculation - Fit tuning".

Step	determine	algorithm	Procedure
1	$C_X, C_{Mie}$	analytical	Determine a first estimate of $C_X$ and $C_{Mie}$ from an analytic equation at a wavelength in the Infrared.
2	$C_Y, C_{phy}$	analytical	Determine a first estimate of $C_Y$ and $C_{phy}$ from analytic equations at two wavelengths; for $C_X$ and $C_{Mie}$ the values from step 1 are taken.
3	$C_X, C_{Mie}, C_Y$	fit	Determine initial values of $C_X, C_{Mie}$ and $C_Y$ by fit; $C_{phy}$ is kept constant at the value from step 2, $C_X, C_{Mie}$ and $C_Y$ are initialized using the values from steps 1 and 2, respectively.
4	$C_{phy}, C_Y, S$	fit	Determine initial values of $C_{phy}, C_Y$ and $S$ by fit; $C_X$ is kept constant at the value from step 3, $C_Y$ is initialized using the value from step 3, $S$ is initialized by the user-setting from the parameter list.
5	All parameters	fit	All parameters are fitted, starting with initial values for $C_X, C_{Mie}, C_{phy}, C_Y$ and $S$ from steps 3 and 4.

Table 4.2: Procedure for inversion of irradiance reflectance spectra of deep water.

Fine-tuning of steps 1 to 4 is done in the "Irradiance reflectance" register card of the "Fit tuning" pop-up window. It is shown in Figure 4.9. Steps 1 and 2 are performed if the check boxes "Analytic estimate of ..." are marked with a hook. Otherwise the initial values from the parameter list or from the previous fit are taken, as described in section 4.2.2. Steps 3 and 4 are tuned in the "Pre-fit" frames. The pre-fits are performed if "max. iterations" is set to a value larger than 1. At step 5 the user can define the wavelength range to be fitted, the intervals between data points, and the maximum number of iterations. The relevant user interface is shown in Figure 4.7.

**Step 1.** The sum of all particles in the water is called total suspended matter (TSM). For this step, its backscattering coefficient  $b_{b,TSM}$  is approximated as wavelength-independent:

$$b_{b,TSM} = b_{b,phy}(\lambda) + b_{b,NAP}(\lambda). \quad (4.1)$$

It can be calculated analytically from the reflectance at any wavelength, for which absorption of phytoplankton and CDOM are either known or can be neglected. The equation of determination is obtained from the irradiance reflectance model of Eq. (2.27) neglecting fluorescence:

$$R(\lambda) = f \cdot \frac{b_{b,W}(\lambda) + b_{b,TSM}}{a(\lambda) + b_{b,W}(\lambda) + b_{b,TSM}}. \quad (4.2)$$

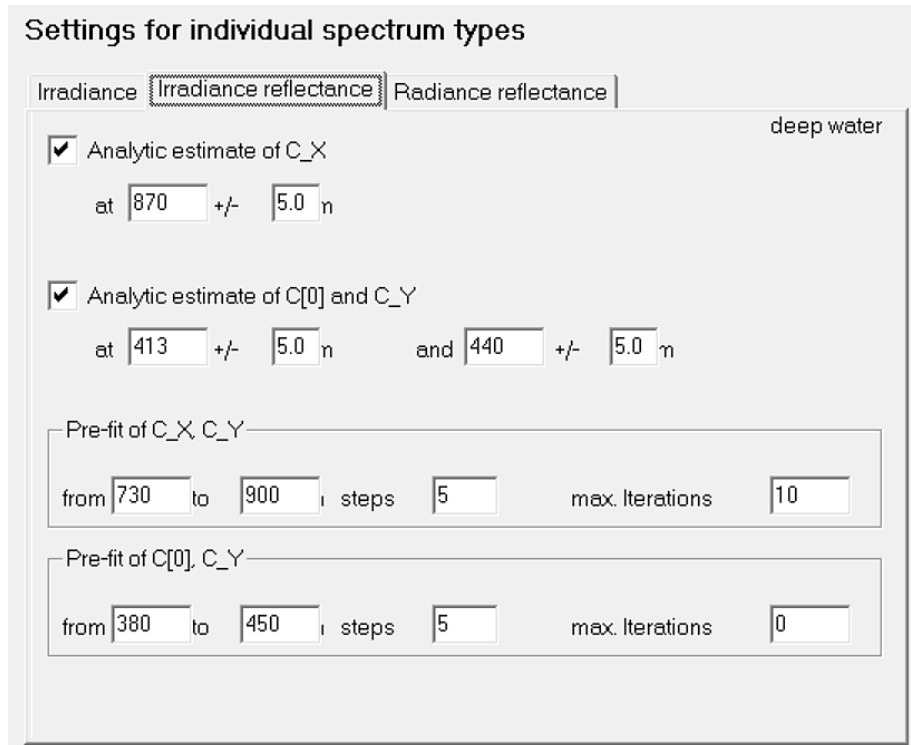


**Figure 4.9:** The register card "Irradiance reflectance" for deep water of the pop-up window "Fit tuning".

If absorption of water and its constituents,  $a$ , is known at a certain wavelength  $\lambda_{IR}$ ,  $b_{b,TSM}$  can be determined as follows:

$$b_{b,TSM} = \frac{a(\lambda_{IR}) \cdot R(\lambda_{IR})}{f - R(\lambda_{IR})} - b_{b,W}(\lambda_{IR}). \quad (4.3)$$

This equation is obtained by solving Eq. (4.2) for  $b_{b,TSM}$ .  $a(\lambda_{IR})$  is calculated according to Eq. (2.1) using as inputs the values from the parameter list. For wavelengths  $\lambda_{IR} > 700$  nm,  $a(\lambda_{IR})$  is typically very close to pure water absorption, except for very high CDOM concentration.

The calculation of  $f$  depends on the selected  $f$  model, cf. section 2.5.1. If  $f$  is parameterized solely as a function of the sun zenith angle (Eqs. (8.1), (8.3)), the  $f$  value resulting from the given sun zenith angle is taken. If  $f$  is parameterized additionally as a function of backscattering (Eqs. (8.2), (8.4)),  $f$  is calculated in two steps. First, the values from the parameter list are taken to calculate backscattering at wavelength  $\lambda_{IR}$  using Eq. (2.11); with that result a first estimate of  $f$  is calculated. In the second step, Eq. (4.3) is applied to calculate  $b_{b,TSM}$  using the  $f$  value from the first step. Then  $f$  is calculated again using Eq. (8.2) or (8.4).

A special algorithm has been implemented for the  $f$  model  $f = \text{constant}$ . Obviously a constant  $f$  needs no further consideration for applying Eq. (4.3). However, in that model  $f$  can be treated as a fit parameter. If fitting  $f$  is activated, an initial value for  $f$  can be calculated in addition to  $b_{b,TSM}$  as described in the following.

### Special case: Initial values for f and $b_{b,TSM}$

Calculation is based on reflectance values at two wavelengths  $\lambda_{IR,1}$  and  $\lambda_{IR,2}$  ( $\lambda_{IR,2} > \lambda_{IR,1}$ ). It requires that  $R(\lambda_{IR,1}) \neq R(\lambda_{IR,2})$ ; if that is not the case,  $f$  is kept constant at the value from the parameter list, and  $b_{b,TSM}$  is calculated as described above.

First the factor  $f$  is eliminated by taking the ratio of Eq. (4.2) for two wavelengths  $\lambda_{IR,1}$  and  $\lambda_{IR,2}$  ( $B_0 = b_{b,TSM}$ ):

$$\frac{R(\lambda_{IR,1}) \cdot (a(\lambda_{IR,1}) + b_{b,W}(\lambda_{IR,1}) + B_0)}{R(\lambda_{IR,2}) \cdot (a(\lambda_{IR,2}) + b_{b,W}(\lambda_{IR,2}) + B_0)} = \frac{b_{b,W}(\lambda_{IR,1}) + B_0}{b_{b,W}(\lambda_{IR,2}) + B_0}. \quad (4.4)$$

Eq. (4.4) assumes that  $B_0$  is the same at  $\lambda_{IR,1}$  and  $\lambda_{IR,2}$ . Multiplication of Eq. (4.4) with the product of both denominators leads to a quadratic expression in  $B_0$  of the form

$$\alpha \cdot B_0^2 + \beta \cdot B_0 + \gamma = 0, \quad (4.5)$$

with

$$\alpha = R(\lambda_{IR,1}) - R(\lambda_{IR,2}); \quad (4.6)$$

$$\beta = R(\lambda_{IR,1}) \cdot (a(\lambda_{IR,1}) + b_{b,W}(\lambda_{IR,1}) + b_{b,W}(\lambda_{IR,2})) - \quad (4.7)$$

$$R(\lambda_{IR,2}) \cdot (a(\lambda_{IR,2}) + b_{b,W}(\lambda_{IR,1}) + b_{b,W}(\lambda_{IR,2}));$$

$$\gamma = R(\lambda_{IR,1}) \cdot (a(\lambda_{IR,1}) + b_{b,W}(\lambda_{IR,1})) \cdot b_{b,W}(\lambda_{IR,2}) - \quad (4.8)$$

$$R(\lambda_{IR,2}) \cdot (a(\lambda_{IR,2}) + b_{b,W}(\lambda_{IR,2})) \cdot b_{b,W}(\lambda_{IR,1}).$$

It has two solutions:

$$B_0 = \frac{-\beta \pm \sqrt{\beta^2 - 4\alpha\gamma}}{2\alpha}. \quad (4.9)$$

The positive solution gives the correct value of  $B_0$ . This is the algorithm for calculating  $B_0$ . The algorithm for calculating  $f$  is obtained directly from Eq. (4.2):

$$f = R(\lambda_{IR,2}) \cdot \frac{a(\lambda_{IR,2}) + b_{b,W}(\lambda_{IR,2}) + B_0}{b_{b,W}(\lambda_{IR,2}) + B_0}. \quad (4.10)$$

It has been investigated for  $b_{b,phy} = C_{Mie} = 0$  how the accuracy of the retrieved  $C_X$  values depends on the choice of the wavelengths  $\lambda_{IR,1}$  and  $\lambda_{IR,2}$  and on the errors of the initial  $C_Y$  and  $C_X$  values. The more  $\lambda_{IR,1}$  and  $\lambda_{IR,2}$  are shifted towards longer wavelengths, the better are the results. For CDOM absorption below  $1 \text{ m}^{-1}$  the relative error of  $C_X$  is always below 20 % if both wavelengths are above 820 nm. For the MERIS channels  $\lambda_{IR,1} = 870 \text{ nm}$  and  $\lambda_{IR,2} = 900 \text{ nm}$  the relative errors are always below 5 % for  $C_Y \leq 0.5 \text{ m}^{-1}$  and below 12 % for  $C_Y \leq 1 \text{ m}^{-1}$ . Hence, for sensors equipped with two or more channels above 820 nm and for moderate CDOM concentrations the analytical equations are well-suited to determine initial values of  $C_X$  and  $f$ .

The conversion from optical units  $b_{b,TSM}$  to gravimetric concentrations  $C_X$ ,  $C_{Mie}$  is based on the assumption that  $b_{b,phy}(\lambda)$  needs no special treatment and is included in  $b_{b,NAP}(\lambda)$ . It makes use of Eq. (2.16) assuming  $b_X(\lambda) = 1$ . Accordingly,  $b_{b,TSM} = b_b(\lambda) - b_{b,W}(\lambda) = C_X \cdot b_{b,X}^* + C_{Mie} \cdot b_{b,Mie}^* \cdot (\lambda/\lambda_S)^n$ . If  $C_{Mie} = 0$ ,  $C_X$  is calculated as

$$C_X = \frac{b_{b,TSM}}{b_{b,X}^*}. \quad (4.11)$$

Otherwise, i.e. for  $C_{Mie} \neq 0$ , the user-defined ratio  $r_{XM} = C_X/C_{Mie}$  is retained; hence the initial values of  $C_X$  and  $C_{Mie}$  are calculated as follows:

$$C_X = \frac{b_{b,TSM}}{b_{b,X}^* + \frac{b_{b,Mie}^*}{r_{XM}} \cdot \left(\frac{\lambda_{IR}}{\lambda_S}\right)^n}; C_{Mie} = \frac{C_X}{r_{XM}}. \quad (4.12)$$

$C_X$  can be determined in that way with an accuracy in the order of 1 % (Gege and Albert 2005).

**Step 2.** A non-iterative procedure based on two channels was found to be practicable for calculating the initial concentrations of phytoplankton ( $C_{phy}$ ) and CDOM ( $C_Y$ ) at an accuracy in the order of 30 % (Gege and Albert 2005). If particle backscattering and the factor  $f$  are known with little error, e.g. from step 1, the  $C_{phy}$  and  $C_Y$  can be determined analytically from two wavelengths  $\lambda_1$  and  $\lambda_2$ . The equations of determination are obtained from the irradiance reflectance model of Eq. (2.27) neglecting fluorescence:

$$R(\lambda) = f \cdot \frac{b_b(\lambda)}{a_w(\lambda) + C_Y \cdot a_Y^N(\lambda) + C_{phy} \cdot a_{phy}^*(\lambda) + b_b(\lambda)}. \quad (4.13)$$

Only the contributions of pure water, CDOM and phytoplankton to absorption are considered, while NAP absorption and temperature dependencies are neglected. Solving the equation for the sum  $C_Y \cdot a_Y^N(\lambda) + C_{phy} \cdot a_{phy}^*(\lambda)$ , and rationing that equation for two wavelengths yields the following ratio  $R_A$ :

$$R_A := \frac{C_Y \cdot a_Y^N(\lambda_1) + C_{phy} \cdot a_{phy}^*(\lambda_1)}{C_Y \cdot a_Y^N(\lambda_2) + C_{phy} \cdot a_{phy}^*(\lambda_2)} = \frac{f \cdot \frac{b_b(\lambda_1)}{R(\lambda_1)} - a_w(\lambda_1) - b_b(\lambda_1)}{f \cdot \frac{b_b(\lambda_2)}{R(\lambda_2)} - a_w(\lambda_2) - b_b(\lambda_2)}. \quad (4.14)$$

Since all functions on the right-hand side of this equation are known,  $R_A$  can be calculated. Division of nominator and denominator of the center expression by  $C_{phy}$  leads to an equation which has as single unknown parameter the ratio  $C_Y/C_{phy}$ . Rewriting this equation yields the following expression:

$$\frac{C_Y}{C_{phy}} = \frac{R_A \cdot a_{phy}^*(\lambda_2) - a_{phy}^*(\lambda_1)}{a_Y^N(\lambda_1) - R_A \cdot a_Y^N(\lambda_2)}. \quad (4.15)$$

The ratio of CDOM to phytoplankton concentration is calculated using this equation. It is a matter of optimization to determine the best-suited wavelengths  $\lambda_1$  and  $\lambda_2$ .

By inserting  $C_Y = (C_Y/C_{phy}) \cdot C_{phy}$  into Eq. (4.13) and solving Eq. (4.13) at wavelength  $\lambda_3$  for  $C_{phy}$  the following expression is obtained:

$$C_{phy} = \frac{f \cdot \frac{b_b(\lambda_3)}{R(\lambda_3)} - a_w(\lambda_3) - b_b(\lambda_3)}{a_{phy}^*(\lambda_3) + \frac{C_Y}{C_{phy}} \cdot a_Y^N(\lambda_3)}. \quad (4.16)$$

Eq.(4.16) is used to calculate the phytoplankton concentration. It is a matter of optimization to determine the best-suited wavelength  $\lambda_3$ . CDOM concentration is then calculated using Eq. (4.17) with the results from Eqs. (4.15) and (4.16):

$$C_Y = \frac{C_Y}{C_{phy}} \cdot C_{phy}. \quad (4.17)$$

It has been investigated how the accuracy of the ratio  $C_Y/C_{phy}$  and of the  $C_Y$  and  $C_{phy}$  values depends on the choice of the wavelengths  $\lambda_1$ ,  $\lambda_2$  and  $\lambda_3$ , on the errors of  $C_X$  and  $C_{Mie}$  determination from step 1 and on the concentrations  $C_X$  and  $C_{Mie}$ . The results of these studies are as follows:

- $\lambda_1$  should be chosen below 470 nm;
- $\lambda_2$  should be chosen below 500 nm;
- $\lambda_3$  should be chosen below 550 nm.

In each case, preference should be given to shorter wavelengths. A good choice is  $\lambda_2 = \lambda_0$  since  $S$  errors don't affect CDOM absorption at  $\lambda_0$ . For  $\lambda_3$  no separate wavelength must be chosen, it can be set  $\lambda_3 = \lambda_2$ . Consequently, selection of only two wavelengths is implemented in WASI. Their defaults are:  $\lambda_1 = 413$  nm,  $\lambda_2 = 440$  nm.

**Steps 3 and 4.** These steps were suggested by Gege (2002). The later developed steps 1 and 2 make them now unnecessary in most cases, but they are useful under certain conditions, for instance if no suitable infrared channel is available for accurate determination of  $C_X$  or  $C_{Mie}$ , or if  $S$  is fit parameter. Steps 3 and 4 improve the estimates for  $C_Y$ ,  $C_{phy}$ ,  $C_X$  and  $C_{Mie}$  by including additional spectral information, and a start value of  $S$  can be determined. Wavelength range, data interval and maximum number of iterations for the fits of steps 3 and 4 are specified in the "Pre-fit" frames of the register card "Irradiance reflectance" of Figure 4.9. If `maxIterations` is set to 0 or 1, the respective fit is not performed.

**Step 5.** Wavelength range, data interval and maximum number of iterations for the fit of step 5 are specified in the "Final fit" register card of the "Fit tuning" pop-up window, see Figure 4.7. The maximum number of iterations forces the fit routine to stop; the number should be set high enough that a forced stop is exceptional.

#### 4.4.2 Irradiance reflectance of shallow water

Inversion of a shallow water irradiance reflectance spectrum determines in addition to the parameters of deep water several parameters related to the bottom: bottom depth  $z_B$  and areal fractions  $f_n$  of up to 6 bottom albedo spectra. The analytic function  $R^{sh}(\lambda)$  used for inversion is given by Eq. (2.29). Since it consists of as much as 21 parameters, it is very important to initialize the fit parameters with realistic values. Otherwise the probability is large that the Simplex gets lost in the high dimensional search space (up to 22 dimensions) and hence the fit provides completely wrong results. Albert (2004) developed the well-working methodology of Table 4.3 to increase step by step the number of estimated parameters, and he implemented it in WASI.

<b>Step</b>	<b>determine</b>	<b>algorithm</b>	<b>Procedure</b>
1	$z_B$	analytical	Determine a first estimate of $z_B$ from an analytic equation at a wavelength interval in the red.
2	$C_X, C_{Mie}$	analytical	Determine a first estimate of $C_X$ and $C_{Mie}$ from an analytic equation at a wavelength in the Infrared using the $z_B$ value from step 1.
3	$a_{WC}(\lambda)$	nested intervals	Estimate the total absorption spectrum of all water constituents for a wavelength interval in the visible using nested intervals. The required values of $z_B, C_X$ and $C_{Mie}$ are taken from steps 1 and 2.
4	$C_{phy}, C_Y$	fit	Determine a first estimate of $C_{phy}$ and $C_Y$ by fitting the spectrum $a_{WC}(\lambda)$ of step 3.
5	$f_n$	$f_n = 1/N$	The areal fractions of all bottom types are set equal; $N$ = number of considered bottom types.
6	$C_X, C_{Mie}, C_Y, z_B$	fit	Determine a second estimate of $C_X, C_{Mie}, C_Y$ and $z_B$ by fitting a wavelength interval in the infrared.
7	$C_{phy}, C_Y, S, z_B$	fit	Determine a first estimate of $S$ , a second of $C_{phy}$ , and a third of $C_Y$ and $z_B$ by fitting a wavelength interval in the blue.
8	All parameters	fit	All fit parameters are fitted.

**Table 4.3: Procedure for inversion of irradiance reflectance spectra of shallow water.**

Fine-tuning of steps 1, 2, 4, 6, and 7 is done in the "Irradiance reflectance" register card of the "Fit tuning" pop-up window. It is shown in Figure 4.10. Steps 1 and 2 are performed if the check boxes "Analytic estimate of ..." are marked with a hook. Otherwise the initial values from the parameter list or from the previous fit are taken, as described in section 4.2.2. Steps 4, 6 and 7 are tuned in the "Pre-fit" frames. The pre-fits are performed if "max. iterations" is set to a value larger than 1. At step 8 the user can define the wavelength range to be fitted, the intervals between data points, and the maximum number of iterations. The relevant user interface is shown in Figure 4.7.

**Step 1.** The equation (2.29), which parameterizes irradiance reflectance of shallow water, is simplified by setting  $K_{uW}(\lambda) = K_{uB}(\lambda) = K_d(\lambda)$ . The resulting equation,

$$R^{sh}(\lambda) = R(\lambda) - A_1 \cdot R(\lambda) \cdot \exp\{-2K_d(\lambda) \cdot z_B\} + A_2 \cdot R^b(\lambda) \cdot \exp\{-2K_d(\lambda) \cdot z_B\}, \quad (4.18)$$

is solved for  $z_B$ :

$$z_B = \frac{1}{2K_d(\lambda)} \ln \frac{A_1 \cdot R(\lambda) - A_2 \cdot R^b(\lambda)}{R(\lambda) - R^{sh}(\lambda)}. \quad (4.19)$$

Various simulations were performed to study the accuracy of this equation depending on wavelength and on errors of concentration and bottom type (Albert 2004). The wavelength interval 600–650 nm was found to be best-suited, thus it is used by default in WASI. By averaging the  $z_B$  values of that interval, an accuracy of  $z_B$  of typically 20–40 % can be expected at moderate suspended matter concentration (< 10 mg/l) and  $z_B < 10$  m. Such accuracy is sufficient to initialise  $z_B$ .

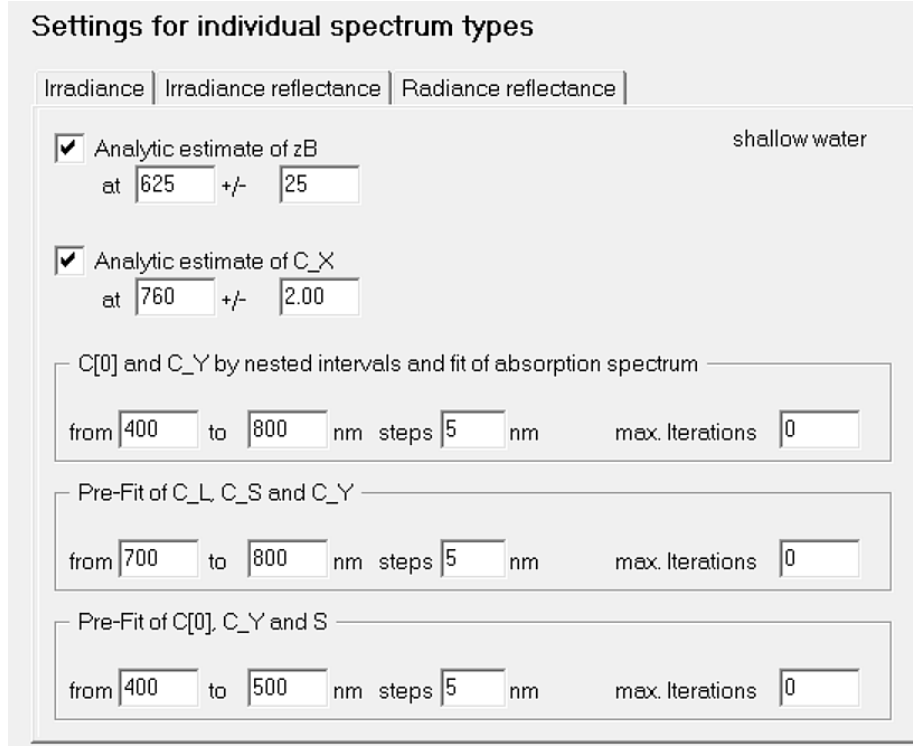


**Figure 4.10:** The register card "Irradiance reflectance" for shallow water of the pop-up window "Fit tuning".

**Step 2.** Like in step 1 of the deep water case, an analytic approximation of the reflectance spectrum is solved for suspended matter backscattering  $b_{b,TSM} = b_b(\lambda) - b_{b,w}(\lambda)$  to obtain an analytic equation for  $b_{b,TSM}$ . The analytic approximation of the reflectance spectrum is given by Eq. (4.18) in which  $R(\lambda)$  is replaced by Eq. (4.2). Solving this equation for  $B_0 = b_{b,TSM}$  yields:

$$B_0 = \frac{\mathfrak{R}^0(\lambda) \cdot [a(\lambda) + b_{b,w}(\lambda)] - b_{b,w}(\lambda)}{1 - \mathfrak{R}^0(\lambda)}, \quad (4.20)$$

where

$$\mathfrak{R}^0(\lambda) = \frac{1}{f} \cdot \frac{R^{sh}(\lambda) - A_2 \cdot R^b(\lambda) \cdot \exp\{-2K_d(\lambda) \cdot z_B\}}{1 - A_1 \cdot \exp\{-2K_d(\lambda) \cdot z_B\}}. \quad (4.21)$$

The conversion from optical units  $B_0 = b_{b,TSM}$  to gravimetric concentrations  $C_X$ ,  $C_{Mie}$  uses Eq. (4.11) or (4.12), as for deep water.

Simulations of Albert (2004) showed that for  $z_B > 2$  m the accuracy is typically better than 20 % for  $C_X + C_{Mie} < 5$  mg/l and better than 40 % for  $C_X + C_{Mie} < 25$  mg/l if 760 nm is taken as reference wavelength, which is used as default in WASI. Such accuracy is sufficient for initializing  $C_X$  and  $C_{Mie}$ .

**Step 3.** Because Eq. (4.18) cannot be solved analytically for  $C_Y$  and  $C_{phy}$ , an intermediate step is required to estimate the total absorption of all water constituents,  $a_{WC}$ . This is done iteratively by the method of nested intervals, which is described in the following.

At wavelengths of non-negligible absorption of water constituents the values of  $R$  and  $K_d$  depend on  $a_{WC}$ . When  $R$  is calculated using Eq. (4.2) and  $K_d$  using Eq. (2.17), values for  $b_b$  and  $a$  have to be assigned first.  $b_b$  is calculated using Eq. (2.11) neglecting  $b_{b,phy}(\lambda)$ ; for its critical parameters  $C_X$  and  $C_{Mie}$  the values from step 2 are taken.  $a$  is calculated using Eq. (2.1); the value of  $a_{WC}$  in that equation is treated as unknown and determined iteratively as follows. In the first step  $R$  and  $K_d$  are calculated using a start value  $A_0$  for  $a_{WC}$  in Eq. (2.1), and with these  $R$  and  $K_d$  values  $R^{sh}_0$  is calculated using Eq. (4.18). In the next steps  $A_0$  is replaced in a systematic way with different  $A_i$  values until one of the following stop criteria is reached: (1) the ratio  $\delta = R^{sh}_i / R^{sh}_0 - 1$ , which is a measure of the deviation between calculated value  $R^{sh}_i$  and measurement  $R^{sh}$ , is below a threshold  $\delta_{min}$ ; (2) the number of iterations exceeds a threshold  $i_{max}$ . The rule for calculating  $A_{i+1}$  from  $A_i$  is as follows:

$$A_{i+1} = \begin{cases} A_i + \frac{\Delta}{i} & \text{if } \delta < 0 \\ A_i - \frac{\Delta}{i} & \text{if } \delta > 0 \end{cases} \quad (4.22)$$

The value of the last iteration,  $A_{i+1}$ , is assigned to  $a_{WC}$ . These iterations are performed wavelength for wavelength. The wavelength range 400–800 nm and a wavelength interval of 5 nm were found suitable, thus these are used by default in WASI. As a result an estimate of the spectrum  $a_{WC}(\lambda)$  is obtained.  $A_0 = 5 \text{ m}^{-1}$ ,  $\Delta = 1 \text{ m}^{-1}$ ,  $\delta_{min} = 0.01$  and  $i_{max} = 100$  are set as defaults in WASI. Wavelength range, wavelength interval, and  $i_{max}$  can be changed in the frame labeled "C[0] and C\_Y by nested intervals and fit of absorption spectrum" of Figure 4.10.  $A_0$ ,  $\Delta$ , and  $\delta_{min}$  can be changed by editing the WASI5.INI file.

**Step 4.** A first estimate of the two parameters  $C_{phy}$  and  $C_Y$  is determined by fitting the spectrum  $a_{WC}(\lambda)$  from step 3 with the Simplex algorithm using Eqs. (2.2) and (2.7). The function  $a_{NAP}(\lambda)$  of Eq. (2.2) and the parameters  $C_1 \dots C_5$  of Eq. (2.7) are set to zero in this step. For wavelength range, wavelength interval, and  $i_{max}$  the same values are taken as in step 3.

**Step 5.** The areal fractions  $f_n$  of all those bottom types are set equal which are marked as fit parameters.

**Steps 6 and 7.** These steps can be tuned by the parameters in the two "Pre fit ..." frames of Figure 4.10.

**Step 8.** Wavelength range, data interval and maximum number of iterations are specified in the "Final fit" register card of the "Fit tuning" pop-up window, see Figure 4.7. The maximum number of iterations forces the fit routine to stop; the number should be set high enough that a forced stop is exceptional.

#### 4.4.3 Radiance reflectance of deep water

The radiance reflectance of deep water above the surface,  $r_{rs}(\lambda)$ , is calculated using Eq. (2.34); that below the surface,  $r_{rs}^-(\lambda)$ , according to Eq. (2.30) or (2.31).  $r_{rs}(\lambda)$  has 25 parameters which may be fitted,  $r_{rs}^-(\lambda)$  has 15. This high number of fit parameters makes fit tuning necessary. In particular it is important to find suitable start values of the parameters, i.e. to start with initial values which are not too different from the final results. The user interface

for controlling fit tuning is shown in Figure 4.11. It is accessed from the menu bar via "Options - Invers calculation - Fit tuning".

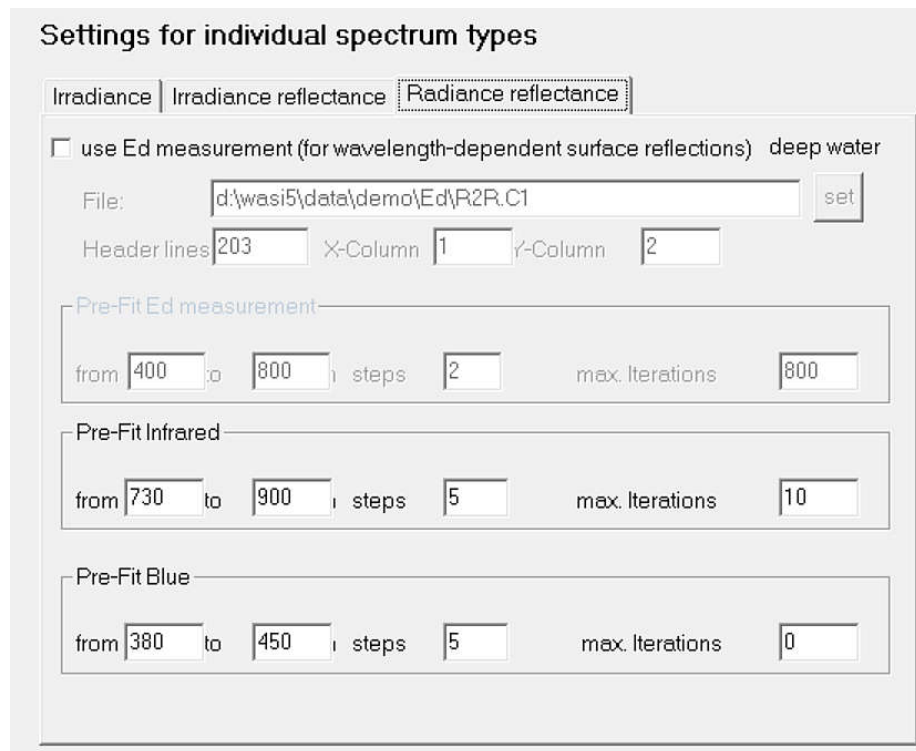


**Figure 4.11:** The register card "Radiance reflectance" for deep water of the pop-up window "Fit tuning".

If a downwelling irradiance measurement is available, the number of fit parameters for  $r_{rs}(\lambda)$  can be reduced by 4 ( $\alpha, \beta, \gamma, \delta$ ). In this case the box "use Ed measurement" should be checked, and the measured spectrum has to be specified.

Most of the initial values are taken from the parameter list in the main window. However, for some parameters an automatic determination is possible: for  $\alpha, \beta, \gamma, \delta$  if an Ed measurement is available, for  $C_x$  and  $\sigma_L$  from a pre-fit in the Infrared, and for  $C_{phy}$ ,  $C_y$ ,  $S$  and  $Q$  from a pre-fit in the Blue. These pre-fits are activated by choosing a value  $>1$  for "max. Iterations". The wavelength intervals, steps and maximum number of iterations have to be specified for each pre-fit. If "max. Iterations" is set to 0 or 1, the corresponding pre-fit is not performed.

#### 4.4.4 Radiance reflectance of shallow water

For inversion of radiance reflectance spectra also the 8 steps of Table 4.3 are performed. The only difference to the case of irradiance reflectance is that all R spectra are replaced by the corresponding  $R_{rs}$  spectra.

#### 4.4.5 Downwelling irradiance

The downwelling irradiance above the water surface,  $E_d(\lambda)$ , is calculated according to Eq. (2.40) as a weighted sum of 3 spectra. Since the curve shapes of these spectra are quite different, it is not possible to obtain similar sum curves by using rather different sets of weights. In other words, the solution of the inversion is unequivocal. Consequently, no fine-tuning of the inversion scheme is necessary.

The downwelling irradiance below the water surface,  $E_d^-(\lambda)$ , is calculated according to Eq. (2.50) using the components of the above-water spectrum  $E_d(\lambda)$ . For  $E_d(\lambda)$  either the parameterization of Eq. (2.40) can be chosen, or a measured spectrum can be taken. The selection is done in the register card "Irradiance" of the pop-up window "Fit tuning", which is shown in Figure 4.12. It is accessed from the menu bar via "Options - Invers calculation - Fit tuning".

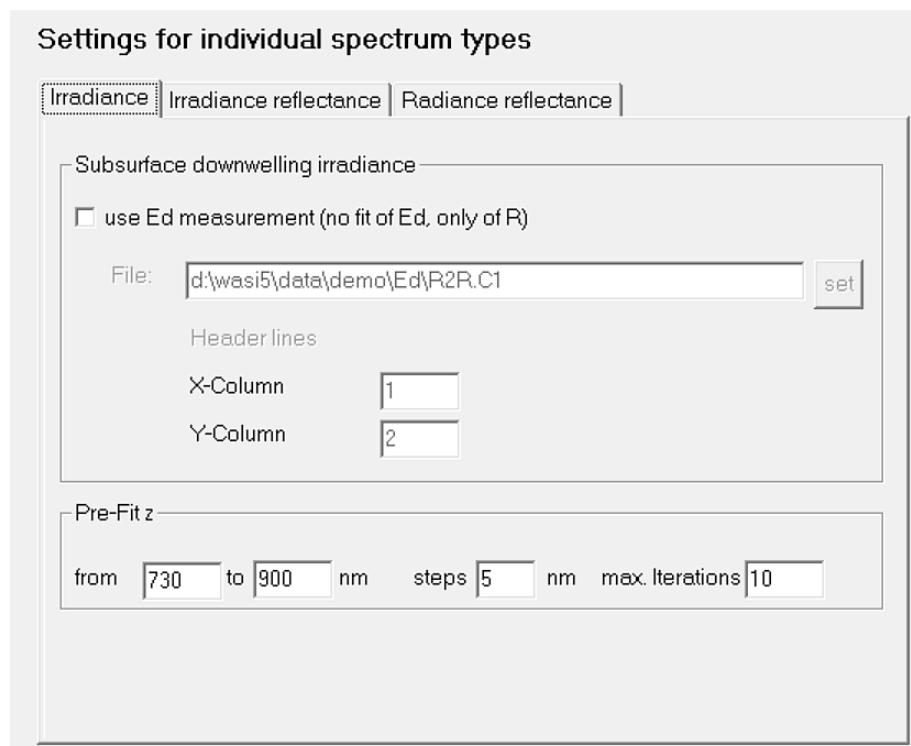


Figure 4.12: The register card "Irradiance" of the pop-up window "Fit tuning".

Downwelling irradiance spectra below the water surface are not very different from those above the surface, i.e. the curve form of  $E_d^-(\lambda)$  depends much more on the parameters of  $E_d(\lambda)$  than on those of  $R(\lambda)$ . Hence small errors of  $E_d(\lambda)$  cause large errors of the retrieved parameters of  $R(\lambda)$ . Thus the option of using  $E_d(\lambda)$  measurements for fitting  $E_d^-(\lambda)$  must be applied with care; in general it should not be used.<sup>6</sup>

<sup>6</sup> The option has been included for consistency reasons:  $E_d(\lambda)$  measurements are useful for inversion of upwelling radiance and specular reflectance spectra.

## 5. Reconstruction mode

The reconstruction mode is a combination of forward and inverse mode: A spectrum is calculated in the forward mode, and subsequently this spectrum is fitted in the inverse mode. The model parameters of the forward calculation are stored together with the fit parameters of the inversion in one file; the spectrum may be saved or not. Analogously to the forward mode, up to three parameters can be iterated simultaneously. Parameters of the forward mode and of the inverse mode can be chosen differently. The mode is called reconstruction mode because inversion reconstructs model parameters of the forward mode at altered conditions. It is useful for sensitivity studies.

### 5.1 Definition of parameter values

The parameter list on the main window shows all parameters which can be chosen differently in forward and inverse mode. The model parameters of the chosen spectrum type are active (font colour is black), the irrelevant parameters are inactive (font colour is gray). Figure 5.1 shows as example the parameter list in forward mode for the spectrum type “Downwelling irradiance” with the model option “above water”. Calculation of this spectrum type makes use of 7 parameters (sun, f\_dd, f\_ds, H\_oz, alpha, beta, WV). Their actual values can be changed by editing the parameter list.

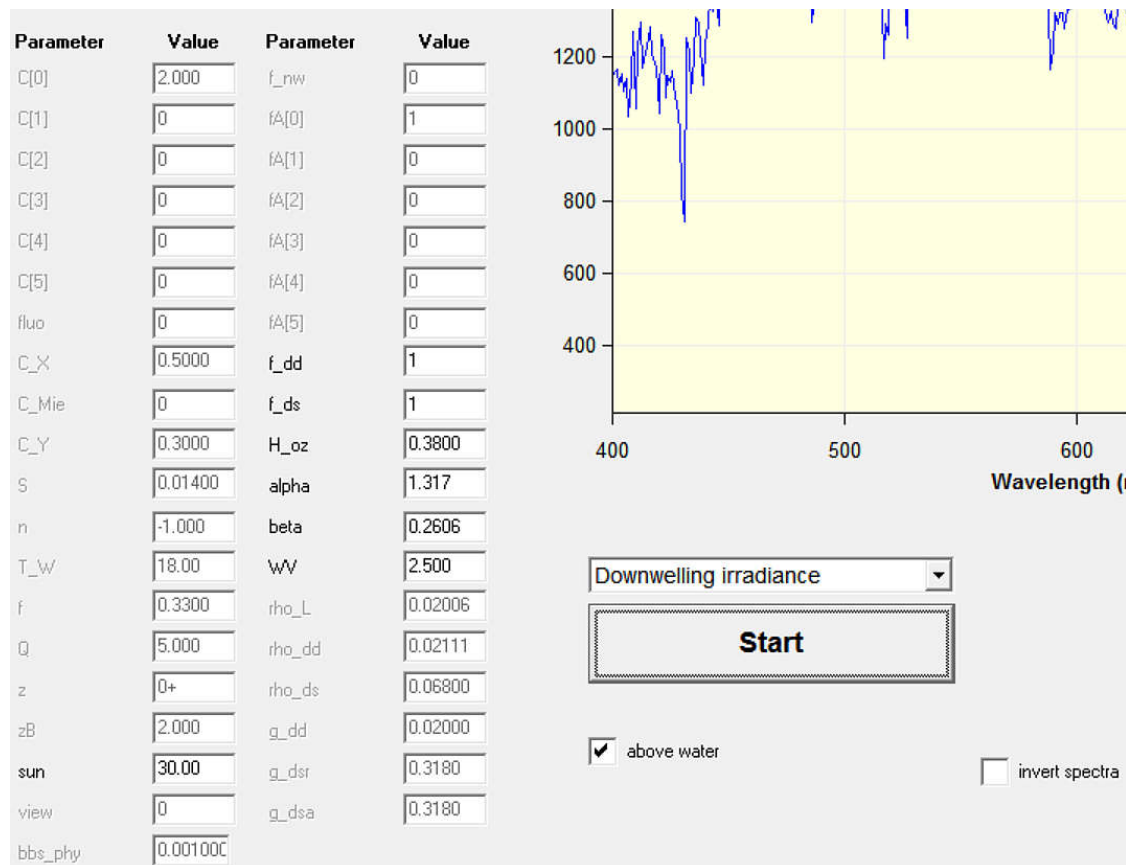
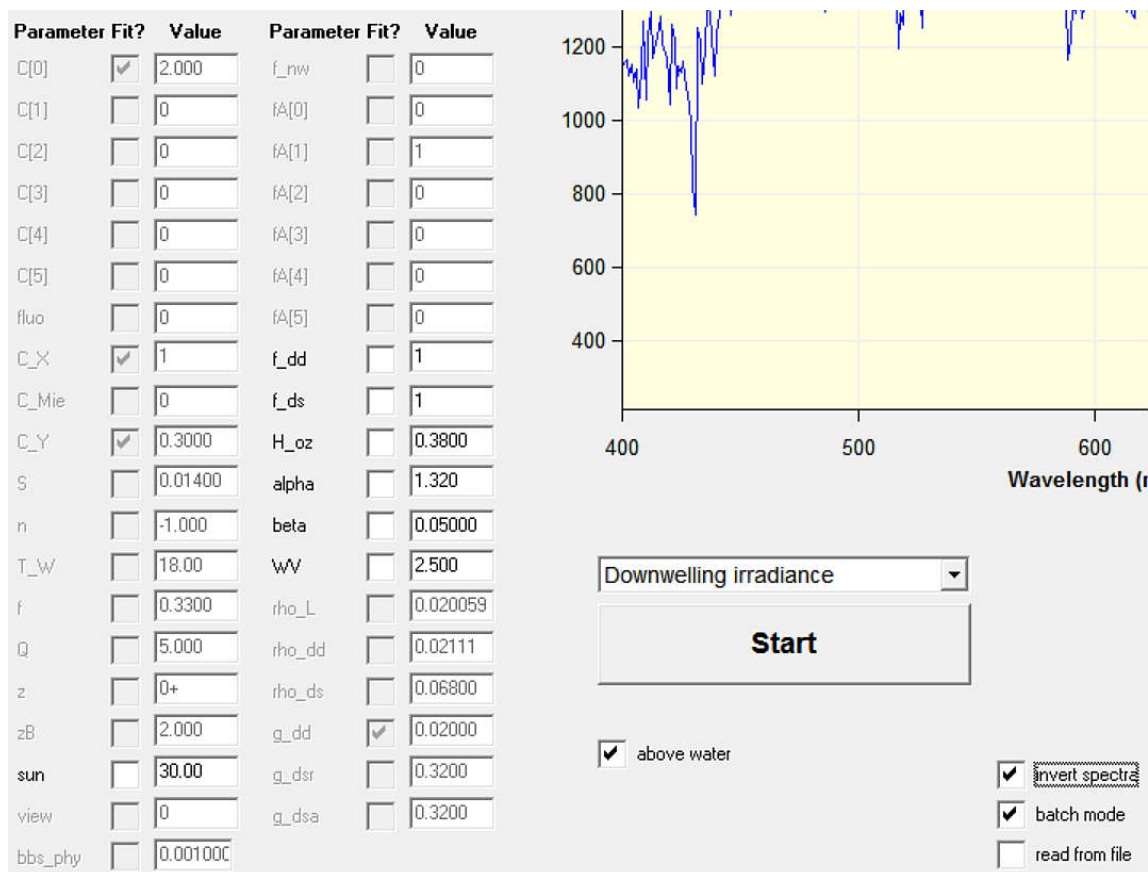


Figure 5.1: Parameter list in forward mode at the example of downwelling irradiance above water.



**Figure 5.2:** : Parameter list in inverse mode at the example of downwelling irradiance above water.

The analogous parameter list for the inverse mode is shown in Figure 5.2. A check box is assigned to each parameter to select whether the parameter should be kept constant during inverse modeling (box is unchecked) or if it should be treated as fit parameter (box is checked). In the first case, the shown value is the parameter value for all calculation steps; in the second case, it is the initial value. By clicking the "invert spectra" check box, the user can quickly switch between the forward and inverse values. In the example of Figure 5.1 and Figure 5.2, the forward and inverse values are chosen identical for four parameters (sun, f\_dd, f\_ds, H\_oz), and differently for three parameters (alpha, beta, WV).

Figure 5.1 and Figure 5.2 are an example how to study propagation of model errors. A different value of the parameter alpha is chosen for forward and inverse calculation, and alpha is not fitted. This is an efficient way to introduce a well-defined model error: the error of the inverse model is attributed to the parameter alpha, and the error is given quantitatively as  $\alpha_{\text{wrong}} - \alpha_{\text{correct}} = 0.5 - 1.317$ . Due to the wrong alpha value, the fit cannot find the correct values of the fit parameters beta and WV. The errors of these parameters depend only on the alpha error. In this way, the sensitivity of beta and WV on alpha errors can be studied. Systematic investigations of such error propagation are the basis of sensitivity studies.

Error propagation can be investigated systematically by iterating the erroneous model parameter during forward calculation. The way to do this is explained in section 3.3.2. Figure 5.3 shows as example how to study systematically the errors caused by wrong values of the parameter alpha: alpha is iterated from 0 to 2 in 11 steps. Thus, 11 spectra are calculated in the forward mode with alpha values of 0, 0.2, ..., 2, and these spectra are subsequently fitted. If alpha is fixed during inversion like in Figure 5.2, a series of inversion results is obtained for a systematically changing error of the parameter alpha.

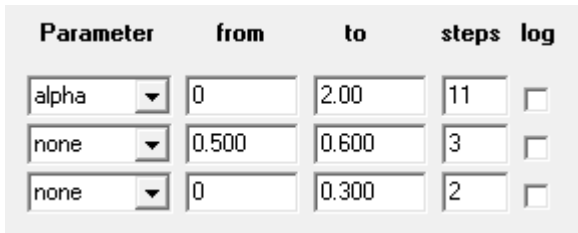


Figure 5.3: Iteration of the parameter alpha.

## 5.2 Definition of output information

The results of fitting a series of spectra are stored in a single file, `FITPARS.TXT`. Figure 5.4 shows as an example a listening of this file for the settings of section 5.1. The first lines explain the file content and summarize relevant information.

The first column of the data block, headed "File", lists the file names of the calculated spectra. Whether the spectra are saved or not, decides the user. As sensitivity studies are generally based on a large number of spectra, usually not all spectra are saved, but only a few for illustration purposes. Thus, a study may be performed in two steps: in the first step, the parameters of interest are iterated over the interesting ranges with few steps, and the resulting spectra are saved; in the second step, the calculations of step 1 are repeated, but with much more steps, and without saving the spectra. How to save forward calculated spectra is described in sections 3.2.4 and 3.3.3, the corresponding pop-up window is shown in Figure 3.3. How to save fit spectra is described in section 4.3.1. Directories selection is described in section 10.2, the corresponding pop-up window is shown in Figure 10.4.

The second column of the data block can be ignored (it is shown for consistency with the inverse mode, where it represents the column of the input spectrum). The third column lists the values of the parameter which is iterated during forward calculation. The abbreviation "fwd" in the heading of this column means "value of forward calculation", the heading's second line specifies the parameter name. If more than one parameter is iterated, similar columns are added. In the example of Figure 5.4, 11 values of the parameter alpha (0, 0.2, ..., 2) were taken

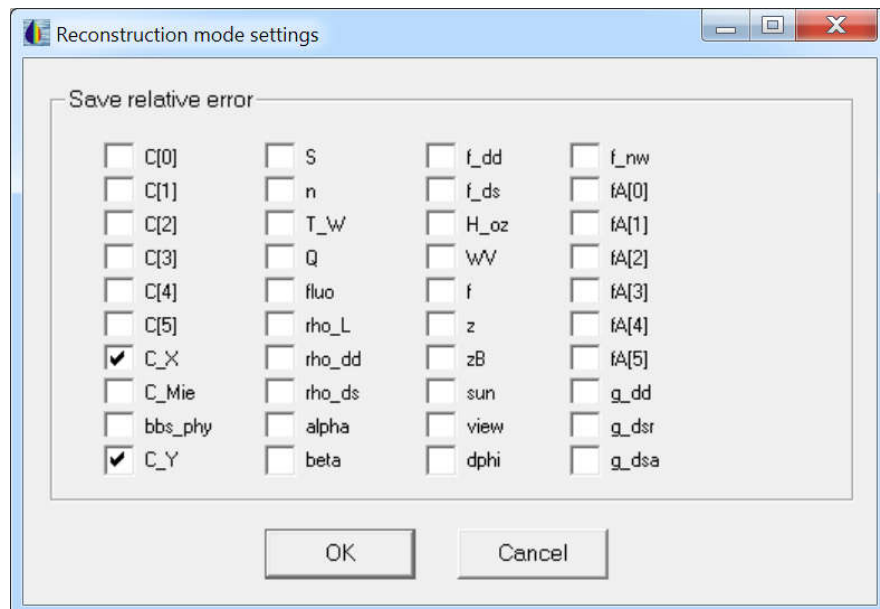
This file was generated by the program WASI Version 4 - Latest update: 2 September 2014									
List of fitted parameters which may differ from one spectrum to the next Common parameter set of all spectra in file: <code>WASI4.INI</code>									
Errors are given in %: error = 100*(inv/fwd-1)									
File	col	fwd	inv	inv	inv	error	error	error	
		alpha	Iter	Resid	beta	WV	alpha	beta	WV
B01	0	0	45	0.0394	0.2035	2.534	5.00E+13	-21.9	1.35
B02	0	0.2000	31	0.0334	0.2252	2.529	150	-13.6	1.16
B03	0	0.4000	29	0.0140	0.2483	2.512	25.0	-4.73	0.493
B04	0	0.6000	29	0.0210	0.2726	2.483	-16.7	4.60	-0.660
B05	0	0.8000	32	0.0691	0.2982	2.443	-37.5	14.4	-2.28
B06	0	1	201	0.132	0.3252	2.392	-50.0	24.8	-4.33
B07	0	1.200	201	0.209	0.3537	2.330	-58.3	35.7	-6.81
B08	0	1.400	201	0.334	0.3595	2.239	-64.3	38.0	-10.4
B09	0	1.600	201	0.460	0.3657	2.153	-68.8	40.3	-13.9
B10	0	1.800	201	0.586	0.3721	2.069	-72.2	42.8	-17.2
B11	0	2.000	201	0.712	0.3787	1.989	-75.0	45.3	-20.4

Figure 5.4: Example of the output file `FITPARS.TXT`.

for forward calculation. Since the other model parameters were hold constant for the series of forward calculations, these are not included in this file; their values are documented in the WASI5.INI file, as indicated in the header information.

All subsequent columns summarize the results which were obtained by fitting the forward calculated spectra. The column "Iter" shows the required number of iterations of the fit routine (see 4.2.4). The column "Resid" lists the residuals, which are a measure for the correspondence between the forward calculated spectrum and the fit curve (see 4.2.3). The subsequent columns tabulate the resulting values of the fit parameters. The abbreviation "inv" in their heading means "value of inverse calculation", the heading's second line specifies the parameter name. Each parameter, for which the check box "Fit?" is marked with a hook in the parameter list, is represented by such a column. In the example of Figure 5.4 these are the parameters beta and WV.

So far the file structure is identical to the inversion of a series of spectra from files (see section 4.3). The specific results of the reconstruction mode are tabulated in the last columns. These columns, labeled "error" and headed by parameter names, list the relative errors of user-selected parameters. The selection which parameters to tabulate, is done in the pop-up window "Reconstruction mode settings", which is shown in Figure 5.5. This window is accessed from the menu bar via "Options – Reconstruction mode", see Figure 10.1. The relative errors are calculated as  $100 * (\text{inv}/\text{fwd} - 1)$ , where "inv" is the fit result of inverse modeling and "fwd" is the parameter value used during forward calculation. Hence, the relative errors are the fit parameter's deviations from the "true" values in percent.



**Figure 5.5:** The pop-up window "Reconstruction mode settings".

## 6. 2D mode

The 2D mode allows visualization and inversion of multispectral and hyperspectral image data using the models described in chapter 2. It is intended primarily to process atmospherically corrected images from airborne sensors and satellite instruments in units of upwelling radiance or radiance reflectance. Please refer to Gege (2014) for a detailed description.

All settings of the 2D mode are made in the popup window shown in Figure 6.1, which is accessed from the menu bar via ‘Options – 2D’.

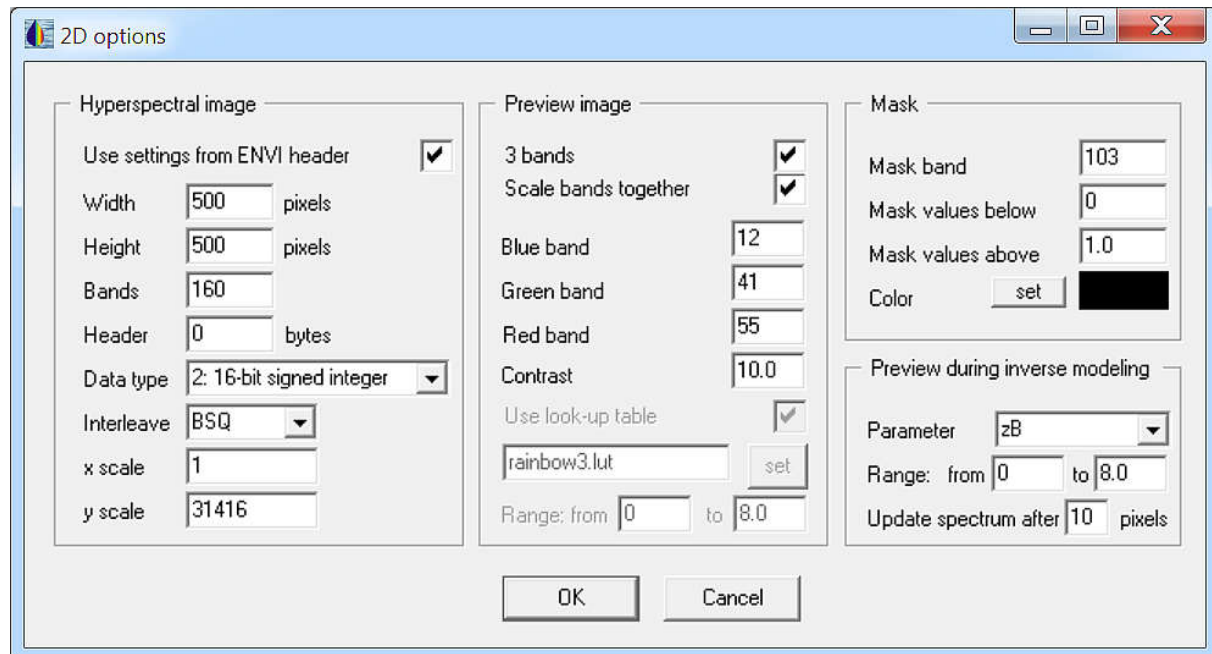


Figure 6.1: Popup window for the options of the 2D mode of WASI.

### 6.1 Image data format

WASI supports the import of multispectral and hyperspectral image data in two formats:

- **ENVI format.** This is the default format.
- **Generic format.** The format details have to be specified by the user.

The selection is made in the panel ‘Hyperspectral image’ of the popup window shown in Figure 6.1. If ‘Use settings from ENVI header’ is marked, the ENVI format is assigned, otherwise the generic format is activated.

The format parameters relevant for multispectral and hyperspectral image data are summarized in Table 6.1. If the ENVI format is chosen, these parameters are imported from the ENVI header file (ENVI 2005), otherwise the user has to specify them in the ‘Hyperspectral image’ panel shown in Figure 6.1. WASI assumes no specific file extension for an image. For images in ENVI format the only requirement is: The ENVI header file must be located in the same directory as the image file, its file name must be the same as the image file name, and its file extension is ‘.hdr’.

Image parameter	WASI name	ENVI header keyword
Number of pixels per line	Width	samples
Number of image lines	Height	lines
Number of bands	Bands	bands
Centre wavelength of each band	(any ASCII table)	wavelength
Spectral resolution (FWHM) of each band	(any ASCII table)	fwhm
Image header offset	Header	header offset
Image data type	Data type	data type
Image interleave type	Interleave	interleave
Bands used for image visualization	Blue band Green band Red band	default bands
Wavelength scale factor	x scale	wavelength units
Intensity scale factor	y scale	-
Geographic information	-	map info

**Table 6.1: Image parameters.**

WASI supports five data types (8-bit byte, 16-bit unsigned integer, 16-bit signed integer, 32-bit signed long integer, 32-bit floating point) and two interleave types (BIL = band interleaved per line, BSQ = band sequential) as input; output is 32-bit floating point BIL or BSQ. Wavelengths are expressed in units of nm. If the ENVI header file uses other units for wavelength, the ‘wavelength scale factor’ specifies the conversion factor (e.g. 1000 if the units are  $\mu\text{m}$ ). The ‘intensity scale factor’ can be used to re-scale all data by division with the specified value; when set to 1, no re-scaling is performed. Band dependent scaling is not supported.

## 6.2 Preview settings

The parameters for visualizing an image are set in the ‘Preview image’ panel shown in Figure 6.1. The preview can show either the values of 3 bands or of 1 band.

- **Show 3 bands.** The box ‘3 bands’ is checked. Displays the image in colors which depend on the chosen channel numbers of the blue, green and red band. To get naturally appearing colors, the bands should be close to 450 nm, 550 nm and 650 nm. The radiometric dynamics of a multi- and hyperspectral image is usually higher than the 8 bit per color of a monitor. This mismatch is adjusted by multiplying the value of each pixel with  $256 \text{ C/M}$ , where C is the contrast and M the maximum value of all unmasked pixels. M is determined automatically, C can be set by the user (the default is 1). If ‘Scale bands together’ is unchecked, M is calculated individually for the red, green and blue bands; otherwise, M is the maximum of the three bands. By default ‘Scale bands together’ is checked.
- **Show 1 band.** The box ‘3 bands’ is unchecked. Displays a single band of the image. If ‘Use look-up table’ is checked, the values of that band are color-coded using a selectable look-up table, otherwise the values are shown as gray values. The range of the displayed values is defined in the ‘Range: from ... to ...’ input fields.

## 6.3 Image import and pixel information

The image is imported by selecting in the menu bar ‘File – Load image’. Moving the mouse over the image opens a small window which displays the coordinates and the values of the preview band(s) at the position of the mouse pointer (Figure 6.2). If the image data are rescaled during import (using ‘y scale’ in Figure 6.1), the rescaled values are shown.

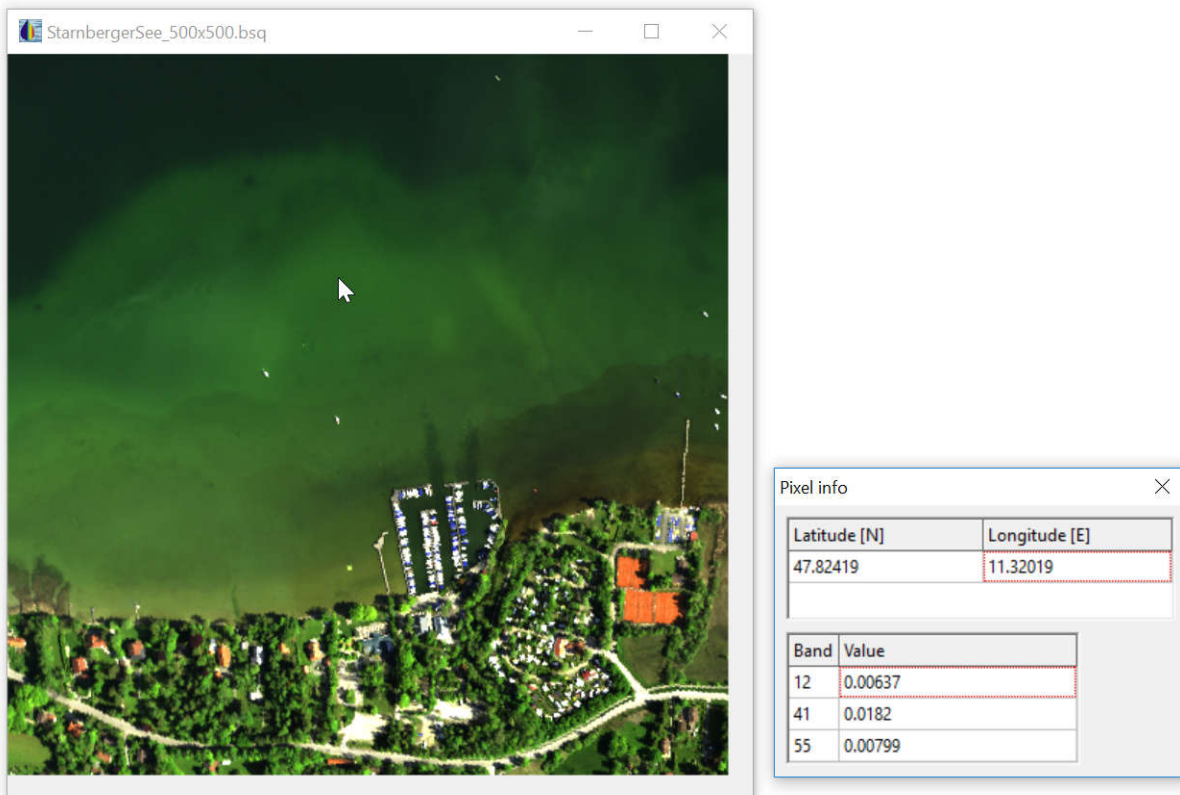


**Figure 6.2: Left:** Imported hyperspectral image (sensor: HySpec VNIR-1600; location: Lake Starnberg, Germany). **Right:** Information for the pixel under the mouse pointer: coordinates and values of the three bands selected for preview.

The user can visualize the spectrum of any pixel by clicking with the mouse on the pixel of interest. By using the arrow keys to move the mouse pointer, the pixel-by-pixel variability can be studied. Mean and standard deviation of an area can be visualized by drawing with the mouse a rectangle. The extracted spectra are displayed in the plot window and can be saved as ASCII file. Inverse modelling can be applied to each spectrum extracted in this way. This feature is useful to determine initial values of fit parameters or to analyze selected pixels for which field data are available.

## 6.4 Image masking

A mask defines the pixels which are ignored during data processing. It is created in the popup window shown in Figure 6.1 using the ‘Mask’ settings. Water is in general darker than land or clouds at wavelengths above 700 nm, hence an infrared band can be taken to define the mask. The box labeled ‘Color’ indicates the chosen color of the mask. The mask color can be changed after pressing the ‘set’ button.

## 6.5 Guidelines for data processing

There are no fixed rules for data processing. This section summarizes the typical steps taken by the author of this manual.

Since more data are publicly available from multispectral satellite instruments than from hyperspectral sensors, an image of the multispectral sensor OLI on board of the Landsat 8 satellite is taken to illustrate the guidelines (Figure 6.3). It was acquired on 13 January 2018 above Costa Rica and shows coastal and inland waters in the Terraba Sierpe national park, which is dominated by mangrove forests. The preview shows bands 1, 3, 4 centered at 443 nm, 562 nm, 655 nm.



Figure 6.3: Image used to illustrate data processing. Landsat 8 scene from 13 January 2018 showing coastal and inland waters at Terraba Sierpe, Costa Rica. Preview settings: Bands 1, 3, 4; contrast 12.

### 6.5.1 Preprocessing

WASI can only process reflectance or radiance data at bottom of the atmosphere, hence the sensor data need some preprocessing before import to WASI. The first steps are calibration and geo-referencing, resulting in a georeferenced image in units of at-sensor radiance with

spectrally well-known band characteristics. This product, known as Level-1b data, is usually created by the data provider. The next step is atmospheric correction. It provides the data in the units required by WASI, i.e., reflectance or upwelling radiance directly above the water surface. Many data providers offer this so-called Level-2 product additionally to the Level-1b data.

The Landsat 8 image shown in Figure 6.3 has been atmospherically corrected using the commercial software ATCOR 4 (courtesy of Nicole Pinnel, DLR). The log file created by ATCOR contains (in xml format) useful information for further processing with WASI: sun elevation  $49.4^\circ$ , horizontal visibility 78 km, ozone column 331 Dobson units. The conversion to units required by WASI is done as follows:

- $\theta_{\text{sun}}$ . The sun zenith angle ‘sun’ is  $90^\circ - \text{sun elevation}$ . Here,  $\theta_{\text{sun}} = 40.6^\circ$ .
- $\beta$ . The turbidity coefficient ‘beta’ is related to horizontal visibility V and aerosol scale height  $H_a$  via  $\beta = \tau_a(550) = 3.91 \cdot H_a/V$  (see section 2.8.1). Here with  $H_a = 1 \text{ km}$ :  $\beta = 0.05$ .
- $H_{\text{oz}}$ . The Dobson units for ozone concentration ‘ $H_{\text{oz}}$ ’ must be divided by 1000 to convert them to cm. Here,  $H_{\text{oz}} = 0.331 \text{ cm}$ .

### 6.5.2 Define mask

WASI can use an arbitrary band of a multi- or hyperspectral image to mask all bands of that image based on a lower and upper brightness threshold. If a land-water mask is included as separate band of the image, it should be selected, but usually such a specific mask is not available. In that case a band should be chosen with a large brightness difference between land and water. Near infrared bands are often well suited since clear water absorbs very strongly above 700 nm, and even more above 800 nm, while vegetation is highly reflecting above  $\sim 740$  nm. The longer the wavelength, the more pronounced are usually the brightness differences between land and water. The example of Figure 6.4 shows that water appears very dark in band 7 of Landsat-8 (1610 nm), while land and clouds are gray or white. This band is therefore useful to define a mask.

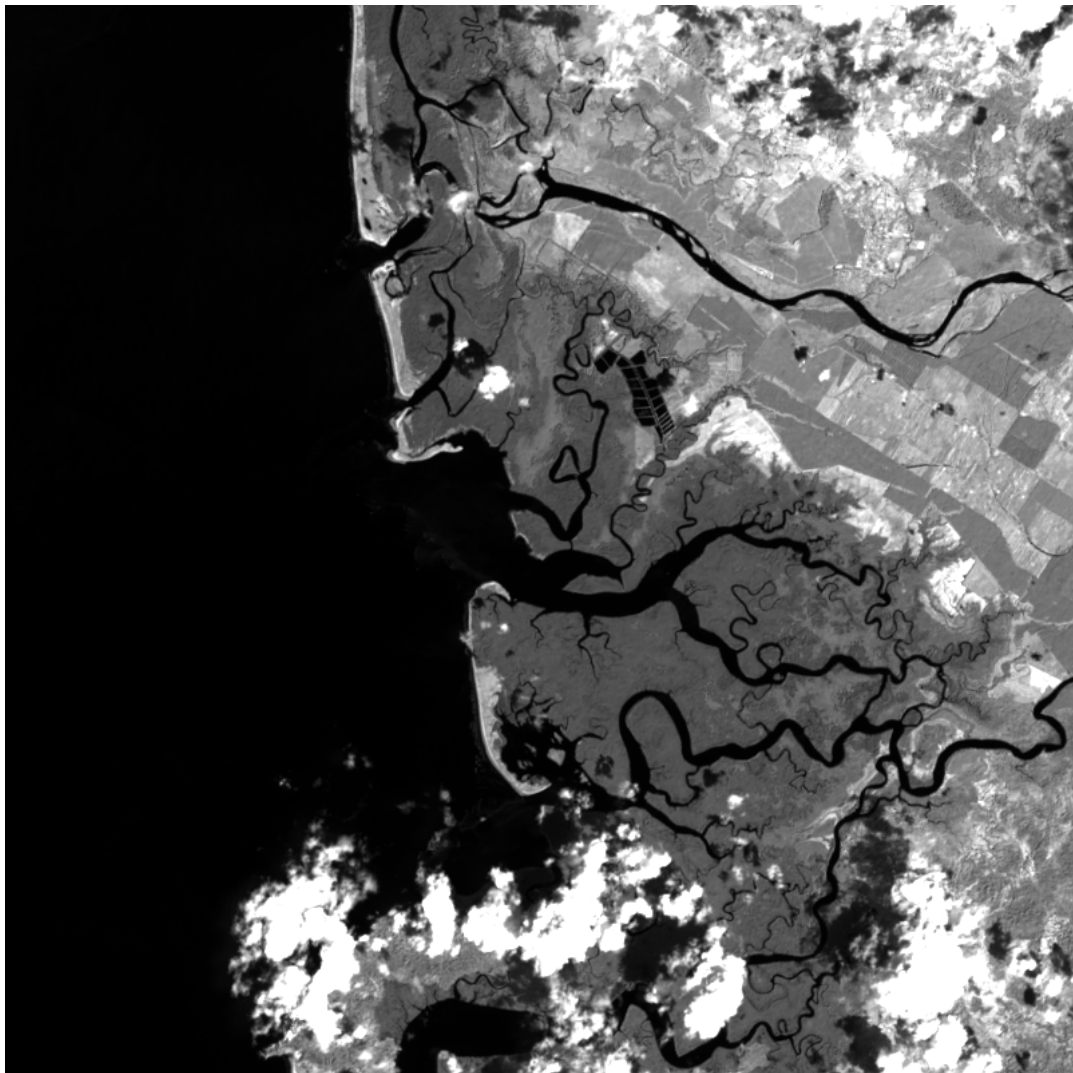


Figure 6.4: Band 7 centered at 1610 nm is used to mask non-water areas.

The mask is defined in WASI by specifying a lower and an upper brightness threshold in the "Mask" panel of Figure 6.1. The lower threshold is usually zero. A first guess for the upper threshold can be obtained with WASI by moving the mouse across the image and observing the typical values of water and non-water pixels. After entering the first guess in the 'Mask values above' field of the 'Mask' panel, the selected band is masked as shown in Figure 6.5. If too many water pixels are masked, the chosen value should be increased; if too many non-water pixels remain, the value should be reduced. Most critical are usually cloud shadows, which can be as dark as water or even darker.

*Note:* Masked water pixels are lost for data analysis, while non-masked land pixels can usually be identified as non-water pixels in the processed image and masked at a later stage. Thus conservative masking is recommended in case no band is available that allows a clear separation between land and water.

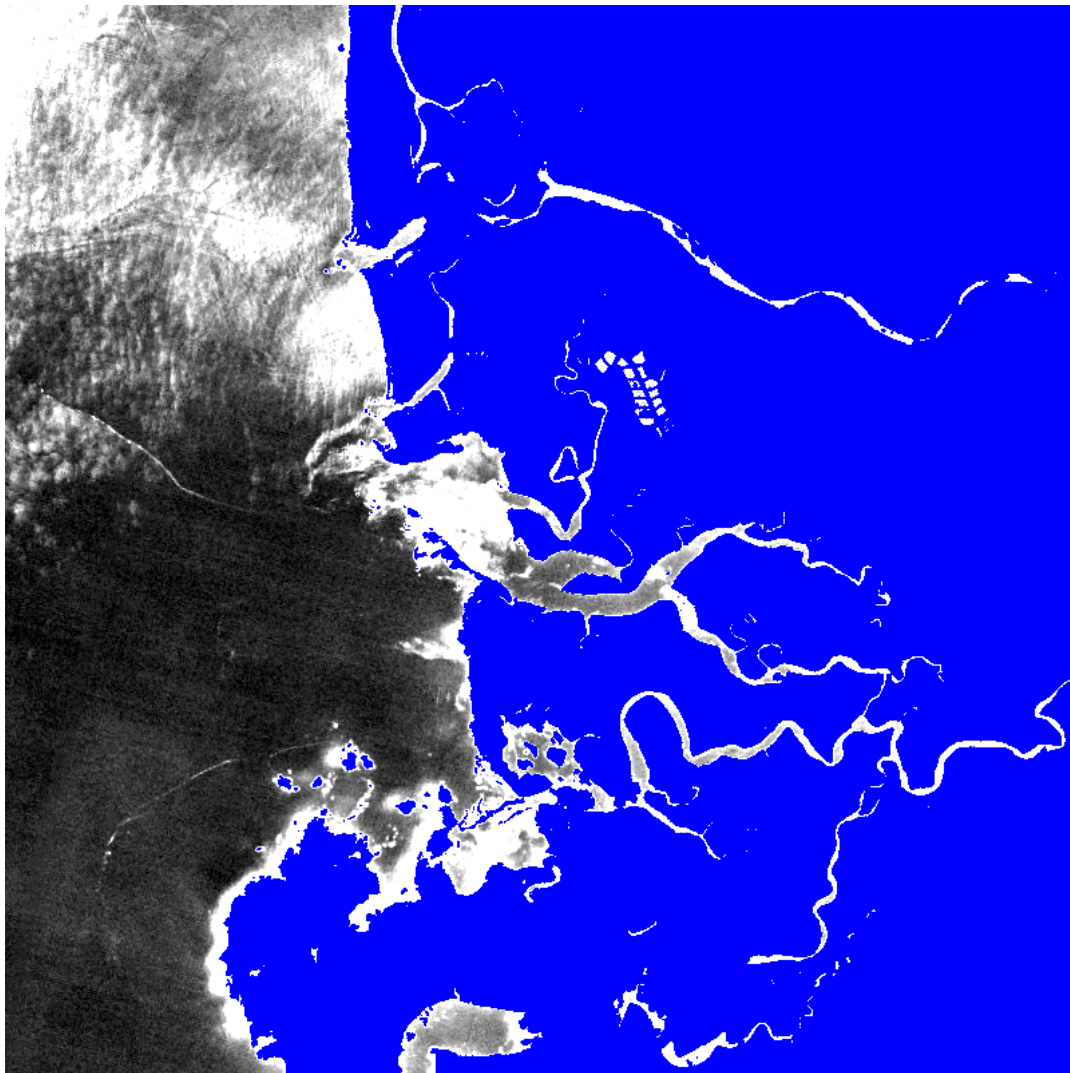
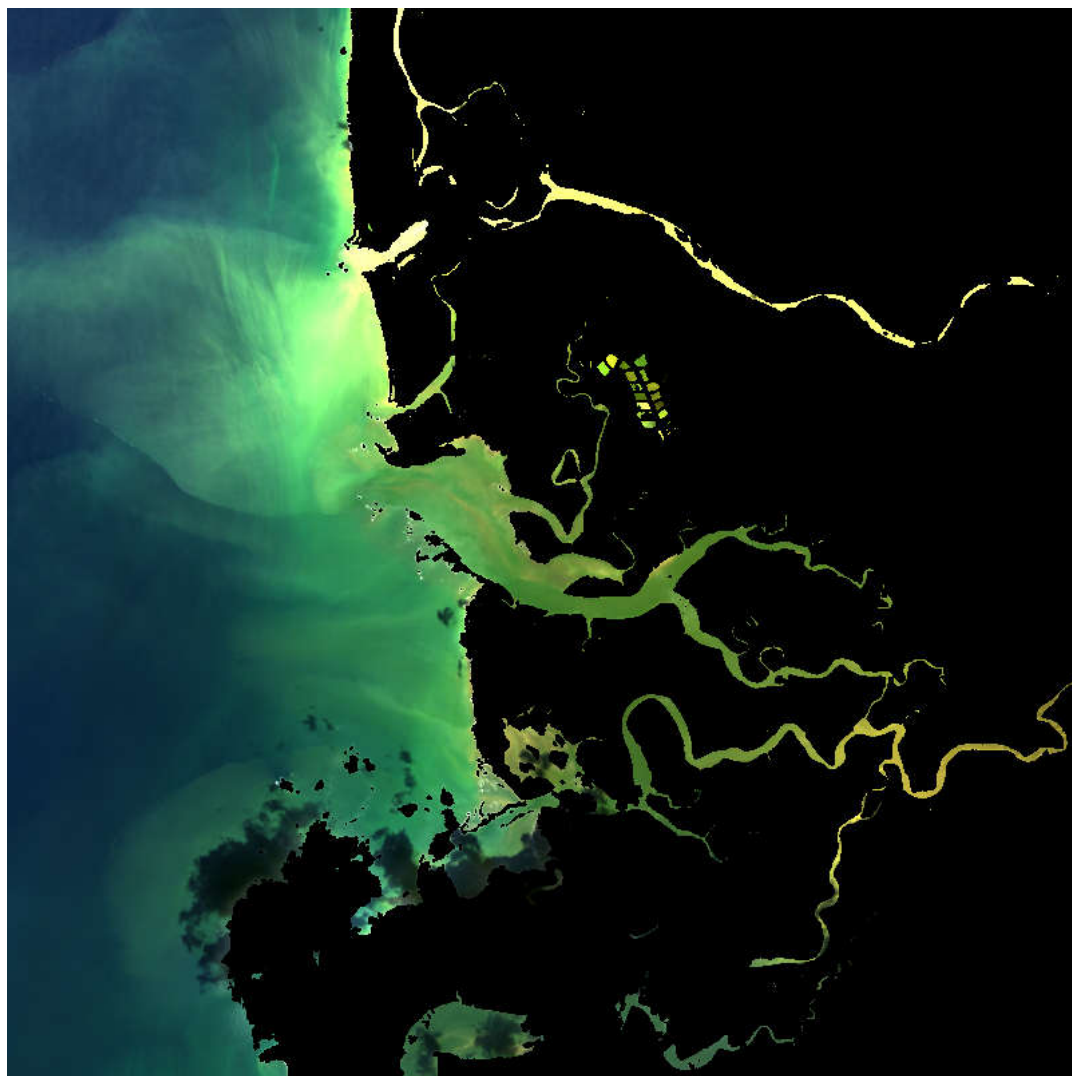


Figure 6.5: Band 7 with the masked pixels shown in blue. Preview settings: band 7, range 0 to 0.003, contrast 4. Mask settings: mask band 7, mask values below 0, mask values above 0.003.

### 6.5.3 Load masked image

After the mask has been defined as described in section 6.5.2, a masked color image can be displayed by checking ‘3 bands’ in the ‘Preview image’ panel shown in Figure 6.1. After the bands have been selected, the image must be loaded again for updating the preview. Figure 6.6 shows the masked version of the image from Figure 6.3. If the water areas appear too dark or too bright, the contrast should be increased or decreased, respectively. Water can now be better distinguished from land, and since the contrast is now adjusted to water, more details can be seen in the water areas of Figure 6.6 compared to Figure 6.3. The comparison with Figure 6.3 shows that the gray areas in the lower part of Figure 6.6 are cloud shadows.



**Figure 6.6:** Masked image used for further processing. Preview settings: bands 1, 3, 4; contrast 3. Mask settings: mask band 7, mask values below 0, mask values above 0.003. The color of the mask was changed to black compared to Figure 6.5.

#### 6.5.4 Select preview parameter

The progress of data processing is visualized by changing the color of the latest processed pixel to a gray value which corresponds to the result of a certain fit parameter (see Figure 6.8). The parameter and its range are selected in the ‘Preview during inverse modeling’ panel of Figure 6.1. Values below or equal to ‘Range: from’ are coded black, values above or equal to ‘Range: to’ are coded white, and the other values are coded on a linear gray scale for the chosen range.

### 6.5.5 Define fit settings

In this step the user has to choose the model parameters and to decide which parameters to fit and which to keep constant for data analysis. The options provided by WASI and the recommended strategy of data analysis are described in chapter 4. The strategy can be summarized as follows:

**Use pre-knowledge.** Whenever a good guess of a parameter is available, it should be used. In this example, the parameters ‘sun’, ‘H\_oz’ and ‘beta’ are known from pre-processing (see section 6.5.1), hence their values are taken (green marks in Figure 6.7).

**Set boundary conditions for fit.** Choose the wavelength range, maximum residual and maximum number of iterations as described in sections 4.2.3 and 4.2.4. Since the parameter values of adjacent pixels are usually similar, it is recommended to deactivate ‘Initial values identical for all spectra’ in the ‘Initial values’ register card of the pop-up window ‘Fit tuning’ (Figure 4.8).

**Estimate parameter ranges.** The high contrast of Figure 6.6 allows distinguishing between different water types. This makes it possible to identify representative areas and to analyze their spectra as described in chapter 4. Clicking the mouse brings the spectrum of the selected pixel to the main window; drawing a rectangle with the mouse extracts the mean spectrum and the standard deviation. It is recommended to apply inverse modeling to a few spectra that represent the color range in the area of interest. In this way the approximate range of each potential fit parameter can be determined.

**Decide which parameters to fit and which to keep constant.** The interactive analysis of a few pixels from the previous step allows ranking the parameters according to their contribution to the observed variability within the area of interest. Parameters that have a clear influence on the reflectance spectrum and change significantly should be selected as fit parameters, the others as constants. The number of fit parameters should always be kept as low as possible to minimize errors introduced by spectral ambiguities.

Figure 6.7 shows the chosen settings for the Landsat 8 example. The water is known to be deep and turbid, hence the deep water model is applied, making the shallow water parameters zB and fA[i] irrelevant. The interactive fit of a few pixels showed that the standard set of fit parameters for optically deep water (C[0], C\_X, C\_Y and g\_dd) can be used to model conveniently the reflectance spectra of the studied pixels. These were therefore selected as fit parameters, with the typical values found in the pre-fits used for initialization (red marks in Figure 6.7).

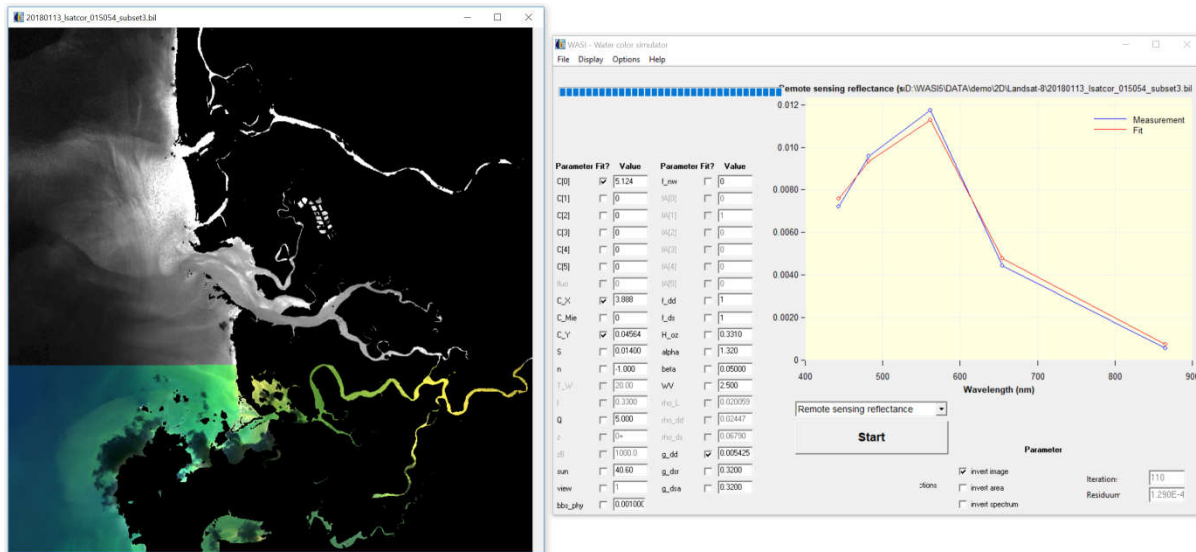
Parameter Fit?	Value	Parameter Fit?	Value
C[0]	<input checked="" type="checkbox"/> 5	f_nw	<input type="checkbox"/> 0
C[1]	<input type="checkbox"/> 0	fA[0]	<input type="checkbox"/> 0
C[2]	<input type="checkbox"/> 0	fA[1]	<input type="checkbox"/> 1
C[3]	<input type="checkbox"/> 0	fA[2]	<input type="checkbox"/> 0
C[4]	<input type="checkbox"/> 0	fA[3]	<input type="checkbox"/> 0
C[5]	<input type="checkbox"/> 0	fA[4]	<input type="checkbox"/> 0
fluo	<input type="checkbox"/> 0	fA[5]	<input type="checkbox"/> 0
C_X	<input checked="" type="checkbox"/> 4	f_dd	<input type="checkbox"/> 1
C_Mie	<input type="checkbox"/> 0	f_ds	<input type="checkbox"/> 1
C_Y	<input checked="" type="checkbox"/> 0.3	H_oz	<input type="checkbox"/> 0.3310
S	<input type="checkbox"/> 0.014	alpha	<input type="checkbox"/> 1.320
n	<input type="checkbox"/> -1.000	beta	<input type="checkbox"/> 0.05
T_W	<input type="checkbox"/> 20.00	wv	<input type="checkbox"/> 2.5
f	<input type="checkbox"/> 0.3300	rho_L	<input type="checkbox"/> 0.020059
Q	<input type="checkbox"/> 5.000	rho_dd	<input type="checkbox"/> 0.0245
z	<input type="checkbox"/> 0+	rho_ds	<input type="checkbox"/> 0.0679
zB	<input type="checkbox"/> 1000.0	g_dd	<input checked="" type="checkbox"/> 0.02000
sun	<input type="checkbox"/> 40.6	g_dsr	<input type="checkbox"/> 0.3200
view	<input type="checkbox"/> 1	g_dsa	<input type="checkbox"/> 0.3200
bbs_phy	<input type="checkbox"/> 0.00100C		

Figure 6.7: Parameter settings for processing the masked Landsat 8 image shown in Figure 6.6. The green marked values are known from preprocessing, the red marked values have been determined by fitting a few representative water pixels of the image, the other values are the defaults of WASI.

### 6.5.6 Run fit

Image data processing is activated by checking ‘invert image’ and pressing the ‘Start’ button. Since the result is stored to file, a file name has to be selected. After the suggested file name is accepted or the own choice is entered, processing starts with the pixel top left and ends with the pixel bottom right. Masked pixels are skipped, non-masked pixels are fitted.

After a pixel has been processed, its color changes to a gray value as explained in section 6.5.4. This allows observing the progress of data processing and identifying potential artifacts in the image of the diagnostic parameter. The correspondence between measured spectra and fit curves can be watched during data processing since an overlay of both curves is continuously updated during processing. A screenshot of the GUI during processing is shown in Figure 6.8. If the preview of the selected fit parameter has unexpected artifacts or the fit curve disagrees frequently from the measurement, data processing should be interrupted using `ctrl-c` and launched again after changing the fit settings or updating the database.



**Figure 6.8:** Screenshot of WASI-2D during data processing. Left: Image preview with the processed pixels in gray, representing the fit parameter  $C_X$  in the range  $0\text{--}10 \text{ g m}^{-3}$ . Right: Fit results of the last processed pixel (fitted values in parameter list, overlay of measurement and fit curve in plot window).

### 6.5.7 Visualize results

The result of data analysis is an image with the file extension `.fit` in ENVI format. It consists of  $N+3$  bands, with  $N$  the number of fit parameters. This image is stored by default in the subdirectory `/fit` of the directory with the image data.

When loading an image with the extension `.fit`, WASI assumes that it is the result of fitting and activates two special features:

**Legend.** A color bar with the parameter name and the selected parameter range is displayed above the image (Figure 6.9, large window).

**Extended pixel info.** Moving the mouse over the image opens a small window (Figure 6.9, small window in the foreground). It lists on the right side the parameter names of all bands. On the left side it shows the coordinates and the parameter value of the selected band at the position of the mouse pointer.

After an image is loaded, a bitmap is automatically stored as file `WASI_img.bmp` in the directory `/WASI5/data/demo/tmp`. It shows the selected band for the complete image, even if it is larger than the preview window and only a part is displayed on screen.

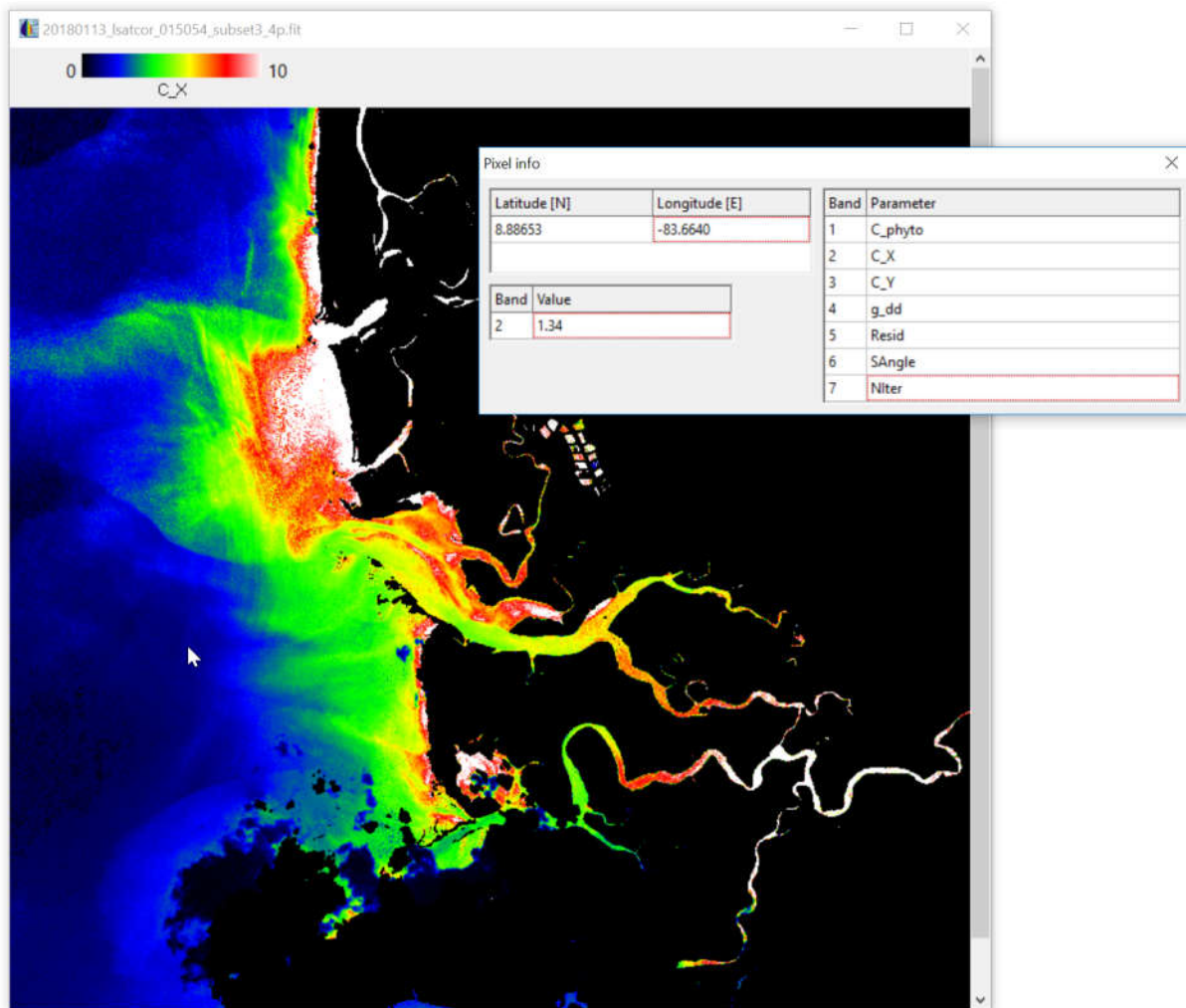


Figure 6.9: Visualization of a fit parameter image in WASI. Large window: Color-coded image of a single fit parameter with legend on top. Small window, left half: coordinates and parameter value of the pixel under the mouse pointer. Small window, right half: Parameter names of all bands.

## 7. Background mode

Alternatively to the usual interactive mode of operation, WASI can also be started from another program through the command

```
WASI5 INI_File
```

In this case the file `INI_File` is read instead of `WASI5.INI`, then calculation is started automatically without opening the graphical user interface, and finally WASI is terminated after the calculations are finished.

This mode of operation is useful for combining WASI with another program. For example, WASI has been combined with a radiative transfer simulation program for the atmosphere (6S) to estimate the influence of errors in atmospheric correction on the retrieval of phytoplankton, Gelbstoff and suspended matter from MERIS and MODIS data (Pyhälähti and Gege, 2001).

## 8. Model options

### 8.1 Downwelling irradiance

The spectrum type "Downwelling irradiance" is activated by selecting in the main window "Downwelling irradiance" from the drop-down list above the "Start" button, see Figure 8.1 right. After the spectrum type is selected, the check box "above water" appears on the screen, and the relevant parameters are activated in the parameter list (Figure 8.1 left). The example of Figure 8.1 shows the parameters of the irradiance model below the water surface (equation (2.50)).

Parameter	Value	Parameter	Value
C[0]	2.000	f_nw	0
C[1]	0	fA[0]	1
C[2]	0	fA[1]	0
C[3]	0	fA[2]	0
C[4]	0	fA[3]	0
C[5]	0	fA[4]	0
fluo	0	fA[5]	0
C_X	0.6000	f_dd	1
C_Mie	0	f_ds	1
C_Y	0.3000	H_oz	0.3000
S	0.01400	alpha	1.317
n	-1.000	beta	0.2606
T_W	20.00	wv	2.500
f	0.3300	rho_L	0.02006
Q	5.000	rho_dd	0.02111
z	0	rho_ds	0.06790
zB	5.000	g_dd	0.02000
sun	30.00	g_dsr	0.3180
view	0	g_dsa	0.3180
bbs_phy	0.00100C		

Downwelling irradiance
   

  
 above water

**Figure 8.1:** Parameter settings of the spectrum type "Downwelling irradiance". Left: Parameter list for in-water calculation. Right: Drop-down list with "Downwelling irradiance" selected as spectrum type and "above water" check box.

A number of options are available for calculating downwelling irradiance. These are set in the register card shown in Figure 8.2. It is accessed from the menu bar via "Options – Models - Irradiance".

The first panel "Reflection factors for downwelling irradiance" is used to specify how reflection of downwelling irradiance at the water surface is calculated. The reflection factor for the direct component,  $\rho_{dd}$ , is calculated by default using the Fresnel equation (the box "Calculate

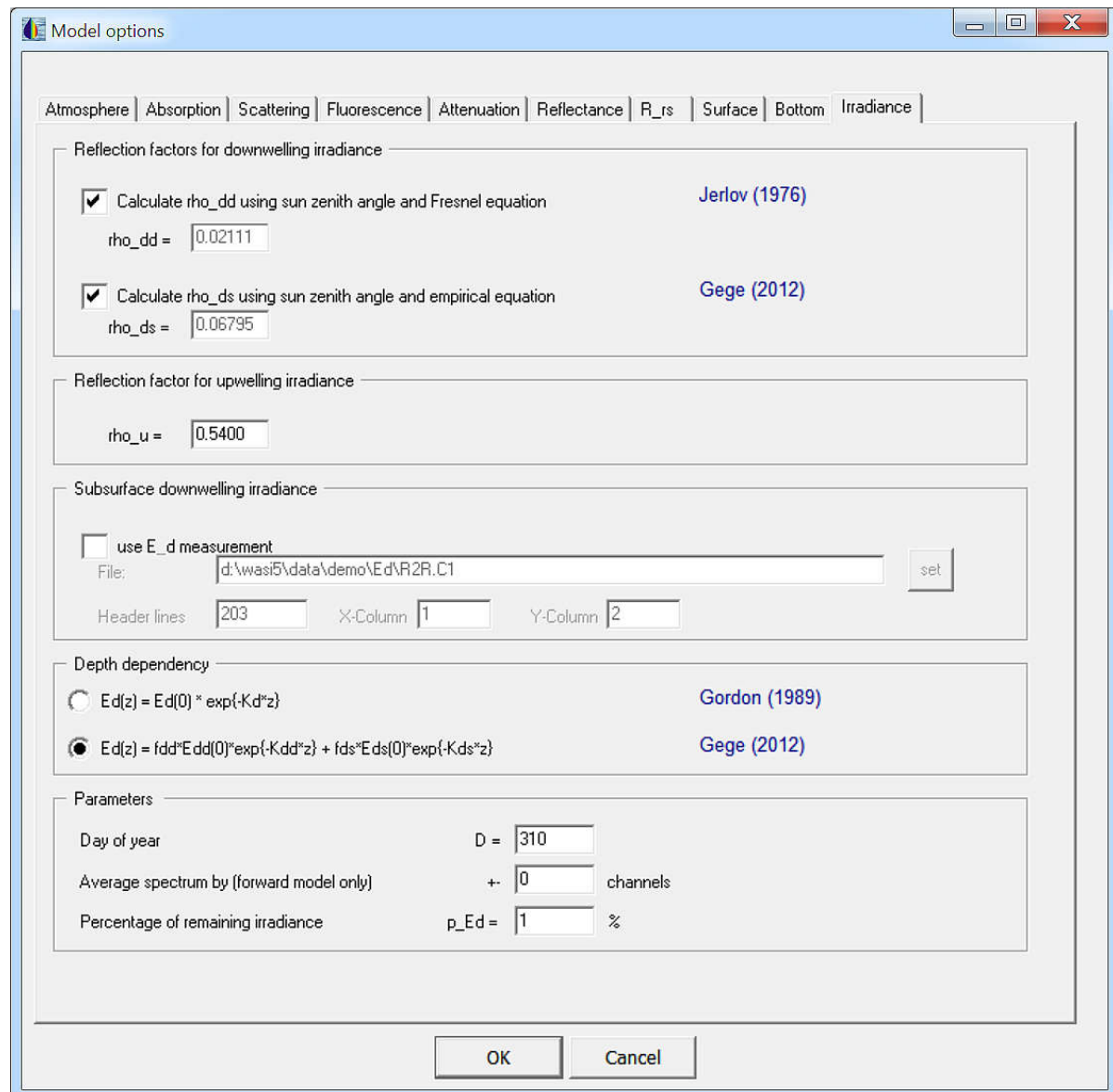


Figure 8.2: The register card "Irradiance" of the pop-up window "Options – Model".

`rho_dd using sun zenith angle and Fresnel equation` is checked). Alternately, a user-defined value can be used (by unchecking that box and entering the desired value in the "rho\_dd" field). Similarly, the reflection factor for the diffuse component,  $\rho_{ds}$ , can either be calculated using equation (2.52) by checking the box "Calculate rho\_ds using sun zenith angle and empirical equation", or the value of  $\rho_{ds}$  can be specified by the user in the "rho\_ds" edit box. The second panel "Reflection factor for upwelling irradiance" is used to specify the value of  $\rho_u$ .

## 8.2 Irradiance reflectance

The spectrum type "Irradiance reflectance" is activated by selecting this type in the main window from the drop-down list above the "Start" button, see Figure 8.3 right. After the spectrum type is selected, the check box "shallow water" appears on the screen, and the relevant parameters are activated in the parameter list (Figure 8.3 left). Irradiance reflectance is always calculated in water, thus no "above water" selection box is shown like in Figure 8.1.

Parameter	Value	Parameter	Value
C[0]	2.000	f_nw	0
C[1]	0	fA[0]	1
C[2]	0	fA[1]	0
C[3]	0	fA[2]	0
C[4]	0	fA[3]	0
C[5]	0	fA[4]	0
fluo	0	fA[5]	0
C_X	0.6000	f_dd	1
C_Mie	0	f_ds	1
C_Y	0.3000	H_oz	0.3000
S	0.01400	alpha	1.317
n	-1.000	beta	0.2606
T_W	20.00	wv	2.500
f	0.3300	rho_L	0.02006
Q	5.000	rho_dd	0.02111
z	0-	rho_ds	0.06795
zB	5.000	g_dd	0.02000
sun	30.00	g_dsr	0.3180
view	0	g_dsa	0.3180
bbs_phy	0.00100C		

Irradiance reflectance
   

  
 shallow water

Figure 8.3: Parameter settings of the spectrum type "Irradiance reflectance". Left: Parameter list for deep water calculation. Right: Drop-down list with "Irradiance reflectance" selected as spectrum type and "shallow water" check box.

Irradiance reflectance spectra  $R(\lambda)$  are calculated using the Gordon algorithm, Eq. (2.27), or the Prieur algorithm,  $R(\lambda) = f \cdot b_b(\lambda) / a(\lambda)$ . Both algorithms parameterize  $R(\lambda)$  as a function of absorption and backscattering and thus require as parameters the concentrations of the different phytoplankton classes ( $C_i = C[i]$ ,  $i = 0, 1, \dots, 5$ ), of non-algal particles ( $C_X = C_X$  for type I,  $C_{Mie} = C_{Mie}$  for type II) and of CDOM ( $C_Y = C_Y$ ), and the Angström exponent (n), water temperature ( $T = T_W$ ), proportionality factor (f), and eventually CDOM absorption exponent (S). f can either be treated as a parameter, or it can be calculated as a function of absorption, backscattering and the sun zenith angle.

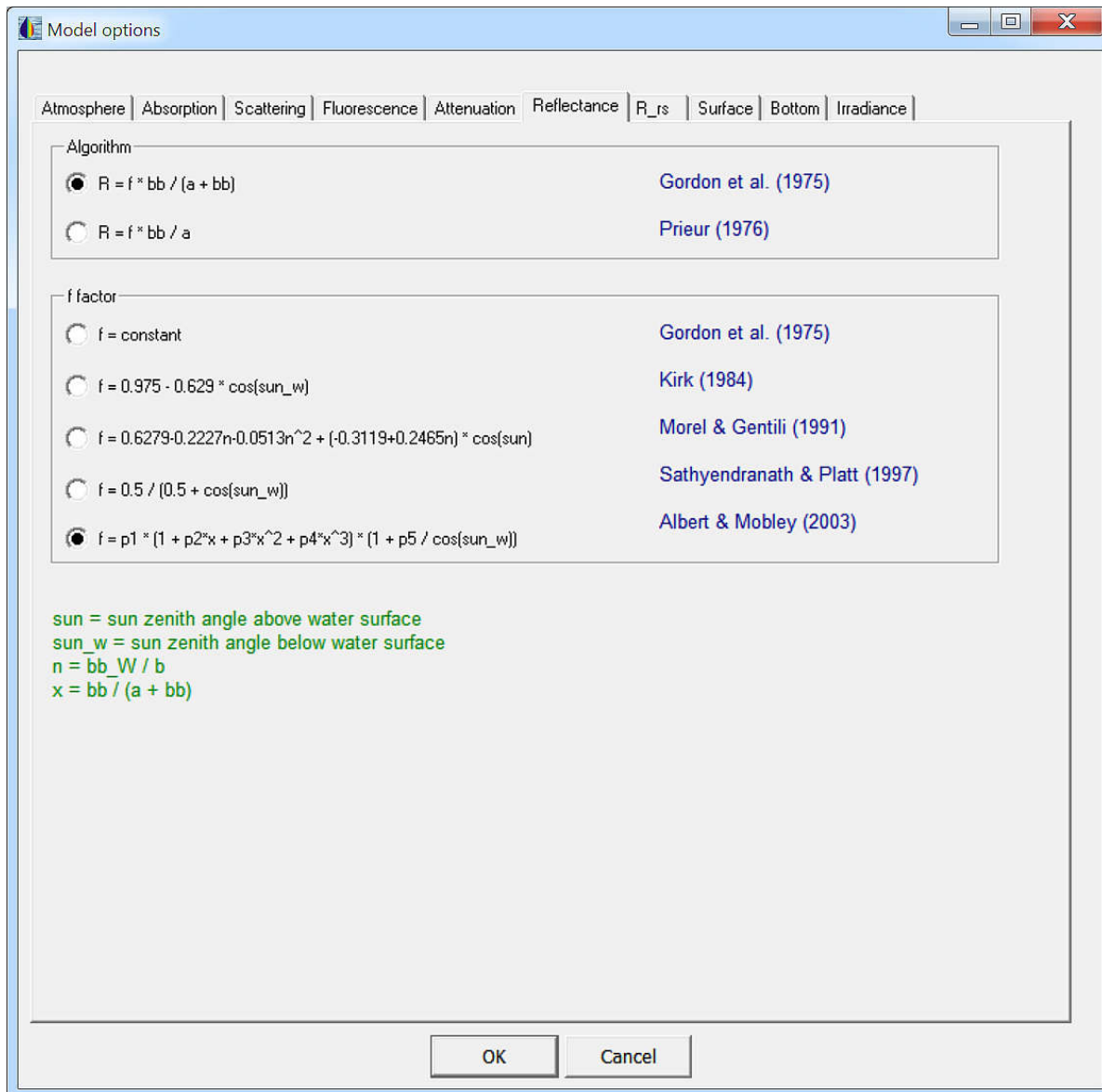


**Figure 8.4:** The register card "Reflectance" of the pop-up window "Model options".

The R algorithm and the f calculation method are selected in the "Reflectance" register card of the "Model options" pop-up window, which is shown in Figure 8.4. The pop-up window is accessed from the menu bar via "Options – Models".

The factor of proportionality,  $f$ , depends on the scattering properties of the water and on the illumination geometry. In WASI,  $f$  can either be treated as a parameter, or it can be calculated using one of the following algorithms:

$$f = 0.975 - 0.629 \cdot \cos \theta'_{\text{sun}} \quad (8.1)$$

$$f = 0.6279 - 0.2227 \cdot \eta_b - 0.0513 \cdot \eta_b^2 + (-0.3119 + 0.2465 \cdot \eta_b) \cdot \cos \theta_{\text{sun}} \quad (8.2)$$

$$f = \frac{0.5}{0.5 + \cos \theta_{\text{sun}}} \quad (8.3)$$

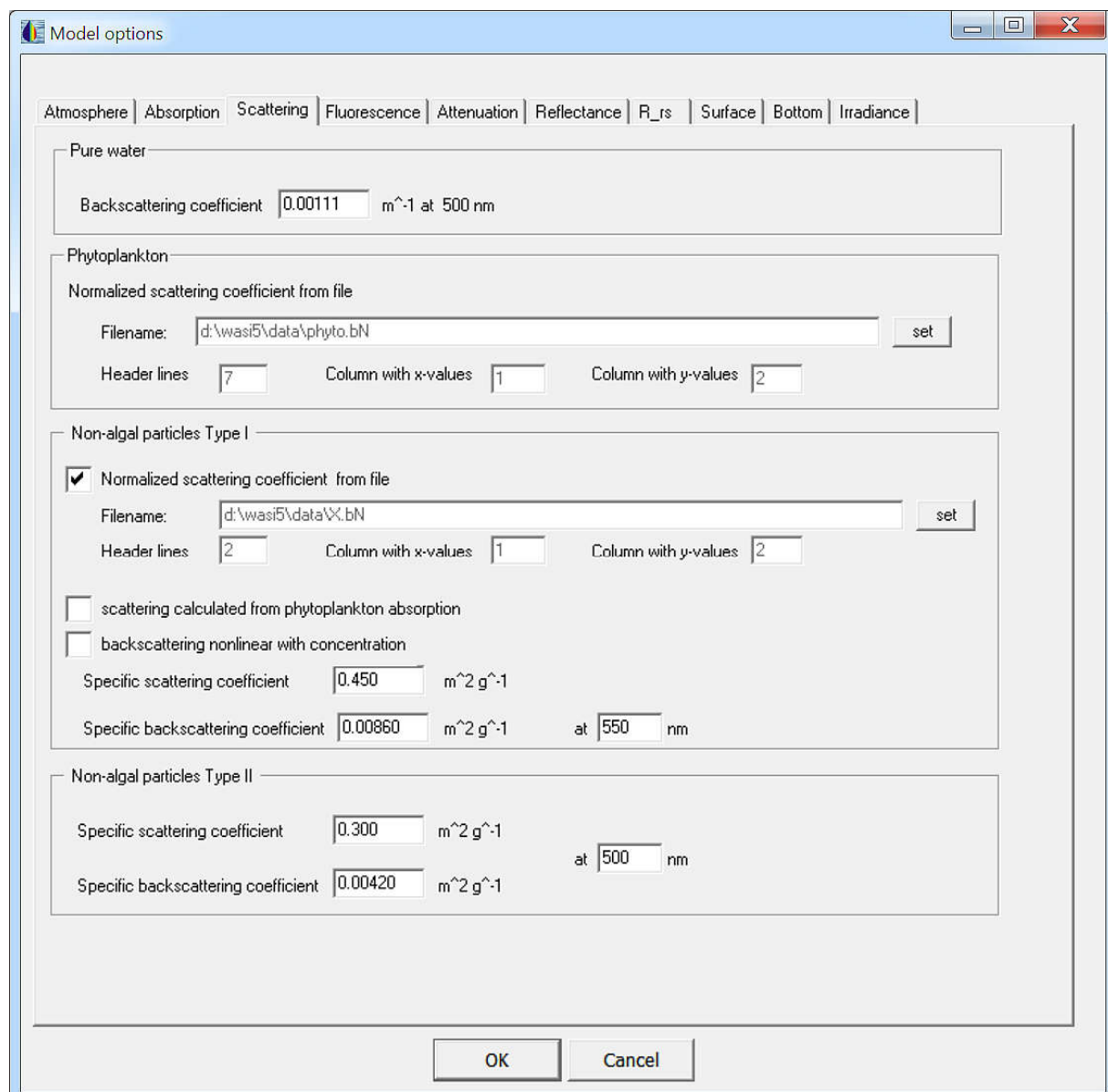


Figure 8.5: The register card "Scattering" of the pop-up window "Model options".

$$f = 0.1034 \cdot (1 + 3.3586 \cdot x - 6.5358 \cdot x^2 + 4.6638 \cdot x^3) \cdot \left(1 + \frac{2.4121}{\cos \theta'_{\text{sun}}}\right). \quad (8.4)$$

Equation (8.1) is from Kirk (1984), (8.2) from Morel and Gentili (1991), (8.3) from Sathyendranath and Platt (1997), and (8.4) from Albert and Mobley (2003).  $\theta_{\text{sun}}$  is the sun zenith angle above the water surface,  $\theta'_{\text{sun}}$  below the surface. The factor  $\eta_b$  in Eq. (8.2) is the ratio  $b_{b,w}/b_b$ . The factor  $x$  in Eq. (8.4) is  $b_b/(a+b_b)$  for the Gordon algorithm and  $b_b/a$  for the Prieur algorithm.

The options for calculating absorption are described in section 8.3. Those for calculating scattering and backscattering are set in the register card "Scattering" of the pop-up window "Model options", see Figure 8.5.

### Backscattering by particles of type I

In Figure 8.5 the box "correlate with phytoplankton" determines whether  $C_X$  of Eq. (2.16) is treated as an independent parameter (no hook), or if  $C_X = C_0$  is set, with  $C_0 = C[0]$  denoting phytoplankton concentration (hook). In case-1 water types suspended matter is highly correlated with phytoplankton, hence it is suggested to mark the box for case-1 waters, but not for case-2 waters.

The boxes "scattering function from file" and "scattering function calculated from phytoplankton absorption" are exclusive, i.e. one of both is marked with a hook. They determine how the function  $b_X(\lambda)$  of Eq. (2.16) is selected: it is either read from file ("scattering function from file" is marked) or it is calculated from the specific absorption spectrum of phytoplankton (the other box is marked). Calculation is useful when suspended matter and phytoplankton are highly correlated, i.e. for case-1 waters; otherwise a spectrum independent from phytoplankton should be taken. If no information about the spectral dependency of particle backscattering is available, it is a good idea to use a constant function  $b_X(\lambda) = 1$ . This provides good results for instance in Lake Constance (Heege 2000). By default,  $b_X(\lambda) = 1$  is read from the file `x.b`. To assign another file, select it by pressing the "set" button.

The box "nonlinear with concentration" determines whether the specific backscattering coefficient  $b_{b,X}^*$  of Eq. (2.16) is treated as constant (no hook), or if it is calculated as  $A \cdot C_L^B$  (hook).  $B$  is the value in the input field "Power of  $C_L$ ", which is visible only in the nonlinear case. The value in the input field "Specific backscattering coefficient" corresponds to  $b_{b,L}^*$  in the linear case, and to  $A$  in the nonlinear case. The "at ... nm" input field of Figure 8.5 specifies the wavelength where the specific backscattering coefficient is valid. After a scattering function is read from file or calculated from phytoplankton absorption, it is normalized at that wavelength.

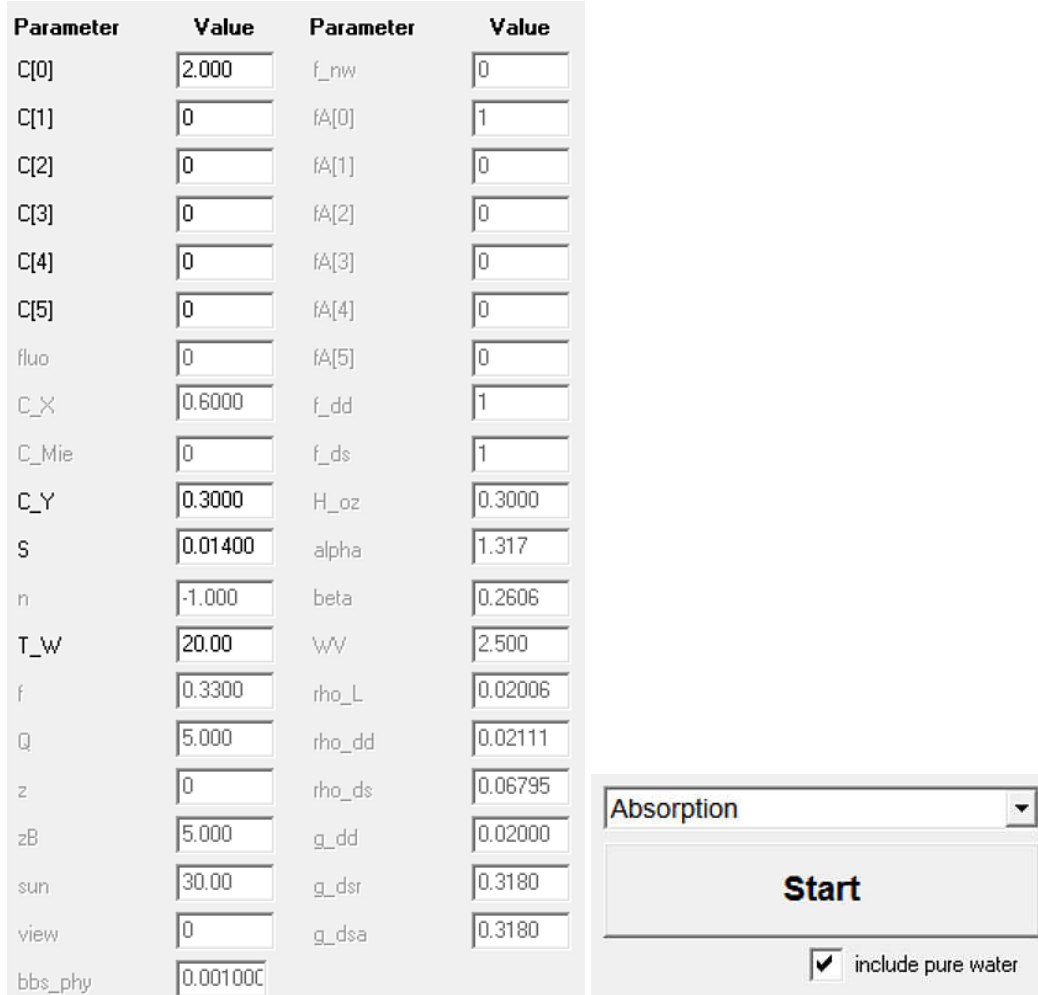
### Backscattering by particles of type II

The value in the input field "Specific backscattering coefficient" of the "Suspended particles type II" section of Figure 8.5 corresponds to  $b_{b,Mie}^*$  of Eq. (2.16). The "at ... nm" input field specifies the wavelength  $\lambda_S$  of Eq. (2.16).

### 8.3 Absorption

The spectrum type "Absorption" is activated by selecting in the main window "Absorption" from the drop-down list above the "Start" button, see Figure 8.6 right. After the spectrum type is set to "Absorption", the check box "include pure water" (Figure 8.6 right) appears on the screen, and the relevant parameters are activated in the parameter list (Figure 8.6 left).

The spectrum type "Absorption" supports two options: include or exclude pure water absorp-



Parameter	Value	Parameter	Value
C[0]	2.000	f_nw	0
C[1]	0	fA[0]	1
C[2]	0	fA[1]	0
C[3]	0	fA[2]	0
C[4]	0	fA[3]	0
C[5]	0	fA[4]	0
fluo	0	fA[5]	0
C_X	0.6000	f_dd	1
C_Mie	0	f_ds	1
C_Y	0.3000	H_oz	0.3000
S	0.01400	alpha	1.317
n	-1.000	beta	0.2606
T_W	20.00	wv	2.500
f	0.3300	rho_L	0.02006
Q	5.000	rho_dd	0.02111
z	0	rho_ds	0.06795
zB	5.000	g_dd	0.02000
sun	30.00	g_dsr	0.3180
view	0	g_dsa	0.3180
bbs_phy	0.00100C		

**Figure 8.6:** Parameter settings of the spectrum type "Absorption". Left: Parameter list. Right: Drop-down list with "Absorption" selected as spectrum type and "include pure water" check box.

tion. If pure water absorption is included (check box is marked with a hook), the absorption spectrum of the water body is calculated using Eq. (2.1). Otherwise (no hook) absorption of the water constituents alone is calculated using Eq. (2.2).<sup>7</sup>

Parameters of the absorption model are the concentrations of the 6 phytoplankton classes ( $C_i = C[i]$ ,  $i = 0, 1, \dots, 5$ ), the concentration of non-algal particles ( $C_X = C_X$ ,  $C_{Mie} = C_{Mie}$ ), CDOM concentration ( $C_Y = C_Y$ ), and eventually the exponent of CDOM absorption ( $S$ ) and

<sup>7</sup> Most spectrum types included in WASI depend on the absorption of the water body. For all types which use absorption implicitly, the absorption spectrum includes pure water, i.e. absorption is calculated according to Eq. (2.1).

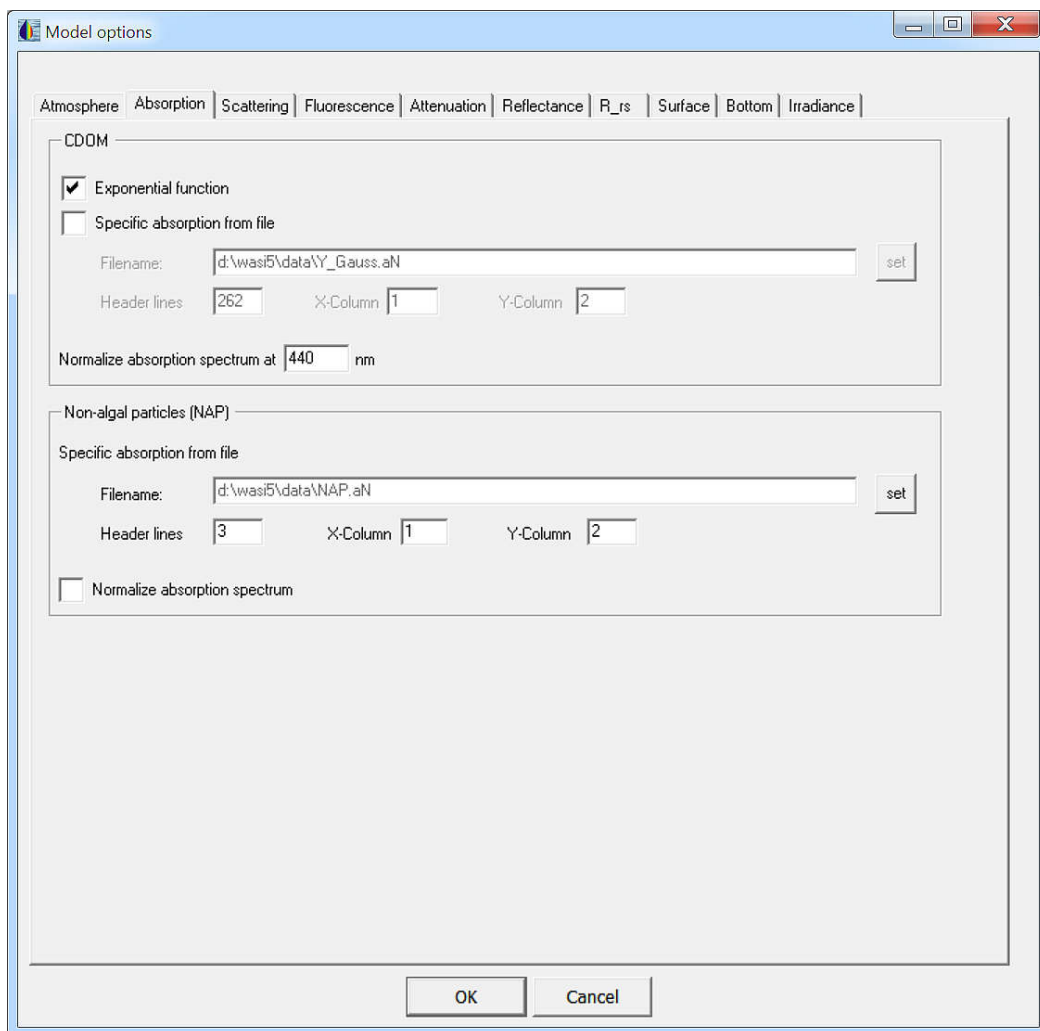


**Figure 8.7: The register card "Absorption" of the pop-up window "Model options".**

water temperature ( $T = T_W$ ).  $T$  is model parameter if pure water absorption is included; it is not required for calculating absorption of the water constituents.

Whether  $S$  is model parameter or not depends on the choice of the normalized CDOM absorption spectrum  $a_Y^*(\lambda)$ . It can either be read from file, or it can be calculated using Eq. (2.5). The selection is done in the "Absorption" register card of the pop-up window "Model options", which is shown in Figure 8.7. The corresponding boxes "Exponential function" and "Specific absorption from file" are exclusive, i.e. one of both is marked with a hook. The input field "Normalize absorption spectrum at ... nm" specifies the wavelength  $\lambda_0$  where  $a_Y^*(\lambda)$  is normalized.

The input spectrum  $a_{NAP}^N(\lambda)$  for NAP absorption may be normalized after it is read from file, or not. The selection is done via the check box "Normalize absorption spectrum" of the "Detritus" section of Figure 8.7. Normalization is performed at the same wavelength  $\lambda_0$  as for CDOM. When  $a_{NAP}^N(\lambda)$  is normalized, NAP concentration  $C_{NAP}$  is given in units of absorption at the wavelength  $\lambda_0$ , otherwise it is given in the units of the input file. By default,  $a_{NAP}^N(\lambda)$  is normalized.

The 10 input spectra  $a_w(\lambda)$ ,  $daw/dT(\lambda)$ ,  $a_Y^*(\lambda)$ ,  $a_{NAP}^N(\lambda)$ ,  $a_i^*(\lambda)$  with  $i=0..5$ , are read from files. These can be replaced by other spectra by pressing the corresponding "set" button and selecting the file name.

## 8.4 Bottom reflectance

The spectrum type "Bottom reflectance" is activated by selecting this type in the main window from the drop-down list above the "Start" button, see Figure 8.8 right. After the spectrum type is set to "Bottom reflectance", the check box "radiance sensor" (Figure 8.8 right) appears on the screen, and the relevant parameters are activated in the parameter list (Figure 8.8 left).

Parameter	Value	Parameter	Value
C[0]	2.000	f_nw	0
C[1]	0	fa[0]	1
C[2]	0	fa[1]	0
C[3]	0	fa[2]	0
C[4]	0	fa[3]	0
C[5]	0	fa[4]	0
fluo	0	fa[5]	0
C_X	0.6000	f_dd	1
C_Mie	0	f_ds	1
C_Y	0.3000	H_oz	0.3000
S	0.01400	alpha	1.317
n	-1.000	beta	0.2606
T_W	20.00	wv	2.500
f	0.3300	rho_L	0.02006
Q	5.000	rho_dd	0.02111
z	0	rho_ds	0.06795
zB	5.000	g_dd	0.02000
sun	30.00	g_dsr	0.3180
view	0	g_dsa	0.3180
bbs_phy	0.001000		

Bottom reflectance
   

  
 radiance sensor

**Figure 8.8:** Parameter settings of the spectrum type "Bottom reflectance". Left: Parameter list. Right: Drop-down list with "Bottom reflectance" selected as spectrum type and "radiance sensor" check box.

If the box "radiance sensor" is checked, the bottom reflectance is calculated for a radiance sensor using Eq. (2.39). Otherwise, it is calculated for an irradiance sensor using Eq. (2.38).

Bottom albedo (irradiance reflectance) is calculated as a weighted sum of 6 albedo spectra. The weights  $f_n = fa[n]$ ,  $n = 0..5$ , are the relative areas of the 6 bottom types within the sensor's field of view. Consequently, it is  $\sum f_n = 1$ , thus only 5 of the  $f_n$  are independent parameters, while one is calculated using  $\sum f_n = 1$ . Which of the weights is adjusted in this manner is defined in the register card "Bottom" of the pop-up window "Model options", see Figure 8.9. It is accessed from the menu bar via "Options – Models" (see Figure 10.1). The selection is

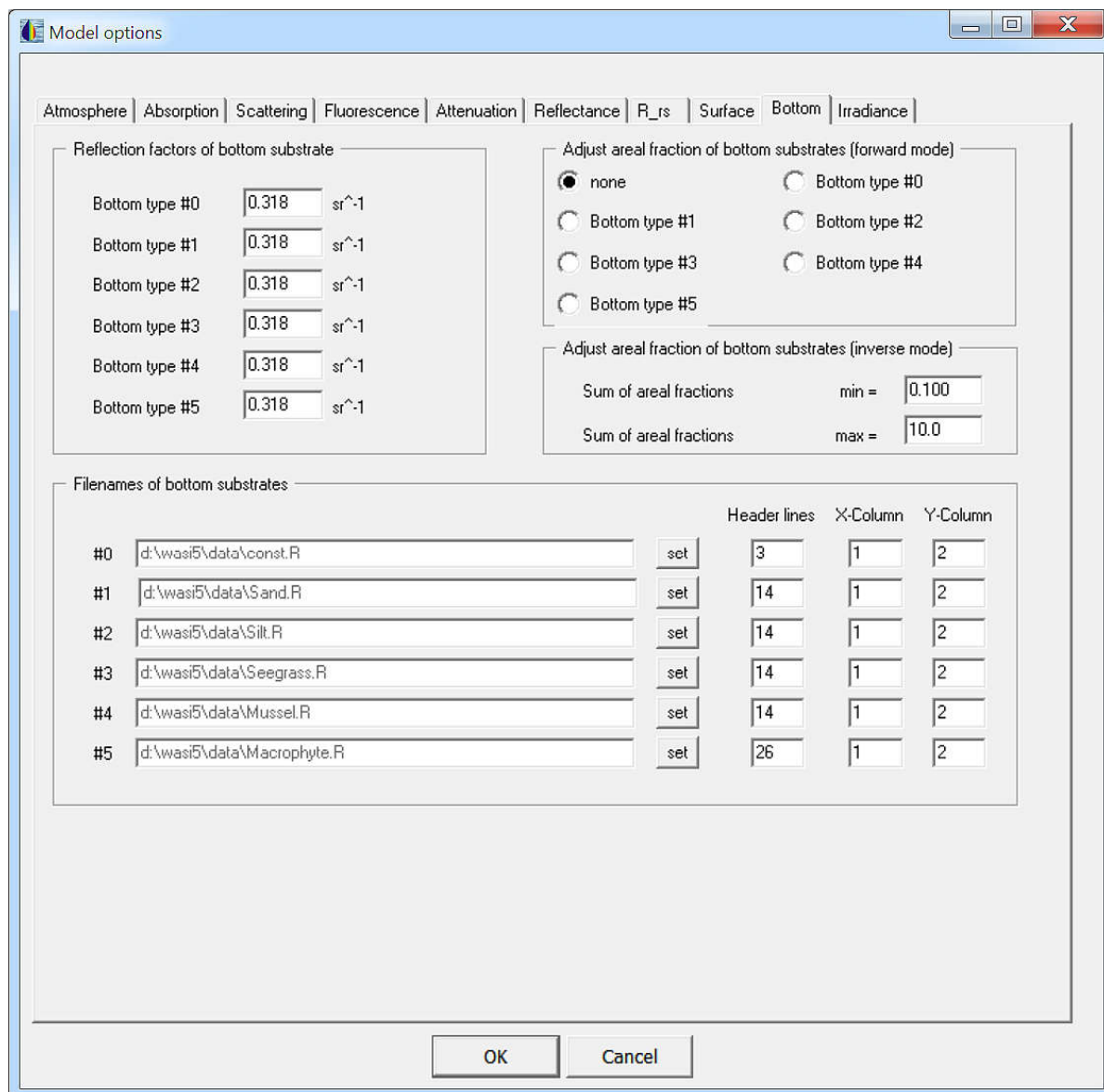


Figure 8.9: The register card "Bottom" of the pop-up window "Model options".

done in the box "Adjust areal fraction of bottom substrates (forward mode)". If "none" is selected, the weights are not automatically adjusted.

For a radiance sensor the bottom reflectance spectra are weighted additionally to  $f_n$  with reflection factors  $B_n$ , which are the ratio of radiance reflected in the direction of the sensor relative to the downwelling irradiance. For an isotropic (Lambertian) reflecting surface it is  $B_n = 1/\pi = 0.318 \text{ sr}^{-1}$ , thus  $0.318 \text{ sr}^{-1}$  are the default values for all  $B_n$ 's. The reflection factors can be set for each surface type individually in the register card "Bottom" of the pop-up window "Model options", see "Reflection factors of bottom substrate" section of Figure 8.9.

## 9. Implicit spectra

All calculations of WASI make use of spectral data which are either imported from file or calculated during run-time. In particular some calculated spectra can be of interest, for instance to estimate spectral details of the radiation or bulk optical properties of the atmosphere or the water body, or for comparison with independent measurements. All implicit spectra can be visualised using the "Display" item of the menu bar as shown in Figure 9.1.

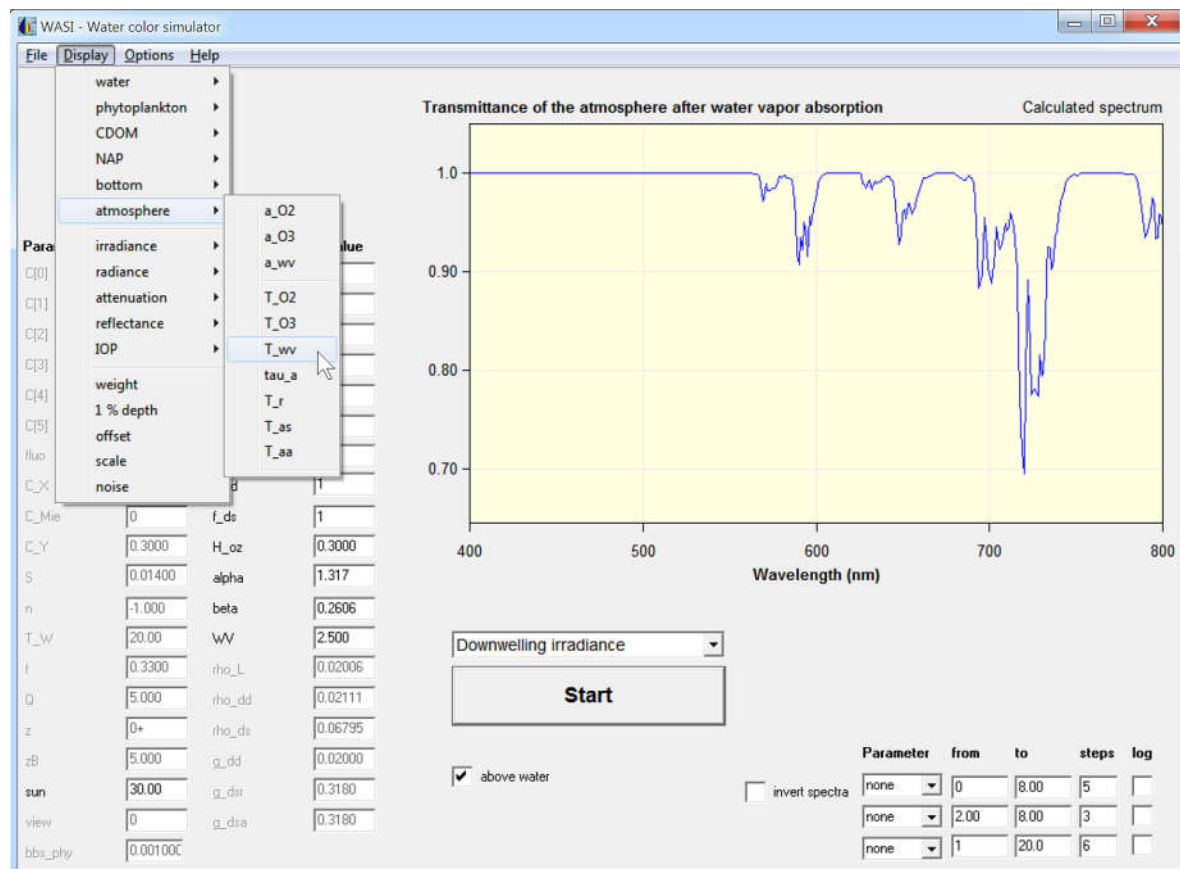


Figure 9.1: Visualizing of an implicit spectrum using the "Display" menu item.

The example of Figure 9.1 shows how to visualise an implicit spectrum of atmosphere modelling, here the atmospheric transmittance after water vapor absorption,  $T_{wv}(\lambda)$ , which is calculated using Eq. (2.49). A visualised spectrum can be exported to file using a dialog window which pops up after selecting "File – Save" as shown in Figure 9.2.

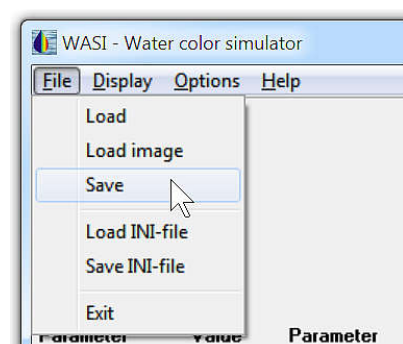


Figure 9.2: Saving an implicit spectrum.

**Transmittance of the atmosphere after water vapor absorption**

This file was generated by the program WASI  
 Version 5.0 (64bit) - Latest update: 18 June 2019  
 Documentation in directory: d:\wasi5\data\demo\tmp  
 Parameter values in files: WASI5.INI, CHANGES.TXT  
 Screenshot of plot in file: WASI\_plot.bmp  
 Average from 400 to 700 nm

No. 1  
 Avg 0

380.00 1  
 381.00 1  
 382.00 1  
 383.00 1  
 384.00 1  
 385.00 1  
 386.00 1  
 387.00 1  
 388.00 1  
 389.00 1  
 390.00 1

Figure 9.3: First lines of an exported spectrum.

The file format of exported spectra is ASCII text. An example is shown in Figure 9.3.

Spectra calculated during run-time can be of particular interest. When these are exported, also the parameter values used for calculation should be documented. This can be done by updating the file WASI5.INI as shown in Figure 9.4 and archiving a copy of this file.

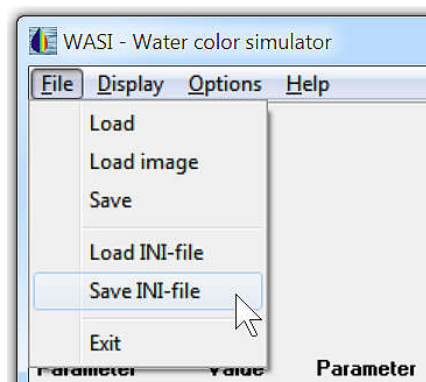


Figure 9.4: Documenting the parameter settings.

A summary of all implicate spectra of WASI is given in Appendix 5 (input spectra) and Appendix 6 (internal spectra).

## 10. Program options

The "Options" item of the menu bar on top of the WASI window is the entry point to all program settings. Figure 10.1 shows the main menu bar of WASI and the structure of the "Options" tree. The various program settings are grouped in 9 thematic areas; one of these ("Invers calculation") is further divided into 2 themes. When one of the themes is selected, a pop-up window shows up which allows inspecting and modifying the settings.

The pop-up windows of the first four thematic areas are described in the previous chapters:

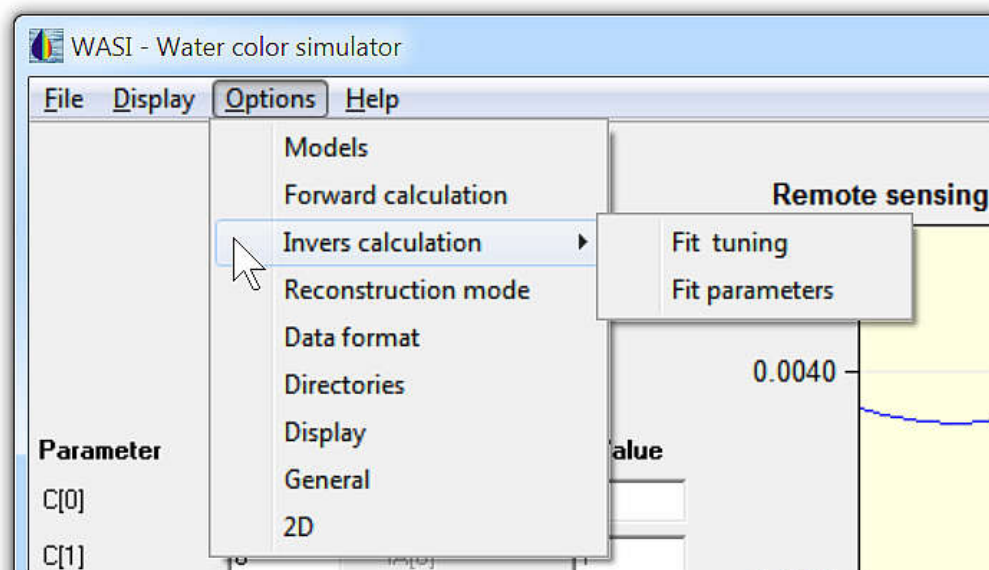


Figure 10.1: The structure of the "Options" menu.

"Models" in chapter 8 (Figure 8.2, Figure 8.4, Figure 8.5, Figure 8.7), "Forward calculation" in chapter 3 (Figure 3.3), "Invers calculation" in chapter 4 (Figure 4.4 to Figure 4.12), and "Reconstruction mode" in chapter 5 (Figure 5.5). The pop-up window "2D" of the 2D mode is described in chapter 6 (Figure 6.1). The pop-up windows of the four remaining themes are described in the following.

### 10.1 Data format

The pop-up window for specifying parameters related to data formats is shown in Figure 10.2. The window consists of three sections entitled "Wavelengths of calculated spectra", "File format of measurements" and "Batch processing" to specify the most common format parameters.

**Wavelengths of calculated spectra.** The wavelength range and the data interval of the calculated spectra can be selected in two ways:

- If the spectra shall be calculated at equidistant wavelengths, the check box "x-values from file" has to be unchecked. The first wavelength is specified in the "xmin" field, the last wavelength in the "xmax" field, and the intervals in the "dx" field.

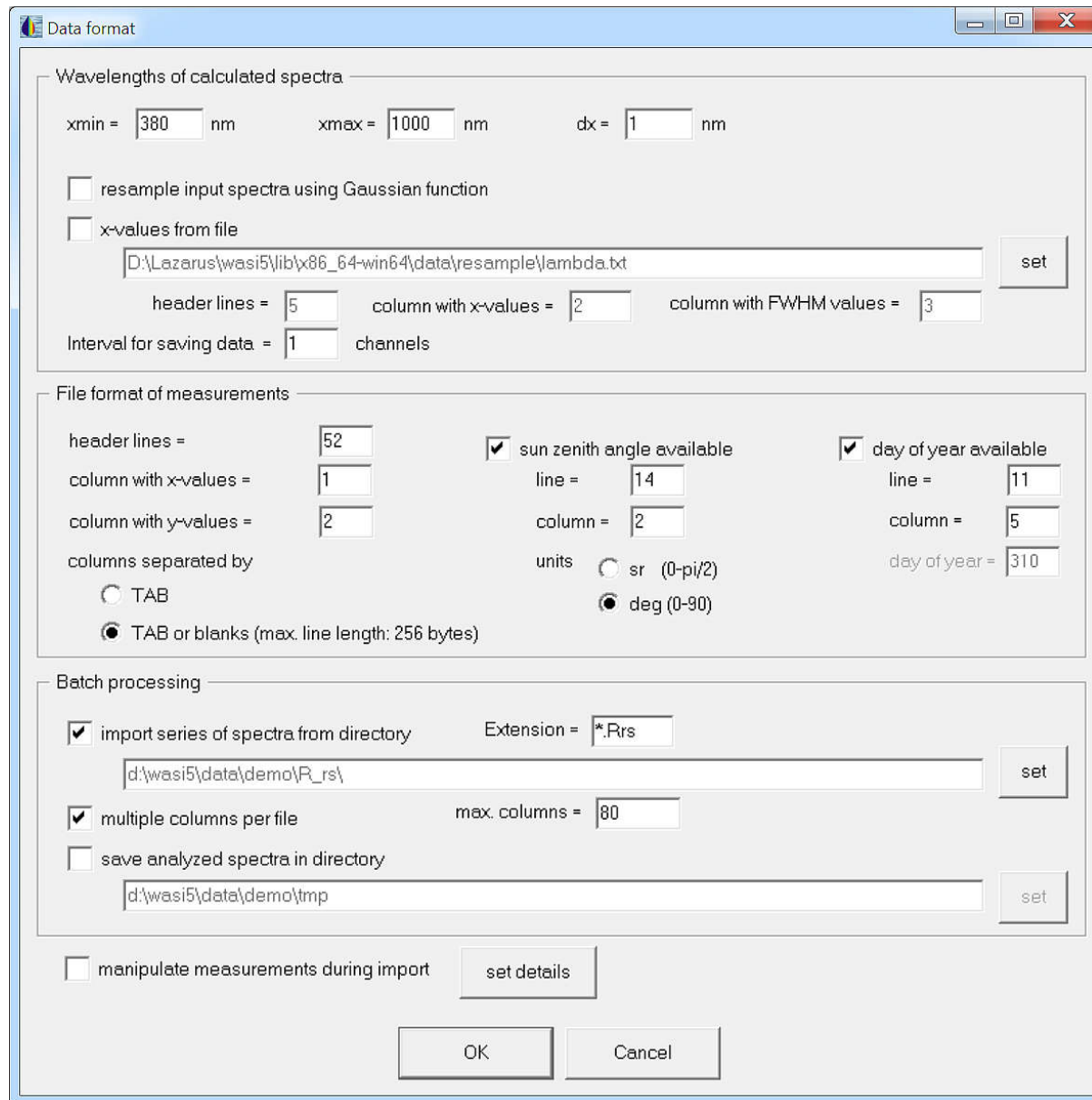


**Figure 10.2: The pop-up window "Data format".**

- For non-equidistant intervals, e.g. if calculations should be performed for channels of a specific sensor, the wavelengths are read from an ASCII table. In this case the box "x-values from file" must be marked with a hook, and the corresponding file must be set. The sensor file can be changed by pressing the button "set", which causes the opening of a file-selection window. The number of lines in the ASCII file that are skipped are specified in the "header lines" input field; the column with the wavelengths is specified in the "column with x-values" field.

The model curves can account for the spectral resolution of a sensor by activating “Resample input spectra using Gaussian function” and specifying the bands’ full width at half maximum (FWHM). If no sensor file is used (“x-values from file” is not checked), the spectral resolution specified in the “FWHM” input field is used for all bands. Otherwise, the sensor file must list the center wavelengths and the corresponding FWHMs of all bands. “Column of FWHM values” specifies the corresponding row of the sensor file.

If calculated spectra should be saved to file at reduced data interval, the "Interval for saving data" can be set to a value > 1.

**File format of measurements.** This section specifies the data format of input spectra. Any ASCII table can be used as input. Basic settings which need to be specified are the number of header lines, column of x-values, and column of y-values. The columns can be separated either by TAB or by an arbitrary number of blanks. However, for large multi-column tables which have lines longer than 256 bytes, only TABs are supported as column separators.

If the sun zenith angle is provided in the input file, mark the box "sun zenith angle available" with a hook and specify line, column and units. If the day of year is provided in the input file, mark the box "day of year available" with a hook and specify line and column; otherwise, specify it in the "day of year" box.

**Batch processing.** The batch mode can be used to process automatically a series of files, i.e. to import one file after the other in WASI, analyze each file by inverse modeling, and store the resulting fit parameters to file. This mode is activated by marking the box "import series of spectra from directory" with a hook. The user has to choose path and files after clicking the "set" button. Alternately, if the path is already set, the file extension can be changed in the input box "Extension".

The batch mode supports files which contain several spectra in the format  $(x, y_1, y_2, \dots, y_N)$ . To read such tables, mark the box "multiple columns per file" with a hook and specify the maximum number of spectra per file, N, by editing the "max. columns" box. The first spectrum  $y_1$  is specified via "Column with y-values" in the section "File format of measurements".

While the fit parameters are always saved automatically in the batch mode, the user can choose if he wants to save also each calculated spectrum. This selection is done by activating or deactivating the box "save analyzed spectra in directory". The directory in which the calculated spectra are stored, is chosen by clicking the corresponding "set" button.

**Manipulate measurements during import.** This check box indicates whether measurements are manipulated during import or not. Pressing the "set details" key opens the popup-window shown in Figure 10.3. It specifies the files and their format used for manipulation.

A measurement  $M(\lambda)$  can be manipulated by subtracting a function  $a(\lambda)$  and/or multiplying a function  $b(\lambda)$  using the equation

$$M'(\lambda) = [M(\lambda) - a(\lambda)] \times b(\lambda). \quad (10.1)$$

$M'(\lambda)$  is the manipulated measurement after import in WASI. The original data are not affected by this operation. Both options are disabled by default to avoid accidental manipulation. An application of Eq. (10.1) is radiometric calibration of raw data  $M(\lambda)$  from units of digital numbers to calibrated spectra  $M'(\lambda)$  in units of radiance or irradiance by specifying a dark current file  $a(\lambda)$  and a response file  $b(\lambda)$ .

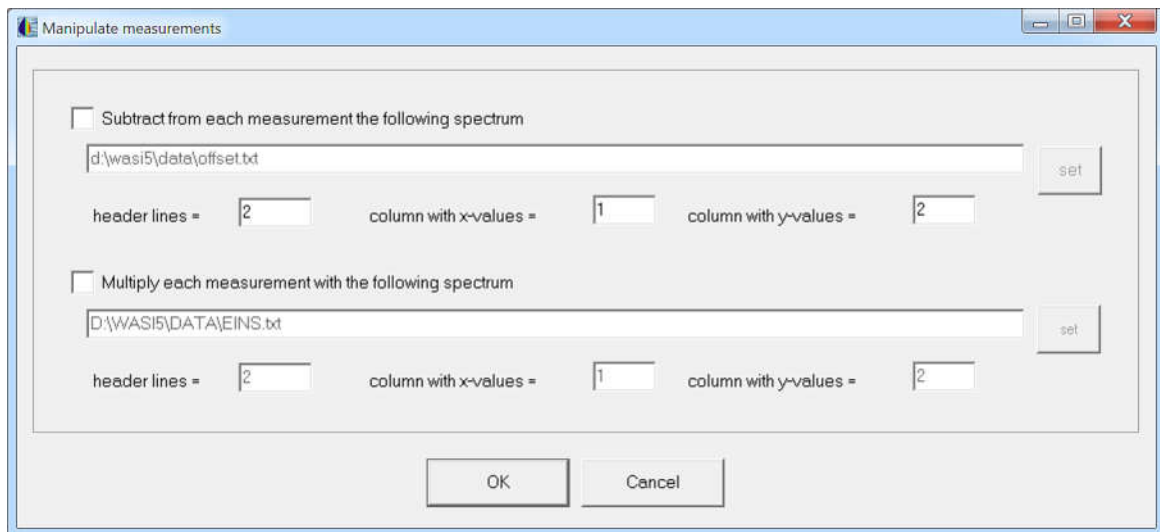


Figure 10.3: The pop-up window "Manipulate measurements".

## 10.2 Directories

The directories for reading import spectra and for saving the results are selected in the "Directories" pop-up window. It is accessed from the menu bar via "Options – Directories" (see Figure 10.1) and shown in Figure 10.4. The pre-selected directories can be changed by entering a new directory name or by pressing the button "set" and selecting a directory from the displayed directory tree (not shown).

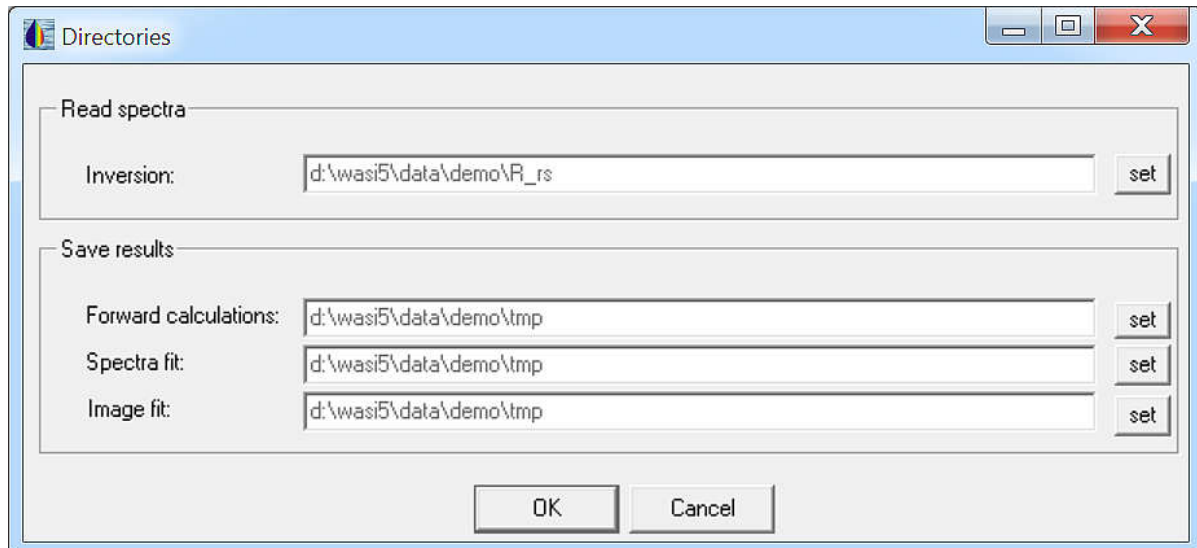


Figure 10.4: The pop-up window "Directories".

## 10.3 Display options

The pop-up window for settings concerning visualisation is shown in Figure 10.5. It appears when the thematic area "Display" is selected in the "Options" menu (see Figure 10.1).

**Range of x and y values.** The range of the displayed x-values is defined by the values in the fields "xmin =" and "xmax =". The range of the displayed y-values is either defined by the values in the fields "ymin =" and "ymax =", or adjusted automatically to the actual spectrum if the check box "autoscale" is marked with a hook. In the latter case the input fields for ymin and ymax are deactivated. By default the autoscale option is activated.

**Spectrum information.** On top right of the plot window the file name of the actual spectrum can be displayed, either excluding or including the path. The selection is made using the check boxes "display filename" and "display path".

**Layout.** The spectra can be plotted either on a blank background, or on a coarse or fine grid. The selection is made using the check boxes "display grid" and "display subgrid". The background colour can be changed by pressing the "set" button and selecting the desired colour in the upcoming popup-window (not shown).

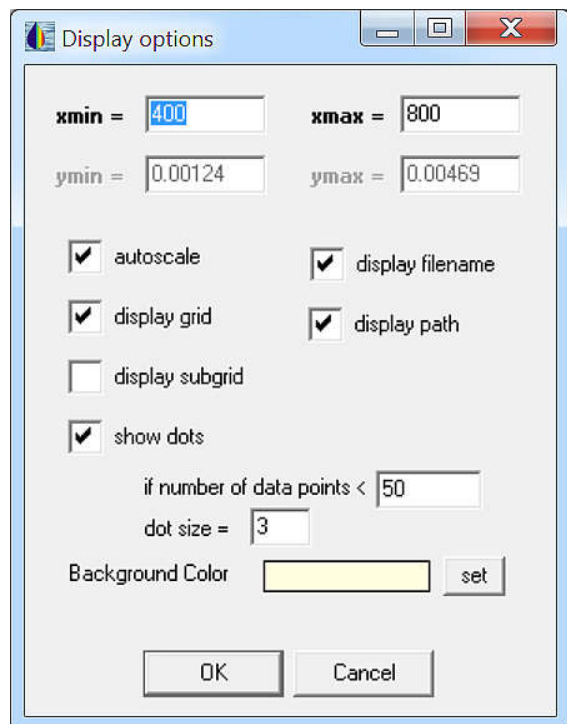


Figure 10.5: The popup-window "Display options".

## 10.4 General options

The pop-up window for some general settings is shown in Figure 10.6. It appears when the thematic area "General" is selected in the "Options" menu (see Figure 10.1).

Four yes-no-decisions can be made:

- The check box "save INI file automatically" selects whether or not the file WASI5.INI is updated automatically at program termination.

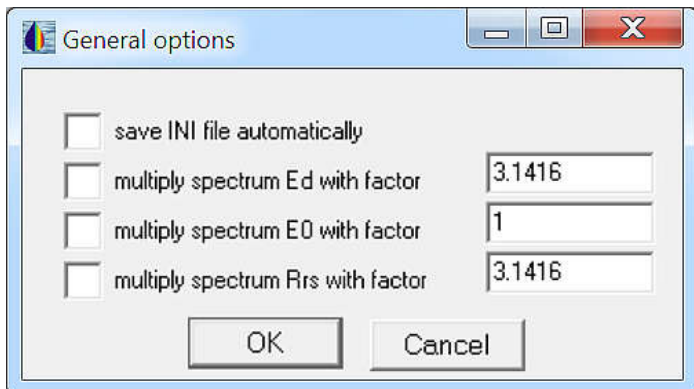


Figure 10.6: The pop-up window "General options".

- The check box "multiply spectrum Ed with factor" allows to multiply automatically each downwelling irradiance spectrum  $E_d(\lambda)$ , which is read from file, with a factor whose value is set in the adjacent input field. This is useful if  $E_d(\lambda)$  was measured as radiance upwelling from a horizontally oriented diffuse reflecting panel,  $L_{up}(\lambda)$ . In this case it is  $E_d(\lambda) = \pi \cdot \rho \cdot L_{up}(\lambda)$ , where  $\rho$  is the panel's reflectance. The conversion factor is set to  $\pi = 3.1416$  by default, which corresponds to  $\rho = 1$ .
- The check box "multiply spectrum E0 with factor" allows to multiply automatically the spectrum of the extraterrestrial solar irradiance,  $E_0(\lambda)$ , with a conversion factor. This is useful if the spectrum  $E_0(\lambda)$  is given in units which are different from the units of the other irradiance spectra. For example, the spectrum  $E_0(\lambda)$  provided with WASI is given in units of  $\mu\text{W cm}^{-2} \text{ sr}^{-1}$ , while the common units in WASI are  $\text{mW m}^{-2} \text{ sr}^{-1}$ . This leads to a conversion factor of 0.1.
- The check box "multiply spectrum rrs with factor" allows multiplying automatically all radiance reflectance spectra  $r_{rs}(\lambda)$  (those read from file as well as those forward calculated) with a factor whose value is set in the adjacent input field. This provides a fast way to convert  $r_{rs}(\lambda)$  to irradiance reflectance  $R(\lambda)$  using the model of Eq. (2.30),  $r_{rs}^-(\lambda) = R(\lambda)/Q$ . The conversion factor is set to  $Q = \pi = 3.1416$  by default, which represents the idealized case of isotropic reflection.

## 11. References

- E. Aas (1987): Two-stream irradiance model for deep waters. *Applied Optics* 26(11), 2095-2101.
- M. R. Abbott and R. M. Letelier (1999): Algorithm theoretical basis document chlorophyll fluorescence (MODIS product number 20). *NASA*.
- Y. H. Ahn, A. Bricaud, A. Morel (1992): Light backscattering efficiency and related properties of some phytoplankton. *Deep-Sea Res.* 39, 1835-1855.
- A. Albert, C. D. Mobley (2003): An analytical model for subsurface irradiance and remote sensing reflectance in deep and shallow case-2 waters. *Optics Express* 11, 2873-2890. <http://www.opticsexpress.org/abstract.cfm?URI=OPEX-11-22-2873>.
- A. Albert (2004): Inversion technique for optical remote sensing in shallow water. *Ph.D. thesis, University of Hamburg*. <http://www.sub.uni-hamburg.de/opus/volltexte/2005/2325/>
- A. Albert, P. Gege (2005): Inversion of irradiance and remote sensing reflectance in shallow water between 400 and 800 nm for calculations of water and bottom properties. *Applied Optics* 45(10), 2331-2343.
- D. Antoine, D. A. Siegel, T. Kostadinov, S. Maritorena, N. B. Nelson, B. Gentili, V. Vellucci, and N. Guillocheau (2011): Variability in optical particle backscattering in contrasting bio-optical oceanic regimes. *Limnol. Oceanogr.* 56: 955–973.
- M. Babin, A. Morel, and B. Gentili (1996): Remote sensing of sea surface Sun-induced chlorophyll fluorescence: consequences of natural variations in the optical characteristics of phytoplankton and the quantum yield of chlorophyll a fluorescence. *Int. J. Remote Sens.* 17, 2417–2448.
- M. Babin, D. Stramski, G.M. Ferrari, H. Claustre, A. Bricaud, G. Obolensky, et al. (2003a): Variations in the light absorption coefficients of phytoplankton, nonalgal particles, and dissolved organic matter in coastal waters around Europe. *J. Geophys. Res.* 108, C7.
- M. Babin, A. Morel, V. Fournier-Sicre, F. Fell, and D. Stramski (2003b): Light scattering properties of marine particles in coastal and open ocean waters as related to the particle mass concentration. *Limnol. Oceanogr.* 48: 843–859.
- R. E. Bird, C. Riordan (1986): Simple solar spectral model for direct and diffuse irradiance on horizontal and tilted planes at the Earth's surface for cloudless atmospheres. *Journal of Climate and Applied Meteorology* 25, 87–97.
- A. Bricaud, A. Morel, L. Prieur (1981): Absorption by dissolved organic matter of the sea (yellow substance) in the UV and visible domains. *Limnol. Oceanogr.* 26, 43-53.
- R. P. Bukata, J. H. Jerome, K. Y. Kondratyev, D. V. Pozdnyakov (1995): Optical Properties and Remote Sensing of Inland and Coastal Waters. *CRC Press, Boca Raton – New York – London – Tokyo*.

- M. S. Caceci, W. P. Cacheris (1984): Fitting Curves to Data. *Byte May 1984: 340-362.*
- K. L. Carder, G. R. Harvey, P. B. Ortner (1989): Marine humic and fulvic acids: their effects on remote sensing of ocean chlorophyll. *Limnol. Oceanogr. 34: 68-81.*
- M. Chami, E. B. Shybanov, T. Y. Churilova, G. A. Khomenko, M. E.-G. Lee, O. V. Martynov, G. A. Berseneva, and G. K. Korotaev (2005): Optical properties of the particles in the Crimea coastal waters (Black Sea). *J. Geophys. Res. 110: C11020.* doi:10.1029/2005JC003008.
- C. Cox, W. Munk (1954): Statistics of the sea surface derived from sun glitter. *J. Marine Res., 13, 198-227.*
- C. Cox, W. Munk (1956): Slopes of the sea surface deduced from photographs of sun glitter. *Bulletin Scripps Inst. Oceanogr. Univ. Calif., 6, 401-488.*
- E. J. D'Sa, R. L. Miller, C. Del Castillo (2006): Bio-optical properties and ocean color algorithms for coastal waters influenced by the Mississippi River during a cold front. *Appl Opt 45, 7410-7428.*
- J. Dera, D. Stramski (1993): Focusing of sunlight by sea surface waves: new results from the Black Sea. *Oceanologia 34, 13-25.*
- R. Doerffer and H. Schiller (2007): The MERIS Case 2 water algorithm. *Int. J. of Remote Sensing 28, 517–535.*
- ENVI (2005): ENVI User's Guide: ENVI Header Format. [http://geol.hu/data/online\\_help/ENVI\\_Header\\_Format.html](http://geol.hu/data/online_help/ENVI_Header_Format.html).
- P. Gege (1994): Gewässeranalyse mit passiver Fernerkundung: Ein Modell zur Interpretation optischer Spektralmessungen. *PhD thesis. DLR-Forschungsbericht 94-15, 171 p.*
- P. Gege (1995): Water analysis by remote sensing: A model for the interpretation of optical spectral measurements. *Technical Translation ESA-TT-1324, 231 pp., July 1995.*
- P. Gege (1998a): Correction of specular reflections at the water surface. *Ocean Optics XIV, November, 10-13, 1998, Kailua-Kona, Hawaii, USA. Conference Papers, Vol. 2.*
- P. Gege (1998b): Characterization of the phytoplankton in Lake Constance for classification by remote sensing. *Arch. Hydrobiol. Spec. Issues Advanc. Limnol. 53, p. 179-193, Dezember 1998: Lake Constance, Characterization of an ecosystem in transition.*
- P. Gege (2000): Gaussian model for yellow substance absorption spectra. *Proc. Ocean Optics XV conference, October 16-20, 2000, Monaco.*
- P. Gege (2002): Error propagation at inversion of irradiance reflectance spectra in case-2 waters. *Ocean Optics XVI Conference, November 18-22, 2002, Santa Fe, USA.*
- P. Gege (2004): The water color simulator WASI: an integrating software tool for analysis and simulation of optical in situ spectra. *Computers & Geosciences, 30, 523-532.*

P. Gege (2005): The Water Colour Simulator WASI. User manual for version 3. *DLR Internal Report IB 564-01/05, 83 pp.*

P. Gege, A. Albert (2006): A tool for inverse modeling of spectral measurements in deep and shallow waters. In: L.L. Richardson and E.F. LeDrew (Eds): "Remote Sensing of Aquatic Coastal Ecosystem Processes: Science and Management Applications", Kluwer book series: Remote Sensing and Digital Image Processing, Springer, ISBN 1-4020-3967-0, pp. 81-109.

P. Gege, N. Pinnel (2011): Sources of variance of downwelling irradiance in water. *Applied Optics 50*, 2192-2203.

P. Gege (2012a): Analytic model for the direct and diffuse components of downwelling spectral irradiance in water. *Applied Optics 51*, 1407-1419.

P. Gege (2012b): Estimation of phytoplankton concentration from downwelling irradiance measurements in water. *Israel Journal of Plant Sciences 60*(1-2), 193-207. DOI: 10.1560/IJPS.60.1-2.193.

P. Gege (2014): WASI-2D: A software tool for regionally optimized analysis of imaging spectrometer data from deep and shallow waters. *Computers & Geosciences 62*, 208-215. <http://dx.doi.org/10.1016/j.cageo.2013.07.022>.

C. Giardino, Brando V.E., Gege P., Pinnel N., Hochberg E., Knaeps E., Reusen I., Doerffer R., Bresciani M., Braga F., Foerster S., Champollion N., Dekker A. (2018): Imaging Spectrometry of Inland and Coastal Waters: State of the Art, Achievements and Perspectives. *Surveys in Geophysics*.

A. Gilerson, J. Zhou, S. Hlaing, I. Ioannou, J. Schalles, B. Gross, F. Moshary, S. Ahmed (2007). Fluorescence component in the reflectance spectra from coastal waters. Dependence on water composition. *Optics Express 15*, 15702-15721.

A. A. Gitelson, G. Dall'Olmo, W. Moses, D. C. Rundquist, T. Barrow, T. R. Fisher, D. Gurlin, J. Holz (2008). A simple semi-analytical model for remote estimation of chlorophyll-a in turbid waters: Validation. *Remote Sensing of Environment 112*, 3582–3593.

H. R. Gordon, O. B. Brown, M. M. Jacobs (1975): Computed Relationships between the Inherent and Apparent Optical Properties of a Flat Homogeneous Ocean. *Applied Optics 14*, 417-427.

H. R. Gordon (1979): Diffuse reflectance of the ocean: the theory of its augmentation by chlorophyll a fluorescence. *Applied Optics 21*, 2489-2492.

H. R. Gordon (1989): Can the Lambert-Beer law be applied to the diffuse attenuation coefficient of ocean water? *Limnol. Oceanogr. 34*(8), 1389-1409.

W. W. Gregg, K. L. Carder (1990): A simple spectral solar irradiance model for cloudless maritime atmospheres. *Limnol. Oceanogr. 35*(8), 1657–1675.

T. Heege (2000): Flugzeuggestützte Fernerkundung von Wasserinhaltsstoffen am Bodensee. *PhD thesis. DLR-Forschungsbericht 2000-40*, 134 p.

- Y. Huot, C. A. Brown, and J. J. Cullen (2005): New algorithms for MODIS sun-induced chlorophyll fluorescence and a comparison with present data products. *Limnol. Oceanogr. Methods* 3, 108–130.
- N. G. Jerlov (1976): Marine Optics. *Elsevier Scientific Publ. Company*.
- J. H. Jerome, R. P. Bukata, J. E. Bruton (1990): Determination of available subsurface light for photochemical and photobiological activity. *J. Great Lakes Res.* 16(3), 436-443.
- K. Kalle (1938): Zum Problem der Meeresswasserfarbe. *Ann. Hydrol. Mar. Mitt.* 66, l-13.
- F. Kasten, A. T. Young (1989): Revised optical air mass tables and approximation formula. *Applied Optics* 28, 4735–4738.
- J. T. O. Kirk (1984): Dependence of relationship between inherent and apparent optical properties of water on solar altitude. *Limnol. Oceanogr.* 29, 350-356.
- J. T. O. Kirk (1991): Volumen scattering function, average cosines, and underwater lightfield. *Limnol. Oceanogr.* 36, 455-467
- L. Kou, D. Labrie, P. Chylek (1993): Refractive indices of water and ice in the 0.65-2.5  $\mu\text{m}$  spectral range. *Applied Optics* 32, 3531-3540.
- Z. P. Lee, K. L. Carder, C. D. Mobley, R. G. Steward, J. S. Patch (1998): Hyperspectral remote sensing for shallow waters. I. A semianalytical model. *Appl. Optics* 37, 6329-6338.
- Z. P. Lee, A. Weidemann, J. Kindle, R. Arnone, K. L. Carder, and C. Davis (2007): Euphotic zone depth: Its derivation and implication to ocean-color remote sensing. *J. Geophysical Research* 112, C03009.
- F.L. Lobo, M. Costa, S. Phillips, E. Young, C. McGregor (2014): Light backscattering in turbid freshwater: A laboratory investigation. *J. Applied Remote Sensing* 8, 083611-1-13.
- Z. Lou (2006): Optical absorption of pure water in the blue and ultraviolet. *Dissertation Texas A&M University*, 115 pp.
- S. Maritorena, A. Morel, and B. Gentili (2000): Determination of the fluorescence quantum yield by oceanic phytoplankton in their natural habitat. *Applied Optics* 39, 6725–6737.
- C. D. Mobley, B. Gentili, H. R. Gordon, Z. Jin, G. W. Kattawar, A. Morel, P. Reinersman, K. Stamnes, R. H. Stavn (1993): Comparison of numerical models for computing underwater light fields. *Appl. Optics* 32, 7484-7504.
- C. D. Mobley (1994): Light and Water. *Academic Press*, 592 pp.
- C. D. Mobley (1999): Estimation of the remote-sensing reflectance from above-surface measurements. *Appl. Optics* 38, 7442-7455.
- A. Morel (1974): Optical Properties of Pure Water and Pure Sea Water. In: *Jerlov, N. G., Steemann Nielsen, E. (Eds.): Optical Aspects of Oceanography*. Academic Press London, 1-24.

- A. Morel (1980): In water and remote measurements of ocean colour. *Boundary-Layer Meteorology* 18, 177-201.
- A. Morel (1988): Optical modeling of the upper ocean in relation to ist biogenous content (case I waters). *J. Geophys. Res.* 93: 10,749–10,768.
- A. Morel, B. Gentili (1991): Diffuse reflectance of oceanic waters: its dependence on Sun angle as influenced by the molecular scattering contribution. *Appl. Optics* 30, 4427-4438.
- A. Morel, S. Maritorena (2001): Bio-optical properties of oceanic waters: A reappraisal. *J. Geophys. Res.* 106: 7163–7180.
- J. L. Mueller, R. W. Austin (1995): Volume 25 of Ocean Optics Protocols for SeaWiFS Validation, Revision 1. *S. B. Hooker, E. R. Firestone, and J. G. Acker, eds., NASA Tech. Memo. 104566. NASA Goddard Space Flight Center, Greenbelt, Md.*
- J. A. Nelder, R. Mead (1965): A simplex method for function minimization. *Computer J.* 7, 308-313.
- G. Nyquist (1979): Investigation of some optical properties of seawater with special reference to lignin sulfonates and humic substances. *PhD Thesis, Göteborgs Universitet, 200 p.*
- T. G. Owens (1991): Energy transformation and fluorescence in photosynthesis. In: *Particle Analysis in Oceanography*, S. Demers, ed. Springer-Verlag, Berlin, pp. 101–137.
- N. Pinnel (2007): A method for mapping submerged macrophytes in lakes using hyperspectral remote sensing. *PhD thesis. Technical University Munich, 165 p.*
- R. W. Preisendorfer, C. D. Mobley (1985): Unpolarized irradiance reflectances and glitter patterns of random capillary waves on lakes and seas, by Monte Carlo simulation. *NOAA Tech. Memo. ERL PMEL-63, Pacific Mar. Environ. Lab., Seattle, WA, 141 pp.*
- R. W. Preisendorfer, C. D. Mobley (1986): Albedos and glitter patterns of a wind-roughened sea surface. *J. Phys. Ocean.*, 16, 1293-1316.
- L. Prieur (1976): Transfers radiatifs dans les eaux de mer. *Thesis, Doctorat d'Etat, Univ. Pierre et Marie Curie, Paris, 243 pp.*
- L. Prieur, S. Sathyendranath (1981): An optical classification of coastal and oceanic waters based on the specific spectral absorption curves of phytoplankton pigments, dissolved organic matter, and other particulate materials. *Limnol. Oceanogr.* 26, 671-689.
- T. Pyhälähti, P. Gege (2001): Retrieval of water quality parameters using different channel configurations. *Proc. ISPRS symposium "Physical measurements & signatures in remote sensing", Jan. 8-12, 2001, Aussous, France.*
- T. I. Quickenden, J.A. Irvin (1980): The ultraviolet absorption spectrum of liquid water. *J. Chem. Phys.* 72(8), 4416-4428.
- R. Röttgers, R. Doerffer, D. McKee, W. Schönfeld (2013): Pure water spectral absorption, scattering, and real part of refractive index model". *Algorithm Theoretical Basis Document*

"The Water Optical Properties Processor (WOPP)". Distribution: Marc Bouvet, ESA/ESRIN, Revision 7, May 2013.

S. Sathyendranath, T. Platt (1988): Oceanic Primary Production: Estimation by Remote Sensing at Local and Regional Scales. *Science*, 241, 1613-1620.

S. Sathyendranath, L. Prieur, A. Morel (1989): A three-component model of ocean colour and its application to remote sensing of phytoplankton pigments in coastal waters. *Int. J. Remote Sensing* 10, 1373-1394.

S. Sathyendranath, T. Platt (1997): Analytic model of ocean color. *Applied Optics* 36, 2620-2629.

K. Schnalzger, 2017. Spektrale Datenbank für den Untergrund der Ostsee sowie Einfluss auf die Bestimmung der Wassertiefe. *Master Thesis University of Augsburg*, 68 pp.

J. N. Schwarz, P. Kowalcuk, S. Kaczmarek, G. Cota, B. G. Mitchell, M. Kahru, F. Chavez, A. Cunningham, D. McKee, P. Gege, M. Kishino, D. Phinney, R. Raine (2002): Two models for absorption by coloured dissolved organic matter (CDOM). *Oceanologia* 44(2), 209-241.

L. Sipelgas, H. Arst, K. Kallio, E. Erm, P. Oja, T. Soomere (2003): Optical properties of dissolved organic matter in Finnish and Estonian lakes. *Nord. Hydrol.* 34, 361-386.

M. M. Tilzer, N. Stambler, C. Lovengreen (1995): The role of phytoplankton in determining the underwater light climate in Lake Constance. *Hydrobiologia* 316, 161-171.

D. A. Toole, D. A. Siegel, D. W. Menzies, M. J. Neumann, R. C. Smith (2000): Remote-sensing reflectance determinations in the coastal ocean environment: impact of instrumental characteristics and environmental variability. *Applied Optics* 39, 456-469.

L. Wang (2008): Measuring optical absorption coefficient of pure water in UV using the integrating cavity absorption meter. *Dissertation Texas A&M University*, 110 pp.

S. G. Warren (1984): Optical constants of ice from the ultraviolet to the microwave. *Applied Optics* 23, 1026-1225.

K. Xue, Y. Zhang, H. Duang, R. Ma (2017): Variability of light absorption properties in optically complex inland waters of Lake Chaohu, China. *J. Great Lakes Research* 43, 17-31.

J. R. V. Zanefeld, E. Boss, A. Barnard (2001): Influence of surface waves on measured and modeled irradiance profiles. *Applied Optics* 40, 1442-1449.

## Appendix 1: Installation

To install WASI 5 on your computer, copy INSTALL\_WASI5.EXE to D:\ and execute it. This program unpacks all files to the directory D:\WASI5. The contents of this directory is as follows:

```
\DATA  
\DOC  
WASI5.EXE  
WASI5.INI  
README.TXT
```

To start WASI, execute the program WASI5.EXE.

If you prefer installing WASI in another directory than D:\WASI5, you need to edit the file WASI5.INI: Replace with a text editor all occurrences of "D:\WASI5\" with your directory.

*Note:* WASI makes no use of the registry.

## Appendix 2: WASI5.INI

WASI5.INI is the initialization file of WASI5. It is read automatically during program start. All program settings are stored in this file. The default file WASI5.INI is shown in the following. A copy of that file is stored in the directory d:\WASI5\DATA\auxiliary.

```
Initialization file for the program WASI - water colour simulator
-----
WASI5.INI version 25 June 2019
WASI5.EXE Version 5.0 (64bit) - Latest update: 25 June 2019

[ Center wavelengths and bandwidths ]
d:\wasi5\data\lambda.txt
5     = Header lines
2     = Column with x-values
3     = Column with FWHM-values

[ offsetS = Measurement offset spectrum ]
d:\wasi5\data\offset.txt
2     = Header lines
1     = Column with x-values
2     = Column with y-values

[ scaleS = Measurement scale spectrum ]
d:\wasi5\data\EINS.txt
2     = Header lines
1     = Column with x-values
2     = Column with y-values

[ noiseS = Measurement noise spectrum ]
d:\wasi5\data\noise.txt
10    = Header lines
1     = Column with x-values
3     = Column with y-values

[ E0 = Extraterrestrial solar irradiance ]
d:\wasi5\data\E0_sun.txt
11    = Header lines
1     = Column with x-values
2     = Column with y-values

[ aO2 = Absorption coefficient of oxygen ]
d:\wasi5\data\O2.a
4     = Header lines
1     = Column with x-values
2     = Column with y-values

[ aO3 = Absorption coefficient of ozone ]
d:\wasi5\data\O3.a
4     = Header lines
1     = Column with x-values
2     = Column with y-values

[ awv = Absorption coefficient of water vapor ]
d:\wasi5\data\WV.a
4     = Header lines
1     = Column with x-values
2     = Column with y-values

[ a_ice = Absorption coefficient of pure ice ]
d:\wasi5\data\ice.a
8     = Header lines
1     = Column with x-values
2     = Column with y-values

[ aw = Absorption coefficient of pure water ]
d:\wasi5\data\water.a
12    = Header lines
1     = Column with x-values
2     = Column with y-values

[ dadT = Temperature gradient of pure water absorption ]
d:\wasi5\data\daWdT.txt
10    = Header lines
1     = Column with x-values
2     = Column with y-values

[ aP[0] = Specific absorption of phytoplankton class no. 0 ]
d:\wasi5\data\phyto.a
12    = Header lines
1     = Column with x-values
2     = Column with y-values
```

```

[ aP[1] = Specific absorption of phytoplankton class no. 1 ]
d:\wasi5\data\cry-lo.a
10   = Header lines
1    = Column with x-values
2    = Column with y-values

[ aP[2] = Specific absorption of phytoplankton class no. 2 ]
d:\wasi5\data\cry-hi.a
11   = Header lines
1    = Column with x-values
2    = Column with y-values

[ aP[3] = Specific absorption of phytoplankton class no. 3 ]
d:\wasi5\data\dia.a
10   = Header lines
1    = Column with x-values
2    = Column with y-values

[ aP[4] = Specific absorption of phytoplankton class no. 4 ]
d:\wasi5\data\dinoflagellates.a
11   = Header lines
1    = Column with x-values
2    = Column with y-values

[ aP[5] = Specific absorption of phytoplankton class no. 5 ]
d:\wasi5\data\green_algae.a
11   = Header lines
1    = Column with x-values
2    = Column with y-values

[ aNAP = Normalized absorption coefficient of non-algal particles ]
d:\wasi5\data\NAP.aN
10   = Header lines
1    = Column with x-values
2    = Column with y-values

[ aY = Normalized absorption coefficient of CDOM ]
d:\wasi5\data\Y_Gauss.aN
262  = Header lines
1    = Column with x-values
2    = Column with y-values

[ bPhyN = Normalized scattering coefficient of phytoplankton ]
d:\wasi5\data\phyto.bN
7    = Header lines
1    = Column with x-values
2    = Column with y-values

[ bXN = Normalized scattering coefficient of suspended particles Type I ]
d:\wasi5\data\X.bN
2    = Header lines
1    = Column with x-values
2    = Column with y-values

[ albedo[0] = Albedo of bottom type #0 = const ]
d:\wasi5\data\const.R
3    Header lines
1    = Column with x-values
2    = Column with y-values

[ albedo[1] = Albedo of bottom type #1 = sand ]
d:\wasi5\data\Sand.R
14   = Header lines
1    = Column with x-values
2    = Column with y-values

[ albedo[2] = Albedo of bottom type #2 = silt ]
d:\wasi5\data\Silt.R
14   = Header lines
1    = Column with x-values
2    = Column with y-values

[ albedo[3] = Albedo of bottom type #3 = sea grass ]
d:\wasi5\data\Seagrass.R
14   = Header lines
1    = Column with x-values
2    = Column with y-values

[ albedo[4] = Albedo of bottom type #4 = mussel ]
d:\wasi5\data\Mussel.R
14   = Header lines
1    = Column with x-values
2    = Column with y-values

[ albedo[5] = Albedo of bottom type #5 = green macrophyte ]
d:\wasi5\data\Macrophyte.R
26   = Header lines
1    = Column with x-values
2    = Column with y-values

```

```

[ a_nw = Albedo of non-water area ]
d:\wasi5\data\10percent.txt
2      = Header lines
1      = Column with x-values
2      = Column with y-values

[ Measurement ]
d:\wasi5\data\demo\rrs\STA10_09.Rrs
17     = Header lines
1      = Column with x-values
2      = Column with y-values
10     = line_sun    = Line with sun zenith angle
2      = col_sun     = Column with sun zenith angle
7      = line_day    = Line with day of year
5      = col_day     = Column with day of year
16     = line_view   = Line with viewing angle
2      = col_view    = Column with viewing angle
7      = line_dphi   = Line with azimuth difference angle
2      = col_dphi    = Column with azimuth difference angle

[ Measurement: Irradiance reflectance, R ]
d:\wasi5\data\demo\R\R.txt
15     = header lines
1      = column with x-values
2      = column with y-values

[ Measurement: Downwelling irradiance, Ed ]
d:\wasi5\data\demo\Ed\Zeiss_R2R.Ed
12     = header lines
1      = column with x-values
2      = column with y-values

[ Measurement: Sky radiance reflected at surface, Ls ]
d:\wasi5\data\demo\L_sky\Ls.txt
17     = header lines
1      = column with x-values
2      = column with y-values

[ Measurement: Attenuation for downwelling irradiance, Kd ]
d:\wasi5\data\demo\Kd\K.prn
5      = Header lines
1      = Column with x-values
3      = Column with y-values

[ gew = Weight function for inversion ]
d:\wasi5\data\EINS.txt
52     = Header lines
1      = Column with x-values
2      = Column with y-values

[ HSI_img = Hyperspectral image ]
d:\wasi5\data\demo\2D\HySpex\StarnbergerSee_500x500.bsq

[ file_LUT[1] = Look-up table for series of simulated spectra ]
d:\wasi5\data\lut\RGB.lut

[ file_LUT[2] = Look-up table for color-coding channels in 2D mode ]
d:\wasi5\data\lut\rainbow3.lut

[ Spectra inverted in batch mode ]
d:\wasi5\data\demo\rrs\STA10_09.Rrs

[ Directories for saving results: FWD, INV, FIT ]
d:\wasi5\data\demo\tmp
d:\wasi5\data\demo\tmp
d:\wasi5\data\demo\tmp

[ General settings and parameters ]
350    = MinX          = lowest x-value allowed for data import and calculation
1000   = MaxX          = highest x-value allowed for data import and calculation
0.10   = MindX         = lowest dx-value allowed for calculation
-100   = MinY          = lowest y-value allowed for display
1.0E+5 = MaxY          = highest y-value allowed for display
400    = xu             = lowest x-coordinate displayed
800    = xo             = highest x-coordinate displayed
0.0013 = yu             = lowest y-coordinate displayed
0.0049 = yo             = highest y-coordinate displayed
350    = xub            = lowest x-coordinate calculated
1000   = xob            = highest x-coordinate calculated
1      = dxb            = wavelength interval for calculation
0      = dsmpl           = resampling distance (channels); 0 = no resampling
1      = dxs             = interval for saving data (channels)
5.00   = FWHM0           = spectral resolution (nm)
1      = FWHM0_min        = lowest allowed spectral resolution (nm)
50.0   = FWHM0_max        = highest allowed spectral resolution (nm)
3      = dotsize          = size of plotted dots
50    = dotMaxN          = max. number of data points to plot dots
600   = PopupDirW         = width of popup window 'directories'
3.1416 = Ed_factor        = multiplicator of spectrum E_down
1      = E0_factor         = multiplicator of spectrum E0

```

```

3.1416 = Rrs_factor           = multiplicator of spectrum R_rs
2      = spec_type            = type of spectrum: 0=E_d, 1=L_up, 2=r_rs, 3=R, 4=R_surf, 5=a, 6=K_d, 7=R_bottom
1      = Model_Ed             = Ed model: 0 = simple, 1 = separation between direct and diffuse component
0      = Model_R               = R model: 0=f*bb/(a+bb), 1=f*bb/a
0      = Model_R_rsA           = Rrs above surface is a function of 0=r_rs(0-), 1=R, 2=both
0      = Model_R_rsB           = Rrs model below surface: 0=f_rs*bb/(a+bb), 1=f_rs*bb/a, 2=R/Q
4      = Model_f               = f model: 0=const, 1=Kirk, 2=Morel+Gentili, 3=Sath.+Platt, 4=Albert+Mobley
0      = Model_f_rs             = f_rs model: 0=Albert, 1=f/Q
0      = Model_Kdd              = Kdd model: 0=Gege, 1=Grötsch
-1     = bottom_fill           = bottom surface type adjusted to yield sum of weights = 1
$00E1FFFF = clPlotBk          = color of plot background
clBlack = clMaskImg           = color of image mask

[ Flags: 0 = FALSE, 1 = TRUE ]
0      = flag_SubGrid          = draw subgrid
1      = flag_Grid              = draw grid
1      = flag_Dots              = draw dots
1      = flag_Autoscale          = autoscale plot
1      = flag_ShowFile           = display filename
1      = flag_ShowPath           = display path
0      = flag_leg_left           = Adjust parameter legend left
1      = flag_leg_top            = Adjust parameter legend top
0      = flag_INI                = save INI file automatically
0      = flag_sv_table           = save forward-spectra as table
0      = flag_save_t              = save calculation time
0      = flag_mult_Ed             = multiply spectrum Ed with factor
0      = flag_mult_E0             = multiply spectrum E0 with factor
0      = flag_mult_Rrs            = multiply spectrum R_rs with factor
0      = flag_x_file              = read x-values from file
0      = flag_fwhm               = use sensor resolution
1      = flag_read_day             = read day of year from file
1      = flag_read_sun              = read sun zenith angle from file
0      = flag_read_view             = Read viewing angle from file?
0      = flag_read_dphi            = Read azimuth difference between sun and viewing angle from file?
1      = flag_sun_unit             = sun zenith angle in deg
0      = Par1_log                 = Logarithmic steps of Parameter 1
0      = Par2_log                 = Logarithmic steps of Parameter 2
0      = Par3_log                 = Logarithmic steps of Parameter 3
1      = flag_batch               = batch mode (including forward mode)
1      = flag_bunt                = change color when calculating a series of spectra
0      = flag_b_SaveFwd            = save all spectra of forward mode
0      = flag_b_SaveInv             = save all spectra of invers mode
0      = flag_b_LoadAll            = load spectra from files
1      = flag_b_Reset              = reset start values
0      = flag_b_Invert             = invert spectra
0      = flag_avg_err              = reconstruction mode: save average errors?
1      = flag_multi                = multiple columns per file
0      = flag_Res_log              = weight residuals logarithmically
1      = flag_Y_exp                = exponential Gelbstoff absorption
1      = flag_surf_inv              = wavelength dependent surface reflections (inversion)
1      = flag_surf_fw               = wavelength dependent surface reflections (forward mode)
0      = flag_fluo                  = include fluorescence of chl-a
0      = flag_MP                   = apply melt pond models
0      = flag_use_Ed                = make use of Ed measurement
0      = flag_use_Ls                = make use of Ls measurement
0      = flag_use_R                 = make use of R measurement
0      = flag_radiom                = reduce radiometric resolution
0      = flag_offset                = add measurement offset
0      = flag_offset_c               = offset is constant
0      = flag_scale                 = add measurement scale
0      = flag_scale_c               = scale is constant
0      = flag_noise                 = add measurement noise
0      = flag_noise_c               = noise is constant
0      = flag_Tab                   = only TAB separates columns
1      = flag_aW                   = include water absorption in bulk absorption
1      = flag_above                 = above water
0      = flag_shallow                = shallow water
1      = flag_L                     = type of bottom reflectance (0: albedo, 1: radiance reflectance)
1      = flag_anX_R                 = analytic determination X start value for R spectra in deep waters
1      = flag_anX_Rsh                = analytic determination X start value for R spectra in shallow waters
1      = flag_anCY_R                = analytic determination C, Y start values for R spectra
1      = flag_anzB                  = analytic determination of zB start value in shallow waters
1      = flag_Fresnel_view            = calculate Fresnel reflectance from viewing angle
1      = flag_bX_file                = scattering coefficient of particles Type I from file
1      = flag_bX_linear              = scattering coefficient of particles Type I linear with C_X
0      = flag_CXisC0                = set C_X = C[0]
0      = flag_norm_D                = normalize NAP absorption spectrum from file at Lambda_0
1      = flag_norm_Y                = normalize Gelbstoff spectrum from file at Lambda_0

[ Settings for batch mode ]
0      = iter_type                = parameter that is iterated
2.0    = rangeMin                 = first value of successive calculation
4.0    = rangeMax                 = last value of successive calculation
1      = rangeDelta                = interval of successive calculation
0      = Par1_Type                 = Parameter 1
0      = Par2_Type                 = Parameter 2
0      = Par3_Type                 = Parameter 3
0      = Par1_Min                  = Minimum of Parameter 1
2.00   = Par2_Min                  = Minimum of Parameter 2
1      = Par3_Min                  = Minimum of Parameter 3

```

```

8.00 = Parl_Max      = Maximum of Parameter 1
8.00 = Par2_Max      = Maximum of Parameter 2
20.0 = Par3_Max      = Maximum of Parameter 3
5    = Parl_N        = Steps of Parameter 1
3    = Par2_N        = Steps of Parameter 2
6    = Par3_N        = Steps of Parameter 3
80   = ycol_max      = Max. number of y-columns

[ Settings for inverse mode ]
[ from to step MaxIter ]
400  800   2   200  = fit settings of pre-fit 1
730  900   5   10   = fit settings of pre-fit 2 (IR region)
380  450   5   0    = fit settings of pre-fit 3 (UV region)
400  900   1   100  = fit settings of final fit
400  800   5   0    = fit of a (shallow water)
700  800   5   0    = fit of R and r_rs in IR region (shallow water)
400  500   5   0    = fit of R and r_rs in UV region (shallow water)
400  800   1   200  = fit of R and r_rs (shallow water)
870  900   0           = LambdaLf = wavelengths for C_X and f initialisation
5    0           = dLambdaLf = wavelength intervals of LambdaLf
760  2           = LambdaLsh = wavelengths for C_X initialisation (shallow water)
2           = dLambdaLsh= wavelength interval of LambdaLsh (shallow water)
413  440   440  = LambdaCY = wavelengths for C[0] and C_Y initialisation
5    5   870   = dLambdaCY = wavelength intervals of LambdaCY
625  25          = LambdazB = wavelength for zB initialisation (shallow water)
25          = dLambdazB = wavelength interval of LambdazB (shallow water)
0.10 0.10         = zB_inimin = zB minimum during initial value determination (shallow water)
0.10 0.10         = CX_inimin = C_X minimum during initial value determination (shallow water)
0.10 0.010        = C0_inimin = C[0] minimum during initial value determination (shallow water)
0.010 5.0          = CY_inimin = C_Y minimum during initial value determination (shallow water)
5.0   1.0          = a_ini   = start value of absorption for nested intervals (shallow water)
1.0   0.010        = da_ini  = initial absorption interval for a_ini (shallow water)
0.010 0.10         = delta_min = threshold of spectrum change for nested intervals (shallow water)
0.10 10            = SfA_min = minimum sum of fA[i] (shallow water)
10   1.00E-4       = SfA_max = maximum sum of fA[i] (shallow water)
1.00E-4 0           = res_max = maximum allowed residuum
0           = res_mode = type of residuum (0=|m-f|^2 = least squares, 1=|m-f|, 2=|1-f/m|)

[ Model constants ]
94   = day          = Day of year
20.0 = T_W0         = Temperature of water absorption spectrum (°C)
1.33000 = nW          = Refractive index of water
550  = Lambda_a      = Reference wavelength for aerosol optical thickness (nm)
440  = Lambda_0      = Reference wavelength for CDOM and NAP absorption (nm)
550  = Lambda_L      = Reference wavelength for scattering of particles Type I (nm)
500  = Lambda_S      = Reference wavelength for scattering of particles Type II (nm)
685.0 = Lambda_f0     = Center wavelength of chl-a fluorescence (nm)
10.62 = Sigma_f0     = Standard deviation of chl-a fluorescence (nm)
0.500 = Q_a          = Portion of emitted fluorescence not reabsorbed within the cell
400  = PAR_min       = PAR range: lower boundary (nm)
700  = PAR_max       = PAR range: upper boundary (nm)
400  = Lmin          = Spectrum average: lower boundary (nm)
700  = Lmax          = Spectrum average: upper boundary (nm)
0.04100 = aNAP440    = Specific absorption coefficient of NAP (m^2/g)
0.00111 = bbW500     = Backscattering coefficient of pure water (1/m)
0.00060 = bbX_A      = Factor A in particle backscattering to concentration relationship (m^2/g)
-0.3700 = bbX_B      = Factor B in particle backscattering to concentration relationship
1.00000 = bb_ice      = Backscattering coefficient of ice (m^-1)
0.00860 = bb_X        = Specific backscattering coeff. of particles Type I (m^2/g)
0.00420 = bb_Mie      = Specific backscattering coeff. of particles Type II (m^2/g)
0.45000 = b_X          = Specific scattering coeff. of particles Type I (m^2/g)
0.30000 = b_Mie        = Specific scattering coeff. of particles Type II (m^2/g)
0.06087 = rho0         = rho_ds polynomial: 0th order value
0.03751 = rho1         = rho_ds polynomial: 1st order value
0.11430 = rho2         = rho_ds polynomial: 2nd order value
0.54000 = rho_Eu       = Reflection factor for upwelling irradiance
0.03000 = sigma_Ed      = Reflection factor for downwelling irradiance
0.02000 = sigma_Lu      = Reflection factor for upwelling radiance
0.00500 = dynamics      = Radiometric resolution
0.03000 = offset_c      = Measurement offset (constant)
1.00000 = scale_c       = Measurement scale factor (constant)
0.00020 = noise_std     = Noise level (standard deviation)
1.00000 = ldd          = Path length of direct irradiance: 0th order value
1.01700 = ldda         = Path length of direct irradiance: 1st order value
1.95000 = lddb         = Path length of direct irradiance: 2nd order value
1.11600 = lds0         = Path length of diffuse irradiance: 0th order value
0.55040 = lds1         = Path length of diffuse irradiance: 1st order value
1.05460 = ld           = Path length factor of total irradiance, Ed
1.00000 = ldd_ice      = Relative path length of direct radiation in ice
6.30000 = Q_ice_p      = Anisotropy factor of downwelling radiation at top of ice layer
1.68000 = Q_ice_m      = Anisotropy factor of downwelling radiation at bottom of ice layer
0.31800 = BRDF[0]       = BRDF of bottom type #0
0.31800 = BRDF[1]       = BRDF of bottom type #1
0.31800 = BRDF[2]       = BRDF of bottom type #2
0.31800 = BRDF[3]       = BRDF of bottom type #3
0.31800 = BRDF[4]       = BRDF of bottom type #4
0.31800 = BRDF[5]       = BRDF of bottom type #5

[ Parameters of 2D module ]
1     = flag_bk_2D      = Invert 2D data in background mode (1=TRUE)

```

```

1      = flag_JoinBands = Identical scaling for 3 preview bands
1      = flag_3Bands   = Preview 3 bands / 1 band
1      = flag_LUT      = Use lookup table
1      = flag_ENVI     = Read ENVI header file
0      = flag_use_ROI = Analyse image for region of interest
0      = flag_scale_ROI= Scale image for region of interest
500    = Width_in     = Input image width
500    = Height_in    = Input image height
100    = Channels_in = Input image channels
7      = Channels_out = Output image channels
0      = HSI_header   = Input image header bytes
0      = frame_min    = First line of processed image
0      = frame_max    = Last line of processed image; 0: all lines
0      = pixel_min     = First column of processed image
0      = pixel_max     = Last column of processed image; 0: all columns
55     = band_R       = Preview band red
41     = band_G       = Preview band green
12     = band_B       = Preview band blue
1      = interleave_in = Input image interleave (0=BIL, 1=BSQ)
1      = interleave_out = Output image interleave (0=BIL, 1=BSQ)
2      = Datentyp     = Input image data type
1000   = x_scale     = Scale factor of x-axis (1=nm, 1000=um)
31416  = y_scale     = Scale factor of y-axis
100    = band_mask   = Preview band of mask
0      = thresh_below = Mask threshold min
1      = thresh_above = Mask threshold max
10     = Plot2D_delta = Interval to plot spectrum
10.00  = contrast    = Preview image contrast
7      = Paro_Type   = Preview parameter during inversion
0      = Paro_Min    = Preview parameter min
10.0   = Paro_Max    = Preview parameter max
15     = N_avg       = Averaged pixels for parameter initialization

[ Model parameters ]
[ forward default start    min     max     step   MaxErr fit sv
  2.00   2     2.00      0      100    0.100  0.0100 1  0   C[0]  = Concentration of phytoplankton class #0 (µg/l)
  0      0     0          0      1000   0.100  0.0100 0  0   C[1]  = Concentration of phytoplankton class #1 (µg/l)
  0      0     0          0      1000   0.100  0.0100 0  0   C[2]  = Concentration of phytoplankton class #2 (µg/l)
  0      0     0          0      1000   0.100  0.0100 0  0   C[3]  = Concentration of phytoplankton class #3 (µg/l)
  0      0     0          0      1000   0.100  0.0100 0  0   C[4]  = Concentration of phytoplankton class #4 (µg/l)
  0      0     0          0      1000   0.100  0.0100 0  0   C[5]  = Concentration of phytoplankton class #5 (µg/l)
  0.500  0.500  1        0.100  1000   0.100  0.0100 1  1   C_X  = Concentration of non-algal particles Type I (mg/l)
  0      0     0          0      125    0.100  0.0100 0  0   C_Mie = Concentration of non-algal particles Type II (mg/l)
0.00100 0.00100 0.00100 0      1.000E-4 1.000E-4 0  0   bbs_phy = Specific backscattering coefficient of phytoplankton (m^2/mg)
  0.300  0.300  0.300   0      50.0   0.0200 0.0100 1  1   C_Y  = CDOM absorption coefficient (m^-1)
0.0140  0.0140  0.0140  0.0250  0.00100 2.000E-5 0  0   S    = Exponent of CDOM absorption (nm^-1)
-1.00   -1.00   -1.00   -2.00   2.00    0.200 0.0500 0  0   n    = Ångström exponent of particle scattering
  20.0   20.0    20.0    0      40.0   1        0.100  0  0   T_W  = Water temperature (°C)
  5.00   5.00    0.500   10.0   0.100  0.0100 0  0   Q    = Anisotropy factor of Lu (1/sr)
0.0210  0.0210  0.0210   0      1.00   0.00200 1.000E-5 0  0   rho_dd = Reflection factor of Edd
0.0201  0.0201  0.0201   0      0.500  0.00200 1.000E-5 0  0   rho_L  = Fresnel reflectance of downwelling radiance
0.0680  0.0680  0.0680   0      50.0   0.00500 1.000E-5 0  0   rho_d  = Reflection factor of Eds
0.2606  0.2606  0.05000 0      20.0   0.02000 0.001000 0  0   beta   = Turbidity coefficient
  1.317  1.317   1.320   -3.000 3.000   0.2000 0.01000 0  0   alpha  = Ångström exponent of aerosols
  1      1     1        0      30.0   0.100  0.0100 0  0   f_dd  = Fraction of direct downwelling irradiance
  1      1     1        0      30.0   0.100  0.0100 0  0   f_ds  = Fraction of diffuse downwelling irradiance
0.380   0.380   0.380    0      5.00   0.0500 0.00100 0  0   H_o2z = Ozone scale height (cm)
  2.50   2.50    2.50    0      20.0   0.100  0.00100 0  0   WV    = Precipitable water (cm)
  0.330   0.330   0.330   0.100  0.900   0.0500 0.00100 0  0   f    = f-factor of R
  0      1     0        0      100   0.100  0.00100 0  0   z    = Sensor depth (m)
  2.00   2      2        0      1000  0.100  0.0100 0  0   zB   = Bottom depth (m)
  30.0   30.0   30.0    0      89.9   5.00   0.100  0  0   sun  = Sun zenith angle (°)
  0      0     0        0      89.9   5.00   0.100  0  0   view = Viewing angle (°)
  0      0     0        0      180   5.00   0.100  0  0   dphi = azimuth difference sun - observer (°)
  0      0.100  0        0      1     0.100  0.05000 0  0   f_nw = Fraction of non-water area
  1      0     0        0      10.0  0.100  0.05000 0  0   FA[0] = fraction of bottom type #0
  0      0     1        0      10.0  0.100  0.05000 0  0   FA[1] = fraction of bottom type #1
  0      0     0        0      10.0  0.100  0.05000 0  0   FA[2] = fraction of bottom type #2
  0      0     0        0      10.0  0.100  0.05000 0  0   FA[3] = fraction of bottom type #3
  0      0     0        0      10.0  0.100  0.05000 0  0   FA[4] = fraction of bottom type #4
  0      0     0        0      10.0  0.05000 0.05000 0  0   FA[5] = fraction of bottom type #5
0.0100  0.0100  0.0100   0      1     0.00500 1.000E-5 0  0   fluo = chl-a fluorescence quantum yield
0.0200  0.0200  0.0200   -1.00  10.0   0.0100 1.000E-4 1  0   g_dd = Fraction of sky radiance due to direct solar radiation
  0.318   0.318   0.320    0      10.0  0.100  0.00100 0  0   g_dsr = Fraction of sky radiance due to Rayleigh scattering
  0.318   0.318   0.320    0      10.0  0.100  0.00100 0  0   g_dsa = Fraction of sky radiance due to aerosol scattering
  0      0     0        -5.00 50.0   0.100  0.00100 0  0   dummy = NOT USED

```

## Appendix 3: Parameters

The following table summarizes the 40 model parameters of all 8 spectrum types. The No.'s are used program-internally as parameter indices.  $\Delta\phi$  is included for future developments and so far not used.

No.	WASI	Symbol	Default	Units	Description
1-6	C[i]	$C_i$	2, 0	$\mu\text{g/l}$	Concentration of phytoplankton class number i, $i = 0..5$
7	C_X	$C_L$	0.5	$\text{mg/l}$	Concentration of non-algal particles of type I
8	C_Mie	$C_s$	0	$\text{mg/l}$	Concentration of non-algal particles of type II
9	C_Y	$Y$	0.3	$\text{m}^{-1}$	CDOM absorption coefficient at wavelength $\lambda_0$
10	S	$S$	0.014	$\text{nm}^{-1}$	Exponent of CDOM absorption
11	n	$n$	-1	-	Exponent of backscattering of non-algal particles type II
12	T_W	$T_w$	18	$^{\circ}\text{C}$	Water temperature
13	Q	$Q$	5	sr	Anisotropy factor of upwelling radiation ("Q-factor")
14	fluo	$\eta_{\text{chl}}$	0.01	-	Quantum yield of chl-a fluorescence
15	rho_L	$\rho_L$	0.02	-	Reflection factor of downwelling radiance
16	rho_dd	$\rho_{dd}$	0.021	-	Reflection factor of direct downwelling irradiance
17	rho_ds	$\rho_{ds}$	0.068	-	Reflection factor of diffuse downwelling irradiance
18	beta	$\beta$	0.2606	-	Turbidity coefficient
19	alpha	$\alpha$	1.317	-	Angström exponent of aerosol scattering
20	f_dd	$f_{dd}$	1	-	Fraction of direct downwelling irradiance
21	f_ds	$f_{ds}$	1	-	Fraction of diffuse downwelling irradiance
22	H_oz	$H_{oz}$	0.38	cm	Ozone scale height
23	WV	WV	2.5	cm	Precipitable water
24	f	$f$	0.33	-	Proportionality factor of irradiance reflectance ("f-factor")
25	z	$z$	1	m	Sensor depth
26	zB	$z_B$	2	m	Bottom depth
27	sun	$\theta_{\text{sun}}$	30	$^{\circ}$	Sun zenith angle
28	view	$\theta_v$	0	$^{\circ}$	Viewing angle (0 = nadir)
29	dphi	$\Delta\phi$	0	$^{\circ}$	Azimuth difference between sun and viewing direction
30-35	fA[n]	$f_n$	1, 0	-	Areal fraction of bottom surface type number n, $n = 0..5$
36	bbs_phy	$b_{b,\text{phy}}^*$	0.001	$\text{m}^2 \text{mg}^{-1}$	Specific backscattering coefficient of phytoplankton
37	g_dd	$g_{dd}$	0.02	$\text{sr}^{-1}$	Fraction of sky radiance due to direct solar radiation
38	g_dsr	$g_{dsr}$	0.318	$\text{sr}^{-1}$	Fraction of sky radiance due to molecule scattering
39	g_dsa	$g_{dsa}$	0.318	$\text{sr}^{-1}$	Fraction of sky radiance due to aerosol scattering
40	f_nw	$f_{nw}$	0	-	Fraction of non-water area

**Forward mode.** Each parameter can be set by the user. When a series of spectra is calculated, iteration can be performed over each of the parameters.

**Invers mode.** The user defines for each parameter if it should be treated as a constant or as fit parameter during inversion.

## Appendix 4: Constants

The following table summarizes the model constants of all 8 spectrum types. They can be changed using the GUI or by editing the WASI5.INI file.

<b>WASI5.INI</b>	<b>Symbol</b>	<b>Units</b>	<b>Default value</b>	<b>Description</b>
Day	d	–	94	Day of year
T_W0	T <sub>0</sub>	°C	20	Reference temperature of spectrum a <sub>w</sub> (λ)
nW	n <sub>w</sub>	–	1.33	Refractive index of water
Lambda_a	λ <sub>a</sub>	nm	550	Reference wavelength for aerosol optical thickness
Lambda_0	λ <sub>0</sub>	nm	440	Reference wavelength for Gelbstoff absorption
Lambda_L	λ <sub>L</sub>	nm	550	Reference wavelength for scattering of large particles
Lambda_S	λ <sub>S</sub>	nm	500	Reference wavelength for scattering of small particles
Lambda_f0	λ <sub>F</sub>	nm	685	Centre wavelength of chl-a fluorescence
Sigma_f0	σ <sub>F</sub>	nm	10.62	Standard deviation of chl-a fluorescence
PAR_min	–	nm	400	PAR range: lower boundary
PAR_max	–	nm	700	PAR range: upper boundary
Lmin	–	nm	400	Spectrum average: lower boundary
Lmax	–	nm	700	Spectrum average: upper boundary
aNAP440	a <sub>NAP</sub> *	m <sup>2</sup> g <sup>-1</sup>	0.041	Specific absorption coefficient of NAP
bbW500	b <sub>1</sub>	m <sup>-1</sup>	0.00111	Backscattering coefficient of pure water at 500 nm
bbX_A	A	m <sup>2</sup> g <sup>-1</sup>	0.006	Factor A in backscattering to conc. relationship
bbX_B	B	–	-0.37	Factor B in backscattering to conc. relationship
bb_X	b <sub>b,X</sub> *	m <sup>2</sup> g <sup>-1</sup>	0.0086	Specific backscattering coefficient of particles Type I
bb_Mie	b <sub>b,Mie</sub> *	m <sup>2</sup> g <sup>-1</sup>	0.0042	Specific backscattering coefficient of particles Type II
b_X	b <sub>X</sub> *	m <sup>2</sup> g <sup>-1</sup>	0.45	Specific scattering coefficient of particles Type I
b_Mie	b <sub>Mie</sub> *	m <sup>2</sup> g <sup>-1</sup>	0.30	Specific scattering coefficient of particles Type II
rho0	–	–	0.06087	rho_ds polynomial: 0th order value
rho1	–	–	0.03751	rho_ds polynomial: 1st order value
rho2	–	–	0.1143	rho_ds polynomial: 2nd order value
rho_Eu	ρ <sub>u</sub>	–	0.54	Reflection factor of upwelling irradiance
sigma_Ed	σ	–	0.03	Reflection factor of downwelling irradiance
sigma_Lu	σ <sub>L</sub> –	–	0.02	Reflection factor of upwelling radiance
dynamics	–	–	0.005	Radiometric resolution
noise_std	–	–	0.0002	Noise level (standard deviation)
Idd	–	–	1	Path length of direct irradiance: 0th order value
Idda	–	–	1.017	Path length of direct irradiance: 1st order value
Iddb	–	–	1.95	Path length of direct irradiance: 2n order value
lds0	–	–	1.1156	Path length of diffuse irradiance: 0th order value
lds1	–	–	0.5504	Path length of diffuse irradiance: 1st order value
Id	κ <sub>0</sub>	–	1.0546	Path length factor of total irradiance, Ed
BRDF[n]	B <sub>n</sub>	sr <sup>-1</sup>	0.318	BRDF of bottom surface no. n, n=0..5

## Appendix 5: Input spectra

The following table summarizes the 34 spectra which are imported from files. For each, a default spectrum is provided in the directory /WASI5/DATA. The user can replace the default spectra by changing the corresponding file description in the WASI5.INI file.

No.	WASI	Symbol	Units	Description
1	x, FWHM	$\lambda$	nm	Wavelengths, Spectral resolution
2	offsetS	–	variable	Measurement offset spectrum
3	scaleS	–	–	Measurement scale spectrum
4	noiseS	–	variable	Measurement noise spectrum
5	E0	$E_0(\lambda)$	$\text{mW m}^{-2} \text{ nm}^{-1}$	Extraterrestrial solar irradiance
6	aO2	$a_o(\lambda)$	$\text{cm}^{-1}$	Absorption coefficient of oxygene
7	aO3	$a_{oz}(\lambda)$	$\text{cm}^{-1}$	Absorption coefficient of ozone
8	aWV	$a_{wv}(\lambda)$	$\text{cm}^{-1}$	Absorption coefficient of water vapor
9	a_ice	$a_{ice}(\lambda)$	$\text{m}^{-1}$	Absorption coefficent of pure ice
10	aW	$a_w(\lambda)$	$\text{m}^{-1}$	Absorption coefficient of pure water
11	dadT	$d a_w(\lambda) / dT$	$\text{m}^{-1} \text{ }^{\circ}\text{C}^{-1}$	Temperature gradient of pure water absorption
12	aP[0]	$a_0^*(\lambda)$	$\text{m}^2 \text{ mg}^{-1}$	Specific absorption coeff. of phytoplankton class no. 0 Default: Mixture of species typical for Lake Constance
13	aP[1]	$a_1^*(\lambda)$	$\text{m}^2 \text{ mg}^{-1}$	Specific absorption coeff. of phytoplankton class no. 1 Default: Cryptophyta type "L"
14	aP[2]	$a_2^*(\lambda)$	$\text{m}^2 \text{ mg}^{-1}$	Specific absorption coeff. of phytoplankton class no. 2 Default: Cryptophyta type "H"
15	aP[3]	$a_3^*(\lambda)$	$\text{m}^2 \text{ mg}^{-1}$	Specific absorption coeff. of phytoplankton class no. 3 Default: Diatoms
16	aP[4]	$a_4^*(\lambda)$	$\text{m}^2 \text{ mg}^{-1}$	Specific absorption coeff. of phytoplankton class no. 4 Default: Dinoflagellates
17	aP[5]	$a_5^*(\lambda)$	$\text{m}^2 \text{ mg}^{-1}$	Specific absorption coeff. of phytoplankton class no. 5 Default: Green algae
18	aNAP	$a_d^*(\lambda)$	–	Normalized absorption coefficient of non-algal particles
19	aY	$a_Y^*(\lambda)$	–	Normalized absorption coefficient of CDOM
20	bPhyN	$b_{phy}^N(\lambda)$	–	Normalized scattering coefficient of phytoplankton
21	bXN	$b_X^N(\lambda)$	–	Normalized scattering coeff. of suspended particles Type I
22	albedo[0]	$a_0(\lambda)$	–	Albedo of bottom type no. 0. Default: Constant
23	albedo[1]	$a_1(\lambda)$	–	Albedo of bottom type no. 1. Default: Sand
24	albedo[2]	$a_2(\lambda)$	–	Albedo of bottom type no. 2. Default: Silt
25	albedo[3]	$a_3(\lambda)$	–	Albedo of bottom type no. 3. Default: Seagrass
26	albedo[4]	$a_4(\lambda)$	–	Albedo of bottom type no. 4. Default: Mussel
27	albedo[5]	$a_5(\lambda)$	–	Albedo of bottom type no. 5. Default: Macrophyte
28	a_nw	$a^{nw}(\lambda)$	–	Albedo of non-water area
29	meas	variable	variable	Measurement: Current input for inverse modeling
30	R	$R(\lambda)$	–	Measurement: Irradiance reflectance
31	Ed	$E_d(\lambda)$	$\text{mW m}^{-2} \text{ nm}^{-1}$	Measurement: Downwelling irradiance
32	Ls	$L_s(\lambda)$	$\text{mW m}^{-2} \text{ nm}^{-1} \text{ sr}^{-1}$	Measurement: Sky radiance reflected at surface
33	Kd	$K_d(\lambda)$	$\text{m}^{-1}$	Measurement: Attenuation for downwelling irradiance
34	gew	$g(\lambda)$	–	Weight function for inversion

## Appendix 6: Calculated spectra

Various spectra are calculated during run-time as intermediate results, depending on the actual spectrum type and calculation options. The spectra  $b_X(\lambda)$ ,  $a_Y^*(\lambda)$ ,  $E_d(\lambda)$ ,  $L_s(\lambda)$ ,  $K_d(\lambda)$ ,  $R(\lambda)$  can replace input spectra. Each spectrum can be displayed and exported to file as explained in chapter 9.

WASI GUI	Symbol	Units	Description
bbW	$b_{b,W}(\lambda)$	$m^{-1}$	Backscattering coefficient of pure water
bX	$b_X(\lambda)$	$- / m^{-1}$	(Normalized) scattering coefficient of suspended particles Type I
b_Mie	$b_{Mie}^* \cdot (\lambda/\lambda_s)^n$	$m^2 mg^{-1}$	Scattering coefficient of suspended particles Type II
bb_Mie	$b_{b,Mie}^* \cdot (\lambda/\lambda_s)^n$	$m^2 mg^{-1}$	Backscattering coefficient of suspended particles Type II
aY*	$a_Y^*(\lambda)$	–	Normalized absorption coefficient of CDOM
T_O2	$T_o(\lambda)$	–	Transmittance of the atmosphere after oxygen absorption
T_O3	$T_{oz}(\lambda)$	–	Transmittance of the atmosphere after ozone absorption
T_wv	$T_{wv}(\lambda)$	–	Transmittance of the atmosphere after water vapor absorption
tau_a	$\tau_a(\lambda)$	–	Aerosol optical thickness
T_r	$T_r(\lambda)$	–	Transmittance of the atmosphere after Rayleigh scattering
T_as	$T_{as}(\lambda)$	–	Transmittance of the atmosphere after aerosol scattering
T_aa	$T_{aa}(\lambda)$	–	Transmittance of the atmosphere after aerosol absorption
Ed0	$E_d(\lambda, 0-)$	$mW m^{-2} nm^{-1}$	Downwelling irradiance just beneath water surface
Ed	$E_d(\lambda)$	$mW m^{-2} nm^{-1}$	Downwelling irradiance
fdd*Edd	$f_{dd} \cdot E_{dd}(\lambda)$	$mW m^{-2} nm^{-1}$	Direct component of downwelling irradiance
fds*Eds	$f_{ds} \cdot E_{ds}(\lambda)$	$mW m^{-2} nm^{-1}$	Diffuse component of downwelling irradiance
E_dsr	$E_{dsr}(\lambda)$	$mW m^{-2} nm^{-1}$	Diffuse component of downwelling irradiance caused by Rayleigh scattering
E_dsa	$E_{dsa}(\lambda)$	$mW m^{-2} nm^{-1}$	Diffuse component of downwelling irradiance caused by aerosol scattering
r_d	$r_d(\lambda)$	–	Ratio of direct to diffuse downwelling irradiance
Lu	$L_u(\lambda)$	$mW m^{-2} nm^{-1} sr^{-1}$	Upwelling radiance
Lr	$\rho_L \cdot L_s(\lambda)$	$mW m^{-2} nm^{-1} sr^{-1}$	Radiance reflected at the water surface
Ls	$L_s(\lambda)$	$mW m^{-2} nm^{-1} sr^{-1}$	Sky radiance
Lf	$L_F(\lambda)$	$mW m^{-2} nm^{-1} sr^{-1}$	Chl-a fluorescence component of upwelling radiance
Kd	$K_d(\lambda)$	$m^{-1}$	Diffuse attenuation coefficient for downwelling irradiance
Kdd	$K_{dd}(\lambda)$	$m^{-1}$	Attenuation coefficient of direct irradiance
Kds	$K_{ds}(\lambda)$	$m^{-1}$	Attenuation coefficient of diffuse irradiance
K_uW	$K_{uW}(\lambda)$	$m^{-1}$	Attenuation of upwelling irradiance backscattered in water
K_uB	$K_{uB}(\lambda)$	$m^{-1}$	Attenuation of upwelling irradiance reflected from the bottom
k_uW	$k_{uW}(\lambda)$	$m^{-1}$	Attenuation of upwelling radiance backscattered in water
k_uB	$k_{uB}(\lambda)$	$m^{-1}$	Attenuation of upwelling radiance reflected from the bottom
R	$R(\lambda)$	–	Irradiance reflectance
r_rs	$r_{rs}(\lambda)$	$sr^{-1}$	Radiance reflectance

Rrs	$R_{rs}(\lambda)$	$\text{sr}^{-1}$	Remote sensing reflectance
Rrs_surf	$R_{rs}^{\text{surf}}(\lambda)$	$\text{sr}^{-1}$	Surface reflectance
rrs_f	$r_{rs,F}(\lambda)$	$\text{sr}^{-1}$	Chl-a fluorescence component of radiance reflectance
f	f	—	f factor
frs	$f_{rs}$	—	$f_{rs}$ factor
Q	Q	$\text{sr}$	Q factor
bottom	$R^b(\lambda)$	—	Bottom albedo
bottom	$r_{rs}^b(\lambda)$	$\text{sr}^{-1}$	Bottom radiance reflectance
a	$a(\lambda)$	$\text{m}^{-1}$	Absorption coefficient
b	$b(\lambda)$	$\text{m}^{-1}$	Scattering coefficient
bb	$b_b(\lambda)$	$\text{m}^{-1}$	Backscattering coefficient
a_calc	—	$\text{m}^{-1}$	Absorption of water constituents + optionally water (inv. mode)
aPh	$\sum C_i \cdot a_i^*(\lambda)$	$\text{m}^{-1}$	Phytoplankton absorption coefficient
aCDOM	$a_{CDOM}(\lambda)$	$\text{m}^{-1}$	CDOM absorption coefficient
aNAP	$a_{NAP}(\lambda)$	$\text{m}^{-1}$	NAP absorption coefficient
bbPh	$b_{b,phy}(\lambda)$	$\text{m}^{-1}$	Phytoplankton backscattering coefficient
bbNAP	$b_{b,NAP}(\lambda)$	$\text{m}^{-1}$	NAP backscattering coefficient
b_calc	$b(\lambda)$	$\text{m}^{-1}$	Scattering of water + constituents (inverse mode)
bb_calc	$b_b(\lambda)$	$\text{m}^{-1}$	Backscattering of water + constituents (inverse mode)
omega_b	$\omega_b(\lambda)$	—	Ratio backscattering over absorption plus backscattering
z_Ed	$z_{Ed}(\lambda)$	m	Depth at which $p_{Ed}$ % of surface irradiance remains

## Appendix 7: Spectrum types

The following table gives for all spectrum types an overview which equation is used for calculation and which parameters can be used as fit parameters. N = maximum number of fit parameters.

Spectrum type	Model options	Symbol	Equation	N	Fit parameters
Absorption	Exclude pure water	$a_{wc}(\lambda)$	(2.2)	10	$C_0 \dots C_5, C_X, C_{Mie}, C_Y, S$
	Include pure water	$a_w(\lambda)$	(2.1)	11	$C_0 \dots C_5, C_X, C_{Mie}, C_Y, S, T$
Attenuation	For downwelling irradiance	$K_d(\lambda)$	(2.17)	13	$C_0 \dots C_5, C_X, C_{Mie}, C_Y, S, T, n, \theta_{sun}$
Surface reflectance	Wavelength dependent	$R_{rs}^{surf}(\lambda)$	(2.25)	10	$\alpha, \beta, \gamma, \delta, \alpha^*, \beta^*, \gamma^*, \delta^*, v, \sigma_L$
	Constant	$R_{rs}^{surf}$	(2.26)	1	$\sigma_L$
Irradiance reflectance	For deep water	$R(\lambda)$	(2.27)	14	$C_0 \dots C_5, D, Y, S, T, C_L, C_S, n, \theta_{sun}$ or $f$
	For shallow water	$R^{sh}(\lambda)$	(2.29)	21	$C_0 \dots C_5, D, Y, S, T, C_L, C_S, n, \theta_{sun}, f_0 \dots f_5, z_B$
Radiance reflectance	For deep water below water surface	$r_{rs}^-(\lambda)$	(2.30)	15	$C_0 \dots C_5, D, Y, S, T, C_L, C_S, n, \theta_{sun}$ or $f, Q$
		$r_{rs}^-(\lambda)$	(2.31)	15	$C_0 \dots C_5, D, X, Y, S, T, C_L, C_S, n, \theta_{sun}, \theta_v$
	For shallow water below water surface	$r_{rs}^{sh-}(\lambda)$	(2.33)	22	$C_0 \dots C_5, D, Y, S, T, C_L, C_S, n, \theta_{sun}, \theta_v$ or $Q, f_0 \dots f_5, z_B$
	For deep water above water surface and wavelength dependent surface reflections	$r_{rs}(\lambda)$	(2.34) and (2.35)	25	$C_0 \dots C_5, D, Y, S, T, C_L, C_S, n, \theta_{sun}$ or $f, Q, \alpha, \beta, \gamma, \delta, \alpha^*, \beta^*, \gamma^*, \delta^*, v, \sigma_L$
		$r_{rs}(\lambda)$	(2.34) and (2.36)	26	$C_0 \dots C_5, D, Y, S, T, C_L, C_S, n, \theta_{sun}$ or $f, \theta_v, Q, \alpha, \beta, \gamma, \delta, \alpha^*, \beta^*, \gamma^*, \delta^*, v, \sigma_L$
		$r_{rs}(\lambda)$	(2.34) and (2.37)	25	$C_0 \dots C_5, D, Y, S, T, C_L, C_S, n, \theta_{sun}$ or $f, Q$ or $\theta_v, \alpha, \beta, \gamma, \delta, \alpha^*, \beta^*, \gamma^*, \delta^*, v, \sigma_L$
	For deep water above water surface and constant surface reflections	$r_{rs}(\lambda)$	(2.34) and (2.35)	16	$C_0 \dots C_5, D, Y, S, T, C_L, C_S, n, \theta_{sun}$ or $f, Q, \sigma_L$
		$r_{rs}(\lambda)$	(2.34) and (2.36)	17	$C_0 \dots C_5, D, Y, S, T, C_L, C_S, n, \theta_{sun}$ or $f, \theta_v, Q, \sigma_L$
		$r_{rs}(\lambda)$	(2.34) and (2.37)	16	$C_0 \dots C_5, D, Y, S, T, C_L, C_S, n, \theta_{sun}$ or $f, Q$ or $\theta_v, \sigma_L$
	For shallow water above water surface and wavelength dependent surface reflections	$r_{rs}^{sh}(\lambda)$	(2.34) and (2.35)	32	$C_0 \dots C_5, D, Y, S, T, C_L, C_S, n, \theta_{sun}, f_0 \dots f_5, z_B, Q, \alpha, \beta, \gamma, \delta, \alpha^*, \beta^*, \gamma^*, \delta^*, v, \sigma_L$
		$r_{rs}^{sh}(\lambda)$	(2.34) and (2.36)	32	$C_0 \dots C_5, D, Y, S, T, C_L, C_S, n, \theta_{sun}, \theta_v, f_0 \dots f_5, z_B, Q, \alpha, \beta, \gamma, \delta, \alpha^*, \beta^*, \gamma^*, \delta^*, v, \sigma_L$
		$r_{rs}^{sh}(\lambda)$	(2.34) and (2.37)	31	$C_0 \dots C_5, D, Y, S, T, C_L, C_S, n, \theta_{sun}, \theta_v, f_0 \dots f_5, z_B, \alpha, \beta, \gamma, \delta, \alpha^*, \beta^*, \gamma^*, \delta^*, v, \sigma_L$
	For shallow water above water surface and constant surface reflections	$r_{rs}^{sh}(\lambda)$	(2.34) and (2.35)	23	$C_0 \dots C_5, D, Y, S, T, C_L, C_S, n, \theta_{sun}, f_0 \dots f_5, z_B, Q, \sigma_L$
		$r_{rs}^{sh}(\lambda)$	(2.34) and	23	$C_0 \dots C_5, D, Y, S, T, C_L, C_S, n, \theta_{sun}, f_0 \dots f_5,$

			(2.36)		$z_B, Q, \sigma_L$
		$r_{rs}^{sh}(\lambda)$	(2.34) and (2.37)	22	$C_0 \dots C_5, D, Y, S, T, C_L, C_S, n, \theta_{sun}, f_0 \dots f_5, z_B, \sigma_L$
Bottom reflectance	For irradiance sensors	$R^b(\lambda)$	(2.38)	6	$f_0 \dots f_5$
	For radiance sensors	$r_{rs}^b(\lambda)$	(2.39)	6	$f_0 \dots f_5$
Downwelling irradiance	Above water surface	$E_d(\lambda)$	(2.40)	5	$\alpha, \beta, \gamma, \delta, v$
	Below water surface for deep water	$E_d^-(\lambda)$	(2.50)	19	$C_0 \dots C_5, D, Y, S, T, C_L, C_S, n, \theta_{sun}$ or $f, \alpha, \beta, \gamma, \delta, v$
Upwelling radiance	Below water surface for shallow water	$E_d^{sh-}(\lambda)$	(2.50)	26	$C_0 \dots C_5, D, Y, S, T, C_L, C_S, n, \theta_{sun}, f_0 \dots f_5, z_B, \alpha, \beta, \gamma, \delta, v$
	Below water surface for deep water	$L_u^-(\lambda)$	(2.66)	20	$C_0 \dots C_5, D, Y, S, T, C_L, C_S, n, \theta_{sun}$ or $f, \theta_v$ or $Q, \alpha, \beta, \gamma, \delta, v$
	Below water surface for shallow water	$L_u^{sh-}(\lambda)$	(2.66)	27	$C_0 \dots C_5, D, Y, S, T, C_L, C_S, n, \theta_{sun}, \theta_v$ or $Q, f_0 \dots f_5, z_B, \alpha, \beta, \gamma, \delta, v$
	Above water surface for deep water and wavelength dependent surface reflections	$L_u(\lambda)$	(2.61)	26	$C_0 \dots C_5, D, Y, S, T, C_L, C_S, n, \theta_{sun}$ or $f, \theta_v$ or $Q, \alpha, \beta, \gamma, \delta, v, \sigma_L^-, \alpha^*, \beta^*, \gamma^*, \delta^*, \sigma_L$
	Above water surface for deep water and constant surface reflections	$L_u(\lambda)$	(2.61)	22	$C_0 \dots C_5, D, Y, S, T, C_L, C_S, n, \theta_{sun}$ or $f, \theta_v$ or $Q, \alpha, \beta, \gamma, \delta, v, \sigma_L^-, \sigma_L$
	Above water surface for shallow water and wavelength dependent surface reflections	$L_u^{sh}(\lambda)$	(2.61)	33	$C_0 \dots C_5, D, Y, S, T, C_L, C_S, n, \theta_{sun}, \theta_v$ or $Q, f_0 \dots f_5, z_B, \alpha, \beta, \gamma, \delta, v, \sigma_L^-, \alpha^*, \beta^*, \gamma^*, \delta^*, \sigma_L$
	Above water surface for shallow water and constant surface reflections	$L_u^{sh}(\lambda)$	(2.61)	29	$C_0 \dots C_5, D, Y, S, T, C_L, C_S, n, \theta_{sun}, \theta_v$ or $Q, f_0 \dots f_5, z_B, \alpha, \beta, \gamma, \delta, v, \sigma_L^-, \sigma_L$

## Appendix 8: Demo data

Some demonstration data are provided in the following subdirectories of the directory d:\WASI5\DATA\demo.

**\2D\HySpex.** Hyperspectral image of the airborne sensor HySpex VNIR-1600 (Figure 6.2).

**\2D\Landsat-8.** Multispectral image of the sensor OLI on board of Landsat-8 (Figure 6.3 to Figure 6.6) and fit results of that image (Figure 6.9).

**\Ed.** Downwelling irradiance measured above water using a ZEISS MCS 501 UV-NIR spectrometer (File Zeiss\_R2R.Ed) and measured under water using a TriOS Ramses ACC VIS sensor (Files Ramses\_\*.Ed). See the file headers for more information.

**\Kd.** Diffuse attenuation coefficients for up- and downwelling irradiance. The two spectra were simulated using HYDROLIGHT.

**\L\_sky.** Sky radiance. The spectrum was simulated using WASI and the spectrum type “Downwelling irradiance”. See the file header for the model parameters.

**\R.** Irradiance reflectance. The spectrum was simulated using WASI for optically deep water. See the file header for the model parameters.

**\rrs.** Radiance reflectance measured under water using a TriOS Ramses ARC VIS sensor (Files Ramses\_\*.rrs). See the file headers for more information.

## Appendix 9: Changes compared to version 4.1

The last version WASI 4.1 was released on 8 September 2015. Since then numerous minor software changes and bug fixes have been made. The main improvements of the current version WASI 5 are as follows:

- The nomenclature was refined for the term *remote sensing reflectance*. The term was used previously for the ratio of upwelling radiance to downwelling irradiance, irrespectively if measured above or under water and whether reflections at the water surface are present or not. This general ratio is now termed *radiance reflectance*, while remote sensing reflectance is restricted now to the ratio of water leaving radiance to downwelling irradiance above the water surface.
- The nomenclature was updated for colored dissolved organic matter (CDOM) and non-algal particles (NAP). The outdated names are Gelbstoff and detritus, respectively.
- Inclusion of NAP absorption in forward and inverse mode, see section 2.1.4.
- NAP concentration is now calculated as sum of  $C_X$  and  $C_{Mie}$ , see Eq. (2.10). Previously it was an independent parameter (called detritus) and related to absorption only.
- Inclusion of phytoplankton backscattering in forward and inverse mode with new fit parameter  $b_{b,phy}^*(\lambda_S)$ , see section 2.2.2.
- New database of bottom substrate albedo, see Figure 2.5. The old spectra can be found in the directory \WASI5\DATA\auxiliary.
- Spectral mixing of water and non-water surfaces was added, see section 2.12.
- Explanation of the parameter symbols in the parameter list, see Figure 3.2.
- Automatic screenshot of the current plot to file WASI\_plot.bmp, see Figure 3.6.
- Automatic screenshot of the current image to file WASI\_img.bmp, see section 6.5.7.
- Detailed description of the 2D mode including guidelines for data processing, see chapter 6.

The inclusion of NAP absorption, phytoplankton backscattering and the exchange of the bottom albedo spectra leads to slightly different model results for the new default settings. To obtain the same results as in WASI 4.1, set  $a_{NAP}^*(\lambda_0) = 0$  and  $b_{b,phy}^*(\lambda_S) = 0$  for optically deep water. For optically shallow water, use additionally the old bottom albedo spectra.

From a developers perspective the most important innovation is the change of the integrated development environment (IDE) from Delphi to Lazarus. Delphi is a commercial software restricted to the Windows operating system, while Lazarus is a free cross-platform software. This opens up the possibility of compiling WASI for other operating systems in the future.